Improving Cold Climate Performance of Heat Pumps Using Market-Available Systems

by

Mary Elizabeth Konrad

A thesis submitted to the
School of Graduate and Postdoctoral Studies in partial
fulfillment of the requirements for the degree of

Masters of Applied Science in Mechanical Engineering

Faculty of Engineering and Applied Science
University of Ontario Institute of Technology (Ontario Tech University)
Oshawa, Ontario, Canada

October 2022

Thesis Examination Information

Submitted by: **Mary Elizabeth Konrad**

Masters of Applied Science in **Mechanical Engineering**

Improving Cold Climate Performance of Heat Pumps Using Market-Available Systems

An oral defense of this thesis took place on October 27th, 2022 in front of the following examining committee:

Examining Committee:

Chair of Examining Committee	Dr. Amirkianoosh Kiani
Research Supervisor	Dr. Brendan D. MacDonald
Examining Committee Member	Dr. Martin Agelin-Chaab
External Examiner	Dr. Jennifer McKellar, Ontario Tech University
	ENE

The above committee determined that the thesis is acceptable in form and content and that a satisfactory knowledge of the field covered by the thesis was demonstrated by the candidate during an oral examination. A signed copy of the Certificate of Approval is available from the School of Graduate and Postdoctoral Studies.

Abstract

Air source heat pumps are an excellent electric alternative to fossil fuel based heating systems for reducing residential greenhouse gas (GHG) emissions, but common mild-climate systems suffer significant performance losses at the low outdoor temperatures experienced in cold climates. Improved heat pumps for cold climates already exist, but they are more expensive and their adoption has been relatively low. An analysis was conducted to assess the status of market-available cold climate heat pump technologies and identify opportunities in the literature that might further improve performance and uptake. A new cascade heat pump system was then proposed for rapid implementation in cold climates, since it is composed of two simple and well-established heat pumps models, compatible for replacing/retrofitting common centrally-ducted natural gas furnaces. Performance modelling and comparative analysis concluded it could out-perform all comparable market-available cold climate systems at -15 °C, with the potential to operate efficiently at even lower temperatures.

Keywords: Heat pump; cold climate; cascade; residential; retrofitting

Author's Declaration

I hereby declare that this thesis consists of original work of which I have authored. This is a true copy of the thesis, including any required final revisions, as accepted by my examiners.

I authorize the University of Ontario Institute of Technology to lend this thesis to other institutions or individuals for the purpose of scholarly research. I further authorize University of Ontario Institute of Technology to reproduce this thesis by photocopying or by other means, in total or in part, at the request of other institutions or individuals for the purpose of scholarly research. I understand that my thesis will be made electronically available to the public.

Mary Elizabeth Konrad

Statement of Contributions

I performed the research, analysis, and modelling for the above manuscript, and presented the findings.

Acknowledgments

I would like to thank my research supervisor, Dr. Brendan MacDonald, for his expertise, support, thoughtful advice, and patience as we navigated this journey amid a pandemic. His unwavering enthusiasm for my thesis project, and dedication to combatting climate change and making meaningful change in the world through engineering, have been both motivating and inspiring.

Thank you as well to my examiners, Dr. Jennifer McKellar and Dr. Martin Agelin-Chaab for taking the time to review my work and provide valuable feedback so that I could learn from your expertise and further improve my thesis.

To the other members of the MacDonald Lab: thank you for making me feel welcome and a part of the team even though circumstance did not give us many opportunities to get to know each other. Thank you as well for your thoughtful feedback on my presentations, it is greatly appreciated.

Thank you to all of my family members and friends for always being there for me and cheering me on through the ups and downs of the last three years. Your presence in my life is invaluable.

Contents

List of Tables

List of Figures

List of Abbreviations and Symbols

Abbreviations

AHRI	Air Conditioning, Heating, and Refrigeration Institute
ccASHP	cold climate air source heat pump
COP	coefficient of performance
c_{p}	specific heat at constant pressure (kJ/kgC)
CSA	Canadian Standards Association
DOE	Department of Energy
EES	Engineering Equation Solver
EXP.	expansion
GHG	greenhouse gas
GWP	global warming potential
h	specific enthalpy, per kg refrigerant (kJ/kg)
HSPF	heating season performance factor
ID	indoor
IHX	internal heat exchanger
$\dot{m}$	mass flow rate (kg/s)
N	compressor speed (RPM)
NRCan	Natural Resources Canada
OD	outdoor
p	pressure (kPa)
$\mathcal{P}$	power consumption
$p-h$	pressure versus enthalpy
$\dot{Q}$	heat transfer (rate) (kW, kBTU, or tons)
q	specific heat, per kg refrigerant (kJ/kg)
R	ratio
s	specific entropy, per kg refrigerant (kJ/kgK)
SI	Système Internationale
SIHX	suction internal heat exchanger
$T-s$	temperature versus entropy
V	compressor displacement volume (m^3/revolution)
VCASHP	vapour compression air source heat pump
VS	variable-speed
$\dot{W}$	work (rate) (kW)
w	specific work, per kg refrigerant (kJ/kg)

Subscripts

1	point 1, expansion valve exit, evaporator inlet
2	point 2, evaporator exit, compressor inlet
3	point 3, compressor discharge, condenser inlet
3i	point 3 when the compression process (2-3) is isentropic
4	point 4, condenser exit, expansion valve inlet
5	point 5, expansion valve exit, evaporator inlet (secondary heat pump)
6	point 6, evaporator exit, compressor inlet (secondary heat pump)
7	point 7, compressor discharge, condenser inlet (secondary heat pump)
8	point 8, condenser exit, expansion valve inlet (secondary heat pump)
air	air
aux	auxiliary
C	compressor
C2	compressor (secondary heat pump)
cond	condenser
cond2	condenser (secondary heat pump)
d	displacement
enc	enclosure
evap	evaporator
evap2	evaporator (secondary heat pump)
exc	excess (beyond the required heating capacity)
exh	exhaust air of the primary evaporator
fan	fan
H	high - rejected
H2	high - rejected (secondary heat pump)
in	inside the home
inj	injected refrigerant
is	isentropic
L	low - absorbed
L2	low - absorbed (secondary heat pump)
load	building load
lost	lost at the compressor
lost2	lost at the compressor (secondary heat pump)
m	motor
out	outside
pinchE	evaporator pinch point
pinchC	condenser pinch point
r	refrigerant
r2	refrigerant (secondary heat pump)
ret	return air
sl	saturated liquid
supp	supply air
sv	saturated vapour

$_{Sys}$	overall system
$_{Sys1}$	System 1
$_{Sys2}$	System 2
$_{th}$	theoretical
$_{tot}$	total

Greek Letters

Δ	differential
η	efficiency
ρ	density (kg/m^3)

Chapter 1

Introduction

1.1 Motivation

Anthropogenic greenhouse gas (GHG) emissions are on the rise and threatening the stability of the global climate [1]. The most recent reports from the International Panel on Climate Change have given us very short timelines during which to reverse this trend and keep global temperatures below a threshold that could avoid triggering dangerous feedback loops, and minimize catastrophic effects on the ecosystems, natural cycles, and climatic norms we depend on [2]. In response, nations around the world are setting ambitious goals to drastically reduce their GHG emissions in the coming years and to meet these targets on time, we need to see substantial reductions happening quickly in all sectors [1]. This thesis project focuses on addressing emissions from Canada's residential building sector, which are predominantly incurred by the space heating required to live in our country's cold climate. In Canada, 56 % of all homes are still heated directly by the burning of fossil fuels [3], and 66 % of residential GHG emissions are attributed to

space heating [4]. Given Canada's relatively clean electricity sector, replacing fossil-fuel-based heating systems with high-efficiency electric alternatives has the potential yield immediate and substantial reductions in residential building emissions. Additionally, as efforts are made to further decarbonize the electricity grid, electrification of heating would allow greener electricity to continue to reduce the carbon footprint of home infrastructure going forward, without the need for subsequent heating system transitions.

Electric vapour compression air-source heat pumps (VCASHPs) offer a promising avenue for energy-efficient electrification of home heating since they can achieve efficiencies more than three times that of standard electric resistance heaters [5], and use only free and ubiquitous outdoor air as a heat source. They are also well-suited to retrofitting homes, since they may be able to directly replace the existing furnace and air conditioner units in common centrally-ducted, forced air systems. The residential VCASHP industry is already well-established internationally, and simple and affordable VCASHPs have a long history of popular use in mild climates where the indoor-outdoor air temperature difference is relatively small year-round. However, these standard single-stage heat pump designs face numerous performance issues when ambient outdoor temperatures drop near or below 0 °C, and most systems shut off at around −5 °C, making them heavily reliant on less efficient or more polluting auxiliary heating systems when operating in cold climates. Improved heat pumps marketed for cold climate use (ccASHPs) are already available, but these new systems have higher upfront costs, and homeowners can be deterred by uncertainty around the projected savings and payback periods. Thus, adoption of heat pump systems in cold climate regions to date has been limited [6]. As of 2019, only 5 % of homes in Canada were using a heat pump for space heating, despite

another 29 % using comparatively inefficient electric resistance heating [7], with higher operating costs.

The urgency of the climate crisis makes the rapid deployment and widespread adoption of ccASHPs a critical challenge that should influence industry design choices. In this regard, there would be inherent benefits to utilizing reliable, inexpensive, and recognized mild-climate heat pumps, that come with pre-existing production lines, supply chains, and trained technicians. Thus, I am motivated to explore if there is a simple way that established, affordable heat pumps could be made to deliver improved cold climate performance, and if so, how such a design would compare to the technologies employed in the cold climate heat pump systems that are already available on the market. The idea I proposed and investigate in this thesis project involves the use of two single-stage, single-speed heat pumps paired together by a shared enclosed airspace to form a two-stage cascade heat pump system. The enclosure can open to operate only one heat pump in certain conditions, to maximize seasonal performance.

More homes in cold climates should be heated using electric heat pumps to reduce emissions from the residential sector. However, determining the best ccASHP designs to prioritize and promote for cold climate applications requires an in-depth understanding of the challenges faced by heat pumps operating at cold outdoor air temperatures, the features and capabilities of ccASHP designs already found on the market and in the literature, as well as robust, comparative studies of side-by-side system performance and energy consumption. Additionally, consideration should be given to designs that address barriers to technology uptake, including simple modifications to existing heat pumps that would offer advantages for rapid deployment and affordability. This thesis will ad-

dress these topics by including a comprehensive analysis of market-available cold climate heat pump technologies and other designs found in the literature, as well as a modelling study of the proposed heat pump design, with a comparison to the market-available cold climate heat pumps.

1.2 Background

1.2.1 Theoretical Carnot heat pumps

The most efficient heat pump cycle is the theoretical Carnot heat pump, which follows the reverse Carnot cycle. The standard Carnot cycle is an ideal, theoretical heat engine which derives the absolute maximum amount of useful work ($\dot{W}_{\mathrm{OUT}}$) possible from the transfer of heat ($\dot{Q}$) from a high temperature reservoir, to a low temperature reservoir. Thus, the *reverse* Carnot cycle is an ideal heat pump which moves heat energy in the opposite direction, from the low temperature reservoir to the high temperature reservoir, driven by a minimal amount of work ($\dot{W}_{\mathrm{IN}}$). A visual representation of these two systems is provided in Figure 1.1.

The Carnot heat pump cycle is made up of four ideal, reversible processes, as shown on the $T - s$ diagram in Figure 1.2:

- ***Process 1-2***: Constant temperature, constant pressure heat absorption from the low temperature reservoir, at the reservoir temperature, T_{L}.
- ***Process 2-3***: Isentropic compression to increase the working fluid temperature to that of the high temperature reservoir, T_{H}.

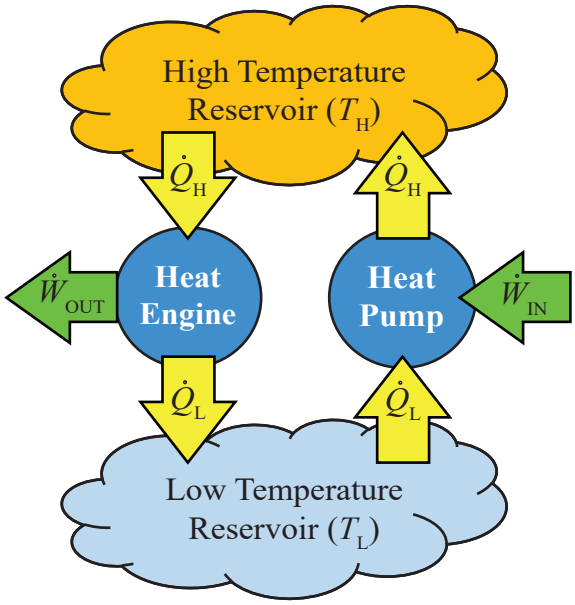

Figure 1.1: A Carnot heat engine and Carnot heat pump operating between high and low temperature reservoirs.

- ***Process 3-4***: Constant temperature, constant pressure heat rejection to the higher temperature reservoir, at the reservoir temperature, T_H.

- ***Process 4-1***: Isentropic expansion to return the working fluid to the initial state.

Since all of these processes are ideal and reversible, the Carnot heat pump's performance is influenced only by the temperatures of the two reservoirs involved, and the cycle demonstrates the theoretical maximum efficiency for the given reservoir temperatures. However, the constraints and behaviours of real-world materials, components, and applications make achieving such a cycle impossible in practice.

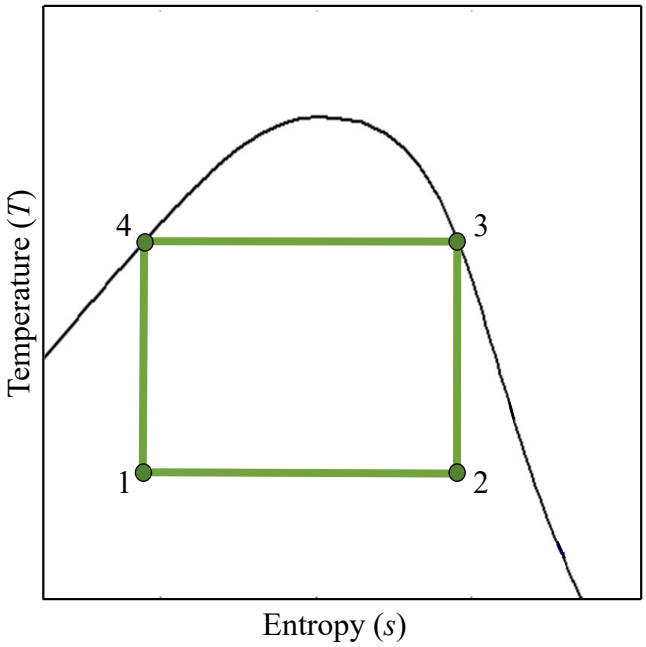

Figure 1.2: $T-s$ diagram of a hypothetical Carnot heat pump using a vapour compression cycle with an azeotropic refrigerant.

1.2.2 Real, ideal heat pumps

Real heat pump cycles commonly follow the vapour compression refrigeration cycle, and leverage the phase change behaviour of azeotropic refrigerants (those which do not change temperature during constant pressure phase change) in order to perform the heat absorption and rejection processes at constant temperature and pressure, as in the Carnot heat pump cycle. This is shown on a $T-s$ diagram in Figure 1.2, where a Carnot heat pump cycle has been created within the vapour dome of an azeotropic fluid. However, to perform this cycle with existing components would be problematic since compressors and turbines can be damaged by the liquid droplets that would be present during the compression (2-3) and expansion (4-1) processes. Thus, in real residential VCASHPs,

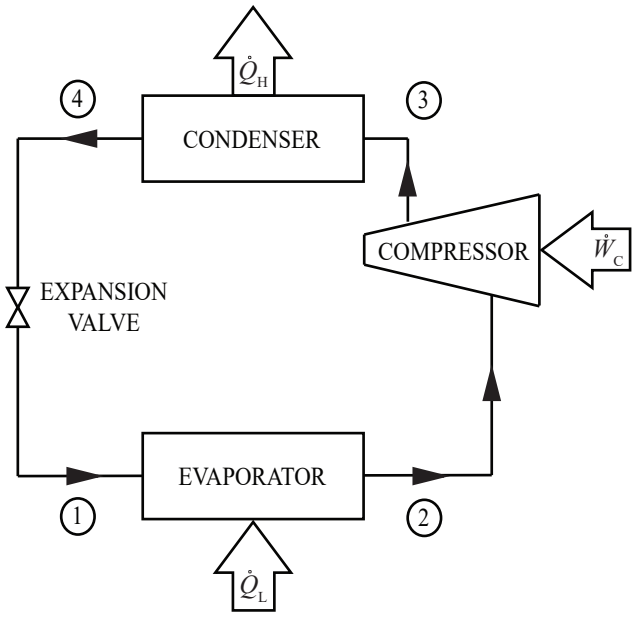

Figure 1.3: A schematic of the components in a real vapour compression heat pump.

the compression process is shifted into the superheated vapour region, and the expansion process is performed by an expansion valve instead of a turbine. The heat absorption (1-2) and heat rejection (3-4) processes are performed using heat exchanger coils (referred to as the evaporator and condenser, respectively) over which air is blown using fans. Figure 1.3 shows the basic components of a standard, single-stage heat pump that uses a vapour compression refrigeration cycle to heat an indoor space.

Real, ideal heat pump cycles differ from the cycle in Figure 1.2 in several ways that are illustrated by the $p - h$ and $T - s$ diagrams in Figure 1.4. Firstly, Point 2 is shifted to the saturation line so that the compression process (2-3) occurs entirely within the superheated vapour region. This results in point 3 having a higher temperature than point 4, as it has moved outside the vapour dome along the line of constant pressure, and thus the heat rejection process (3-4) no longer occurs at constant temperature. The expansion process (4-1) is no longer isentropic, but isenthalpic due to the use of the

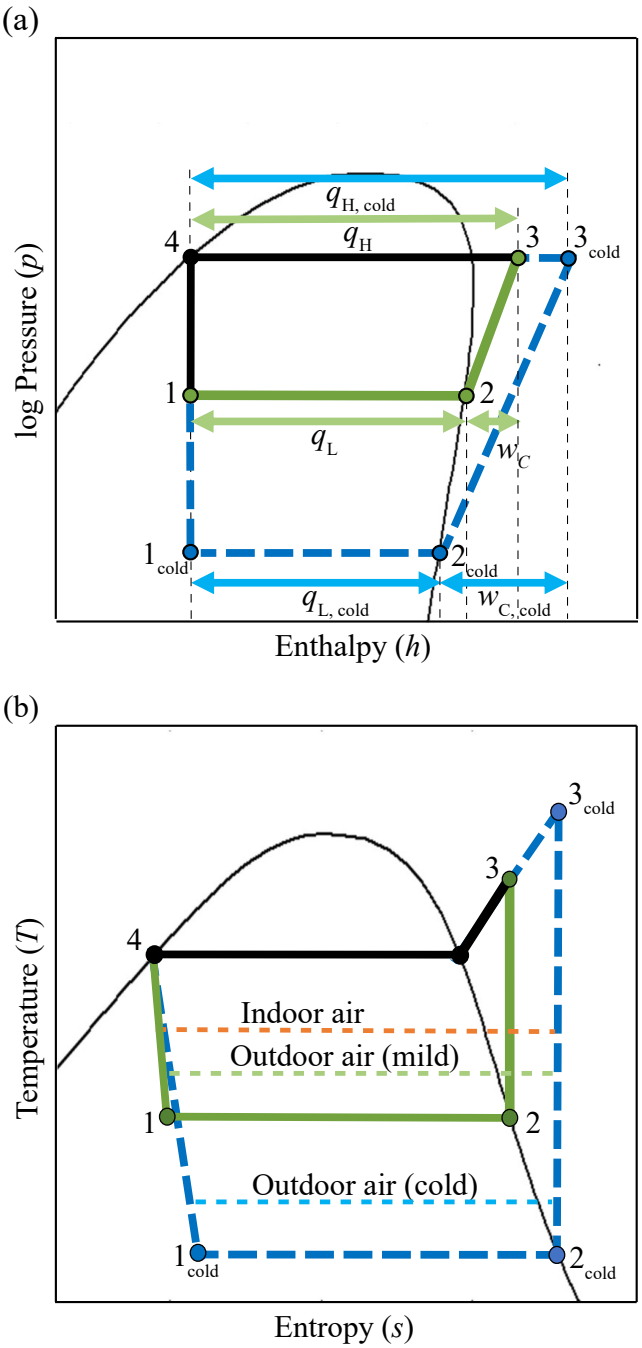

Figure 1.4: (a) Pressure-enthalpy ($p-h$) diagram and (b) temperature-entropy ($T-s$) diagram of the thermodynamic heating cycle of an ideal, standard single-stage heat pump at mild (green cycle) and cold (blue cycle) outdoor air temperatures.

expansion valve. Additionally, real heat exchangers require a temperature difference (ΔT) between the refrigerant inside the coil and the air source/sink in order for heat transfer to occur. The resulting cycles (shown in Figure 1.4) are still considered ideal since they ignore component inefficiencies and pressure losses, and assume all components and pipes to be adiabatic. However, the real, ideal VCASHP cycle is useful for examining the inherent effects of changing indoor/outdoor temperatures on heat pump performance, which will be discussed in Section 1.2.5.

1.2.3 True, non-ideal heat pumps

True heat pump cycles, performed by built systems, are influenced by a variety of additional, unavoidable factors which make them differ from the ideal cycles in Figure 1.4:

- Imperfect piping insulation can lead to heat transfer to or from the surroundings.
- Some amount of superheating is desired at point 2 to ensure complete evaporation occurs before the compressor.
- Some amount of subcooling is desired at point 4 to ensure complete condensation occurs before the expansion valve.
- Fluid friction results in pressure drops along pipe sections.
- Entropy is generated in the compressor due to mechanical friction.
- Compressor efficiency is reduced due to pressure drops at the inlet and outlet valves.
- Compressor volumetric efficiency is imperfect, and varies with the system operating conditions.

- Mass flow rate varies with the density at point 2 and the volumetric efficiency of the compressor.
- Heat generated by the compressor motor preheats the suction gas entering the compressor.
- Heat is lost to the surrounding air from the compressor shell.
- Zeotropic refrigerant mixtures may be used, which exhibit temperature changes during constant pressure evaporation and condensation.
- Frost may accumulate on the evaporator coil, impacting heat transfer and air flow.

The $T-s$ diagram in Figure 1.5 shows a true heat pump cycle, demonstrating several of the phenomena listed above. The position of point 3' demonstrates the effect of heat loss ($\dot{Q}_C$) during the compression process (2-3).

1.2.4 Intentional design elements

Beyond the unavoidable variables described above, a heat pump's cycle and resulting performance are also influenced by a variety of factors which may be intentionally manipulated to improve or optimize heat pump performance for a particular application. These factors include

- refrigerant pipe length and path;
- component and pipe thermal insulation;
- indoor/outdoor heat exchanger size and type;

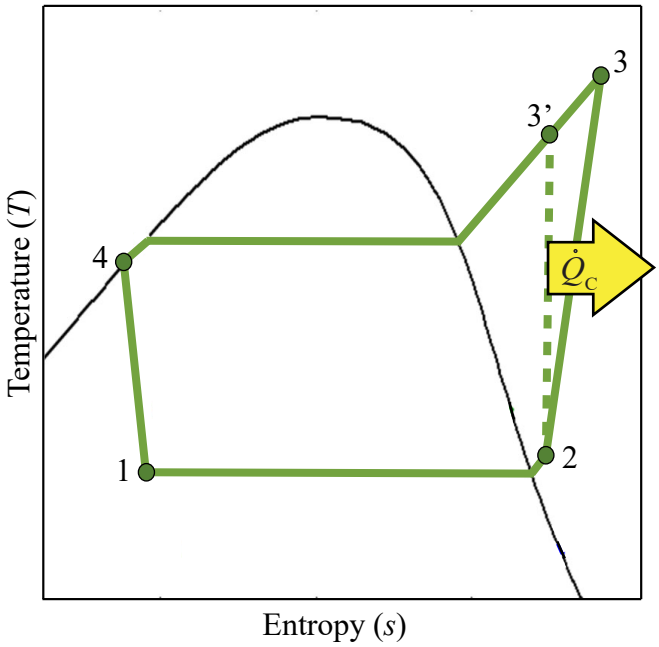

Figure 1.5: $T - s$ diagram of a true, non-ideal heat pump cycle showing heat loss from the compressor ($\dot{Q}_C$).

- compressor speed, type, and special features;
- controlled set points (such as ΔT at the evaporator and condenser, max/min T and p at specific points, and the degrees of superheating and subcooling at points 2 and 4 respectively);
- total mass of refrigerant in the system;
- components and controls which manipulate active refrigerant charge (mass of refrigerant in circulation);
- advanced cycle types and modifications (such as flash injection);
- fan speed, type, and control logic;

- defrost strategy and control logic; and
- system sizing/capacity relative to design heating and cooling loads.

Thus, in order to understand and predict the performance of an existing, built heat pump, design specifications, operational set points, and performance data are needed to determine which of the above factors play a significant role, and what their effect is on the resulting heat pump cycle at different indoor and outdoor temperature conditions.

1.2.5 Cold climate operation

There are a variety of effects that cold climate heating conditions have on heat pump performance, which are summarized in this section, but first it is useful to refer to the real, ideal cycle from Figure 1.4, to observe the effects that decreasing outdoor air temperature have on a standard VCASHP cycle. As outdoor temperature changes, the refrigerant temperature (and corresponding saturation pressure) found in each of the heat pump's two heat exchangers is controlled to maintain a sufficient temperature difference between the air and refrigerant to achieve satisfactory heat transfer (as shown in Figure 1.4). Thus, when heating during cold outdoor air conditions, a corresponding drop in evaporator temperature and pressure is needed to keep the system functioning (as shown by the shift from the green cycle to blue cycle in Fig. 1.4). This requirement for lower evaporator pressure in cold climate heat pumps necessitates system design changes to ensure heating objectives can be achieved.

Reduced performance at cold air temperatures

Decreasing outdoor air temperature causes detrimental changes to the variables that define system heating performance. VCASHP efficiency is most commonly expressed by the ratio between the useful heating output ($\dot{Q}_{\mathrm{H}}$) and electrical energy consumed ($\mathcal{P}_{\mathrm{tot}}$), known as the coefficient of performance (COP) shown in Equation 1.1. For an ideal heat pump cycle system losses are assumed to be negligible, and $\mathcal{P}_{\mathrm{tot}}$ includes only the compressor work ($\dot{W}_{\mathrm{C}}$). Thus, the COP is defined by Equation (1.1), and the relationship between $\dot{Q}_{\mathrm{H}}$ and $\dot{W}_{\mathrm{C}}$ is based on the energy balance reflected in Eqs. (1.2) and (1.3).

$$\mathrm{COP} = \frac{\dot{Q}_{\mathrm{H}}}{\mathcal{P}_{\mathrm{tot}}} \tag{1.1}$$

$$\dot{Q}_{\mathrm{L}} + \dot{W}_{\mathrm{C}} = \dot{Q}_{\mathrm{H}} \tag{1.2}$$

$$\dot{m}_{\mathrm{r}} q_{\mathrm{L}} + \dot{m}_{\mathrm{r}} w_{\mathrm{C}} = \dot{m}_{\mathrm{r}} q_{\mathrm{H}} \tag{1.3}$$

As seen in Fig. 1.4, when the outdoor air temperature drops, so does evaporator temperature and pressure, shifting part of the ideal thermodynamic cycle from the green line to the blue line. The blue (cold) cycle in Fig. 1.4 (a) reveals a decrease in the magnitude of q_{L} as point 2_{cold} moves downward along the saturation line, which must be compensated for by a corresponding increase in the magnitude of the specific compressor work $w_{\mathrm{C,\,cold}}$. This can also be seen in Eq. (1.3), since any decrease in the magnitude of q_{L} requires a corresponding increase in w_{C} to maintain the desired specific heat output (q_{H}) (when mass flow rate $\dot{m}_{\mathrm{r}}$ is constant). This increase in specific compressor work for cold climate heating operation is consistent with the fact that a greater pressure change must be achieved by the compressor, and the result is a decrease in the COP of the system.

The shift from point 2 to 2_{cold} also results in decreased density of the refrigerant at the compressor inlet, which reduces the volumetric efficiency of the compressor [8]. This leads to a decrease in the mass flow rate ($\dot{m}_{\text{r}}$) throughout the system (with constant compressor speed), and a consequent reduction of the heating capacity $\dot{Q}_{\text{H}}$ (as per Eq. (1.3)) [9]. Typically, this reduction in capacity is addressed by operating an auxiliary heating system of another (less efficient) type, which increases costs and lowers the overall system COP.

Increased compressor discharge temperature

As outdoor air temperature decreases, the discharge temperature of the compressor (point 3 in Fig. 1.4) in an the ideal, single stage heat pump increases problematically. This increase is due to the fact that, as evaporator temperature and pressure drop, the point where the isentropic line extending from point 2_{cold} meets the desired condenser pressure (point 3_{cold}) occurs at a higher temperature. Given that real compressors rarely operate isentropically, the actual discharge temperature is even higher. An increasing temperature at point 3_{cold} lowers the efficiency of the compression process, and reduces oil viscosity in the compressor which can cause poor lubrication, leakage, damage, or premature failure [10]. Thus, heat pumps are designed to turn off when unsafe discharge temperatures are reached, thereby limiting their operating temperature range [9–11].

Refrigerant management issues

Two refrigerant management issues common to cold climate heat pumps are known as compressor slugging and flooding, and both involve detrimental uptake of liquid into the

compressor that can cause decreased efficiency, damage, or failure. Slugging refers to a temporary surge of liquid to the compressor that can occur when a heat pump starts up or switches between cooling and heating modes. Due to the need for defrost cycles, VCASHPs operating in cold temperatures perform these startups and mode changes frequently, making slugging a more serious concern. Furthermore, continuous flooding of the compressor can occur at cold temperatures since heat absorption at the evaporator may be insufficient to fully vapourize, or adequately superheat, the refrigerant before it exits the evaporator, heading toward the compressor (at point 2_{cold} in Fig. 1.4) [12]. Addressing these issues may involve devices which contain and control liquid refrigerant, or add supplemental heat to the suction line (at point 2_{cold}), thus preventing undesired liquid from entering the compressor [12].

The active circulating amount, or *charge*, of refrigerant desired for optimal performance of a heat pump system also becomes more variable in a cold climate. Heating and cooling modes usually require different refrigerant charges, and a system is commonly charged according to the mode with the higher refrigerant requirement [13] (usually cooling mode [14]). At a fixed condenser temperature, the optimal refrigerant charge decreases as evaporator temperature drops [15], and the indoor/outdoor temperature difference increases. Thus, in a cold climate where the indoor/outdoor temperature difference in the cooling season (summer) can be very small, and in the heating season (winter) can be very large, the optimal refrigerant charge will vary greatly. Nonoptimal refrigerant charge has a negative effect on system COP and capacity, in both the undercharged, and overcharged condition [16, 17]. Furthermore, overcharge conditions can increase the risk of liquid flood-back and slugging of the compressor [18]. Thus an

effective cold climate design should include the ability to actively modify the amount of refrigerant that is circulating through the heat pump cycle, or otherwise counteract the negative effects of over/under charge.

Other challenges

When evaporator temperature drops below both the dew point of the outdoor air, and the freezing temperature of water, condensation occurs and then freezes on the evaporator heat exchanger coils. This frost layer inhibits air flow and decreases heat transfer, so a defrosting method is needed [19–21], and melted frost must be effectively drained out and away from the basepan to prevent re-freezing and accumulation. The defrosting process may consume additional energy, reduce overall system efficiency, and temporarily interrupt or counteract heat delivery to the home [22]. If the frost layer is incompletely removed and then re-freezes, it can become even more difficult to melt in future defrosting attempts [21]. Thus, an efficient, rapid, and effective defrost method is critical to cold climate VCASHP design.

If a VCASHP system is sized to meet the maximum heating demand of a building in a cold climate, it will be oversized during the shoulder and cooling seasons when demand is lower [9, 23]. An oversized single-speed heat pump will move heat too quickly, causing it to switch on and off frequently, a phenomenon referred to as "short-cycling". Any amount of on-off cycling due to partial load operation degrades system COP [24] since, during the off cycle, refrigerant migrates from the high pressure condenser to the lower pressure evaporator [8]. This migrating refrigerant not only carries energy with it in the wrong direction, but must also be properly redistributed at startup, which

consumes compressor power before useful operation can be resumed [8]. Short-cycling is also uncomfortable for inhabitants of the building, due to the temperature fluctuations [10, 23] and poor humidity control [25, 26] it can cause. For these reasons, regulatory sizing guidelines limit the degree of oversizing (compared to the design cooling load) permitted for single-speed heat pumps [26] thereby necessitating the use of auxiliary heating to supplement output at peak heating demand in cold climates (where peak heating load is drastically larger than peak cooling load) [24]. To avoid excessive on-off cycling, and minimize/eliminate auxiliary heating needs, cold climate designs should allow for modulation of the heating/cooling capacity to match the demand at different outdoor temperatures.

1.3 Literature review

1.3.1 Past reviews of cold climate VCASHP technology

Past reviews reveal extensive activity and progress in the field of cold climate VCASHP heat pump design. There have been several progressive publications providing updated and comprehensive reviews of research papers including one in 2005 by Bertsch et al. [27] and a more recent one in 2018 by Zhang et al. [28]. Discussions of some challenges and technologies relevant to cold climate VCASHPs have also been included in more general reviews of heat pump technology [29–36]. Other reviews have been conducted that provide insight into specialized subsets of VCASHP technological research, with impacts on cold climate performance. Such topics include variable refrigerant flow [37], refriger-

ant injection [38, 39], ejector enhancement [40–43], cascade designs [44, 45], alternative refrigerants [46, 47], improved heat exchanger designs [48], defrosting methods [49–51], and VCASHPs for electric vehicles [52]. Relevant work can be also found in heat pump research focused on cooling in very hot climates [53], high temperature heating [54, 55], and low temperature refrigeration [56], since these applications involve many of the same thermodynamic challenges encountered in cold climate heating. With respect to reviews of industry progress, one 2019 review paper by Jesper et al. [57] examined the performance and application of market-available large-scale heat pumps, but no such review exists for residential heat pumps.

1.3.2 Cascade heat pumps

A cascade heat pump is comprised of two or more separate heat pump cycles where a low temperature cycle rejects heat to a higher temperature cycle by way of a shared heat exchanger or connecting heat transfer fluid loop, in order to span a large temperature difference [58]. A typical two-stage cascade system is shown in Fig. 1.6. One advantage of a cascade design is that the two cycles can use different refrigerants, selected based on properties that make them well-suited to the specific operating conditions of the high or low temperature cycle they will individually perform [58], thereby improving overall system performance. Cascade systems could also allow for the safe use of a refrigerant with superior performance that poses risks in inhabited spaces, since one heat pump cycle could take place entirely outside of the building. Additional benefits of cascade systems are similar to other two-stage cycles (discussed in Section 1.3.3), including reduced pres-

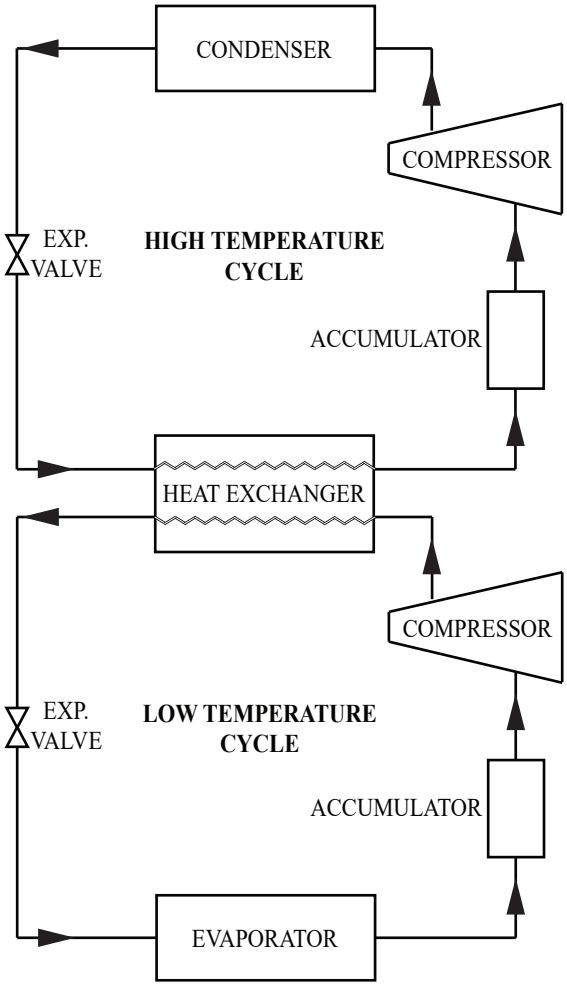

Figure 1.6: Diagram showing the configuration of a typical two-stage cascade heat pump.

sure differences across each compressor, lower high-stage discharge temperatures, and the ability to incorporate different compressor types/sizes, independent compressor controls, and multi-function operation (described in Section 2.2.2) [31,58,59]. While cascade cycles have been studied extensively for use in low temperature refrigeration [45], and are commonly employed when CO_2 is used as a refrigerant [60], they have also been investigated for high temperature dryer systems [54,59,61]; however, their application in cold climate heat pumps is relatively new [58]. Yang et al. [58] provided a brief summary of recent

studies where cascade cycles were employed in cold climate heat pumps and proposed a novel cold climate design which could operate in single-stage or cascade mode, using only R410a refrigerant. Their heat pump could also modify the speed of the lower stage compressor depending on the outdoor temperature and load conditions, and demonstrated safe and reliable operation down to evaporating temperatures of −35 °C. Cascade designs present challenges for defrosting of the outdoor coil, which some researchers have addressed by incorporating thermal energy storage [62, 63]. Several other studies have examined the use of cascade cycles for heating or water heating using an air to water design [64–69], but the application of cascade technology for centrally-ducted residential heat pumps should be explored further.

1.3.3 Multi-function heat pumps

Heat pumps referred to as "multi-function" are those that can switch their operation between two or more configurations that form different cycle types, thereby improving seasonal efficiency by employing the most suitable and efficient cycle type for the load and operating conditions at a given time [10, 58]. Several cold climate cycle modifications/types have been shown to be beneficial to heating performance only below certain ambient outdoor temperatures, including vapour injection [70], two-stage compression [71], tandem compression [14], and cascade operation [59]; therefore, reverting to a standard single-stage cycle in warmer conditions will result in higher efficiency over the entire heating season. Additionally, the ability to operate either one or two compressors in multi-function two-stage or tandem compression heat pumps, helps to increase the

modulating range of the system to meet the widely varying loads and large peak heating demands experienced in cold climates (discussed in Section 1.2.5) [72], thus reducing the need for auxiliary heating. A two-stage multi-function cold climate heat pump developed by the Hallowell brand, called the *Acadia*, used to be sold in North America, before Hallowell went out of business. The *Acadia* operated in four heating modes which were activated at certain temperature thresholds and in response to instantaneous heating demand, as described by Johnson [73]. It's function was similar to the two-stage designs presented by Bertch and Groll [23] and Tian et al. [71], which provide evidence that multi-function heat pumps can yield improved cold climate performance.

1.3.4 Related designs

No peer-reviewed studies have been identified which examine the coupling of two existing heat pump systems via a shared air-space, nor do they discuss the deliberate enclosure and preheating of air space around the outdoor evaporator unit as a method for cold-weather augmentation of heat pump performance. The closest mentions to the latter concept were those of passive "preheating" of air; Kamel and colleagues mentioned that some installers deliberately place heat pumps in sheltered areas beside exhaust air outlets [74], and Loveday described a system which used corrugated roof cladding to passively transmit and preheat air (via incident solar radiation) before delivering it to a heat pump evaporator in the attic space [75]. However, Loveday's system only operated in heating mode, and required a thermal storage tank, a secondary system to extract the energy from said tank, as well as supplementary electric heating throughout the house [75].

1.3.5 Gaps

While several reviews on cold climate heat pump technologies exist, the most recent is now four years old [28], and no reviews were identified which specifically address technological progress and performance of market-available cold climate VCASHPs for the residential sector. Thus there exists an opportunity to provide an up-to-date overview of technologies in market-available residential ccASHPs and to highlight promising innovations in the literature that are not yet being seen on the market, but that could address important challenges. With respect to the proposed add-on design, no studies were found which which attempted to enable the use of unmodified existing heat pumps in cold climates. Similarly, no studies have examined the effect of enclosing the outdoor unit of a heat pump and using air as a medium to transfer heat between the heat pump cycles in a cascade system. While cascade multi-function heat pumps have been studied in the literature with promising results for year-round performance, the two cycles have always been fully integrated into a single system, which poses challenges for defrosting. Thus, the benefits of a system which can be completely de-coupled, like the one proposed in this thesis, should be explored.

1.4 Thesis objectives

The primary objectives of this thesis are to provide useful and up-to-date insight on the scope and status of market-available cold climate technologies, and to highlight additional opportunities that could help to expedite the development and implementation of superior residential cold climate heat pumps which do not rely on auxiliary back up heating,

including a novel design composed of available, inexpensive heat pumps. To accomplish this, the following will be done:

1. Identify and analyse the technologies currently being used in market-available cold climate heat pump systems.

2. Review advancements in the literature regarding cold-climate heat pump technologies, highlighting those which are not found in market-available systems.

3. Model an existing, affordable, single-stage heat pump at varying outdoor air temperatures, for use as both the primary and secondary heat pumps in an add-on cascade heat pump model.

4. Develop a model of the add-on cascade design, to determine if it can meet the heating load of a sample home at three industry standard outdoor air temperatures, while keeping critical operating parameters within reasonable limits.

5. Determine the overall system COP of the proposed system at the three temperature conditions, and compare it to that of the same single-speed heat pump supplemented with an electric heating coil, and to published performance data for other market-available cold climate heat pump systems (supplemented with electric heating as needed).

1.5 Thesis organization

The next chapter (Chapter 2) of this thesis is the analytical review I conducted of the technologies and design strategies currently found in market-available cold climate heat pumps and the literature. Chapter 2 offers insight into the complexity and performance outcomes of current cold climate enhancements, opportunities for further improvement, and provides context and systems for comparison to the proposed add-on cascade configuration that is modelled in this study. Chapter 3 describes the development of the outdoor temperature-dependant models used to predict and compare the performance of the proposed add-on cascade design, to that of a standard heat pump with auxiliary backup (electric resistance heating), and the other market-available cold climate systems that were described in Chapter 2. Chapter 4 discusses the outcomes of the modelling, and the results of the performance comparisons performed. The final chapter (Chapter 5) offers a summary of the conclusions drawn, recommendations for future work, and a description of the contributions offered by this thesis.

Chapter 2

Market-available cold climate heat pumps

The heat pump designs which are currently being sold and marketed in Canada as "cold climate" air source heat pumps (ccASHPs) leverage many of the factors listed above in Section 1.2.3 to improve capacity and efficiency at low outdoor temperatures. A review and thermodynamic analysis of market-available, centrally-ducted cold climate residential heat pumps was conducted in order to gain a better understanding of the effectiveness, complexity, and scope of cold climate technologies currently used in the industry. Additionally, a review of existing literature highlighted innovations that have the potential to further improve cold climate heat pump performance, but are missing from market-available systems. The contents of this chapter will be submitted to *Renewable and Sustainable Energy Reviews* for publishing.

Table 1: Conversion of standard heat pump nominal sizes in SI units (kW), kBTU/hr and tons.

Tons	**kBTU/hr**	**kW**
2.5	30	8.8
3	36	10.6
3.5	42	12.3
4	48	14.1
5	60	17.6

2.1 Market analysis

The heat pumps examined in this review were chosen to provide a comprehensive representation of the VCASHP systems which have already been commercialized for residential use in cold climates, and could be suitable for the replacement of an existing centrally-ducted furnace in a single-detached home. The heat pumps identified were those with outdoor units from the product lines classified as "cold climate air source heat pumps" (ccASHPs) by Natural Resources Canada, with 70 % or more of their rated heating capacity (max output at outdoor and indoor dry bulb temperatures of 8.3 °C and 21.1 °C, respectively) retained when the outdoor temperature drops to −15 °C [121]. Only centrally-ducted heat pumps available in 8.8 kW–17.6 kW (30–60 kBTU/hr or 2.5–5 ton) nominal capacities were considered, as this represents a common capacity range for most single-detached homes. Table 1 provides SI unit conversions for reference, as industry-standard sizing units (tons and kBTU) will be used throughout this thesis.

Table 2: Market-available cold climate heat pumps highlighting key features and heating performance benchmarks.

Brand	Model	Variable Speed?	Comp. Type	Cycle Type	Refrigerant Management	Min. Temp.	Nominal OD/ID Size (kBTU/hr)	Rated[1] Capacity (kBTU/hr)	% Rated Capacity at −15 °C	COP at −15 °C
Mitsubishi	PUZ-HA** (*P-series with Hyper Heat*)	Yes [76–78]	Scroll or twin rotary [76, 79] [80, 81]	Quasi Two-stage (IHX) [76–78]	Power Receiver [76–78]	−25 °C [79–81] [82–84]	36/36 42/42	38 48	100 % 100 %	1.83–2 1.91–2.05
Trane American Standard	TRUZ*****HA[2] ASUZ*****HA [2]									
Gree	FLEXX**HP230V1AO	Yes [85]	Two-stage rotary [85]	Quasi Two-stage (*Flash Tank*) [86]	Accumulator [86]	−30 °C [86]	36/36 60/48	36 48	83 % 89 %	1.83 1.82
Kinghome	GUD**W/A KU**UHO (*Ultranixx*)						60/60	54	81 %	1.8
Tosot	TU**-**WADU (*Unix/Apex*)									
GE	AUH****ZGDA (*Connect*)									
LG	LUU**0HHV (*RED Series*)	Yes [87]	Scroll [87]	Single-Stage (*36*) Quasi Two-Stage (*IHX, 42-48*) [87]	Accumulator [87]	−30 °C [87]	36/36 [88] 42/42 48/48	37.5 [88] 48 50	100 % [88] 100 % 100 %	1.75 [88] 2.04 2.11
LG	LUU**9HV	Yes [89]	Scroll [89]	Single-Stage [89]	Accumulator [89]	−20 °C [89]	36/36	40	87 %	1.83
LG	LUU**8HV	Yes [89]	Twin rotary [89]	Single-Stage [89]	Accumulator [89]	−20 °C [89]	36/36	40	75 %	2
Daikin	RZQ**TAVJU (*Sky Air*)	Yes [90]	Swing (rotary) [90]	Single-Stage Indirect Vapour Injection [90]	Accumulator [90]	−20 °C [91]	30/30	34	100 %	2.09
Samsung	AC0**JXSCCH/AA (*Max Heat*)	Yes [92]	Twin rotary [93]	Single-Stage [93]	Accumulator [93]	−25 °C [93]	30/30 36/36	32 40	107 % 100 %	1.84 1.8
Samsung	AC0**JXADCH/AA	Yes [92]	Twin rotary [94]	Single-Stage [94]	Accumulator [92]	−20 °C [94]	30/30	32	84 %	1.98
Bryant	284ANV0** (*Evolution*)	Yes [95]	Rotary [96]	Single-Stage [95]	Accumulator [95]	−23.3 °C [95]	36/var.	34–35	79 %–80 %	2.02–2.23
Carrier	25VNA4** (*Infinity*)									
Bryant	280ANV0** (*Evolution Extreme*)	Yes [97]	Scroll [97]	Single-Stage [97]	Accumulator, Charge Compensator [97]	−26.1 °C* [98]	36/var. 48/var. 60/var.	33.4–35.6 45.5–46.5 55.5	70 %–94 % 83 % 72 %	2.06–2.2 2.12–2.24 1.99
Carrier	25VNA0** (*Infinity*)	Yes [99]	Scroll [99]	Single-Stage [100]	Accumulator, Charge Compensator [99]	−34.4 °C* [99]	36/var. 48/var. 60/var.	33.4–35.7 45.5–46.5 55.5	70 %–94 % 83 % 72 %	2.06–2.2 2.12–2.24 1.99
Bryant	38MAQB30R–3 (*Preferred*)	Yes [101]	Rotary [102]	Single-Stage [102]	Accumulator [102]	−25 °C [102]	30/var.	29.2–30.2	70 %–76 %	2.34–2.53
Carrier Payne	(*Performance*) (*Mid-Tier*)									
Fujitsu	FO**20RVJCAB	Yes [103]	Scroll [103]	Single-Stage [103]	Accumulator [104]	−23 °C [103]	36/60 48/60	33 42	96 % 83 %	2.25 2.14
Fujitsu	AOUG**LMAS1	Yes [105]	Twin rotary [105]	Single-Stage [105]	Accumulator [105]	−20 °C [105]	36/36	42	78 %	2.02
Rheem	RP20**BJV (*Prestige*)	Yes [106]	Scroll [106]	Single-Stage [107]	Accumulator [106]	−23 °C [107]	36/60 48/60	33 42	96 % 83 %	2.25 2.14
Ruud	UP20**BJV									
Ecoer	EODA18H-4860 (*ESI Ultra*)	Yes [108]	Rotary [108]	Single-Stage [109]	Accumulator [109]	−19.4 °C [110]	48–60/36	36	72 %–77 %	2.08–2.1
Bosch	BOVA-**HDN1-M20G (*IDS Premium*)	Yes [111]	Rotary	Single-Stage [111]	Accumulator [111]	−20 °C [111]	60/48 60/60	48 56	73 % 71 %	2.26 2.38
Bosch	BOVB-**HDN1-M18M (*IDS Plus*)	Yes [112]	Rotary [112]	Single-Stage [113]	Accumulator [113]	−15 °C [112]	60/36	35.2	79 %	2.05
Zephyr	ZE-**HPA	Yes [114]	Rotary [114]	Single-Stage [115]	Accumulator [115]	−25 °C [115]	36/36	36	81 %	1.93
Azur	AZ-**HPA									
Haxxair	HVHD-**E2D	Yes [116]	n.s.	n.s.	n.s.	−30 °C [116]	36/36	36	81 %	1.93
American Standard	4A6V80**A1 (*Platinum 18*)	Yes [117]	Scroll [117]	Single-Stage [117]	n.s.	−23.3 °C [118]	48/48	41	70 %	1.93
Trane	4TWV80**A1 (*TruComfort XV18*)						60/48	52.5	77 %	1.82
American Standard	4A6V00**A1 (*Platinum 20*)	Yes [119]	Scroll [119]	Single-Stage [119]	n.s.	−23.3 °C [120]	60/48	52.5	77 %	1.82
Trane	4TWV00**A1 (*TruComfort XV20i*)									

Table 2 lists the heat pump product lines (outdoor unit models) examined and, for each, presents pertinent information about design, components, and operation, as well as performance benchmarks for comparison. Similar systems sold under more than one name/model have been grouped, and their descriptions merged for simplicity. The model names typically contain numbers (replaced with stars in Table 2) that indicate the so-called "nominal capacity" of the heat pump in units of kBTU/hr. However, it can be seen that the rated heating capacity often varies from those values, and may change depending on which indoor unit is paired with the outdoor unit in question. This section is organized according to the different technological developments demonstrated by the heat pumps, which explain their superior cold climate performance.

2.1.1 Compressor technology

Selection of a suitable compressor is a critical part of cold climate heat pump design because the compressor is the primary driver of power consumption and refrigerant flow rate (and thus heating capacity), and it imposes temperature limitations that can lead to shut-off in cold conditions [11]. Cold climate heat pumps rely on compressor technology to expand the operating temperature range, and mitigate short-cycling. Additionally, for some of the highest-performing models, a custom-designed compressor is needed to facilitate more complex cold climate modifications that are employed. This section discusses types and features of compressors being utilized in the market-available cold climate heat pumps in Table 2.

Compressor type

The compressors being used in market-available VCASHPs for cold climates are either scroll or rotary (rolling piston) type compressors (and modified versions of these), rather than reciprocating compressors, as seen in Table 2. This is common across most of the residential heat pump industry, because both scroll and rotary compressors are smaller in size, last longer, and generate less vibration and noise than reciprocating compressors [122], making them attractive for residential applications in any climate. However, the choice of compressor type is more critical for heat pumps in cold climates due to the fact that the reciprocating compressor is susceptible to a drastic reduction in volumetric efficiency and mass flow rate at the low evaporator pressures that occur when heating in cold outdoor air conditions [8]. At the start of each piston stroke in a reciprocating compressor, the gas remaining in the clearance volume of the cylinder expands until its pressure drops below that of the evaporator. Thus, lower evaporator pressure leads to greater expansion of the clearance volume, and a smaller volume remaining for incoming refrigerant to fill during each stroke [8]. This decrease in intake volume also coincides with a decrease in the density of the refrigerant at low evaporator pressures, thereby further reducing the mass flow rate and the resultant system heating capacity. By contrast, scroll and rotary compressors (shown in Figures 2.1(a) and (b)) have no clearance volume that effects the flow rate [122, 123], so heat pumps with these types of compressors exhibit more stable capacity amid varying outdoor temperatures [8]. Of the 22 distinct ccASHP systems examined, 8 use only scroll type, and 12 use only rotary type compressors. The Mitsubishi *P-series with Hyper Heat* heat pumps use either a scroll or a twin rotary compressor, depending on the exact unit.

Variable compressor speed

Variable-speed compressors are standard in cold climate heat pumps, as they are used in all of the units listed in Table 2. By increasing compressor speed when the outdoor temperature is colder, variable-speed compressors can counteract the effects of decreased refrigerant density at low evaporator pressures, that would otherwise reduce mass flow rate and heating capacity (as described in Section 1.2.5) [124]. Additionally, newer regulations allow for variable-speed heat pumps to be sized to supply a larger portion of the peak home heating demand [125], thereby reducing reliance on supplementary auxiliary heating [26, 126]. Larger variable-speed heat pumps can avoid the short-cycling issues described in Section 1.2.5 because they can reduce compressor speed during periods of lower demand [126, 127]. At loads within the variable capacity range of the system, these heat pumps can run continuously, thereby eliminating COP degradation due to cycling, and improving humidity and temperature control in the home [24, 26].

Variable-speed compressors can more efficiently match varying loads by having smooth modulation [128] over a wide range of speeds. Smooth variation of compressor speed is commonly achieved using a variable-frequency inverter drive to control the speed of the compressor motor Where there are larger variations in load throughout the year, such as in a climate with very cold winters (large winter heating loads), and mild summers (small summer cooling loads), the desired compressor modulating range is increased. Furthermore, in cold climates, the use of increased compressor speed to compensate for decreasing suction density at cold temperatures, further widens the desired modulating range. Due to the role of refrigerant flow in compressor lubrication and motor cooling in hermetic compressors (typical for residential heat pumps), expanding the modulating

range poses design challenges [129, 130]. Industry manufacturers are working to widen the effective range of speeds that can be performed by their variable-speed compressors. For instance, the *R1* scroll compressor featured in the LG *RED* series, claims 50 % higher maximum frequency than a traditional scroll compressor [131].

Typically, heat pumps with variable-speed compressors also have variable or multi-speed indoor and outdoor fans, which can further improve system efficiency by modulating operating speed along with changes in compressor speed to match the required heating output [132]. Modification of fan speed directly affects system capacity since it changes the heat transfer coefficients at the condenser and evaporator heat exchangers. An increase in indoor fan speed can improve efficiency by lowering the required condenser temperature, but may result in discomfort for building inhabitants, so some systems have different modes to prioritize comfort over efficiency [124]. Air flow rates can also influence both system COP and the effectiveness of air distribution through ductwork [133].

Variable-speed heat pumps offer several additional advantages over single-speed and two-speed systems. For example, they show improved steady state performance at partial loads [127, 128, 134] making them more efficient than single-speed systems even without considering on-off cycling. Furthermore, they generate less noise at most load levels, and can use higher startup speeds to accelerate desired temperature changes [135]. For these reasons, most heat pump manufacturers now offer high-performance lines of variable-speed heat pumps, marketed for their superior efficiency and quietness. However, variable-speed inverter drives add complexity and cost [14, 72, 136], so single-speed, and two-speed heat pumps are still commonly selected as the economical option in contexts where their performance is considered satisfactory, such as in milder climates.

Varying compressor speed can increase seasonal efficiency, and improve heating capacity at low outdoor temperatures, but it cannot solve the issues of decreased COP and high compressor discharge temperature that occur at low outdoor air temperatures (explained in Section 1.2.5). As a result, additional cold climate features continue to be developed, and are already being implemented in several of the market-available heat pumps in Table 2. The most significant feature is the inclusion of a vapour injection circuit.

Compressors with vapour injection capability

A quasi two-stage cycle, as described in detail in Section 2.1.2 below, enables heat pumps to have increased performance but requires a compressor that is capable of incorporating vapour injection, which is usually more expensive [137]. These modified compressors allow for additional vapour to be injected through a secondary port partway through the compression process. The scroll compressor, with its multiple compression chambers, is well-suited to the incorporation of one or more injection ports [28], and early vapour injection research focused heavily on this compressor type [39,70]. Figure 2.1(a) shows an example of a scroll compressor with a vapour injection port for quasi two-stage operation. LG uses their injectable *R1* scroll compressor to facilitate a quasi two-stage cycle in the 3.5 and 4 ton sizes of their *RED* heat pump series, found in Table 2. Similarly, the scroll compressor used in some models of the Mitsubishi *P-Series with Hyper Heat* has vapour injection capability.

The twin (two-stage) rotary compressor is also well-suited to vapour injection, since it is possible to feed in additional vapour at an intermediate pressure during the transition

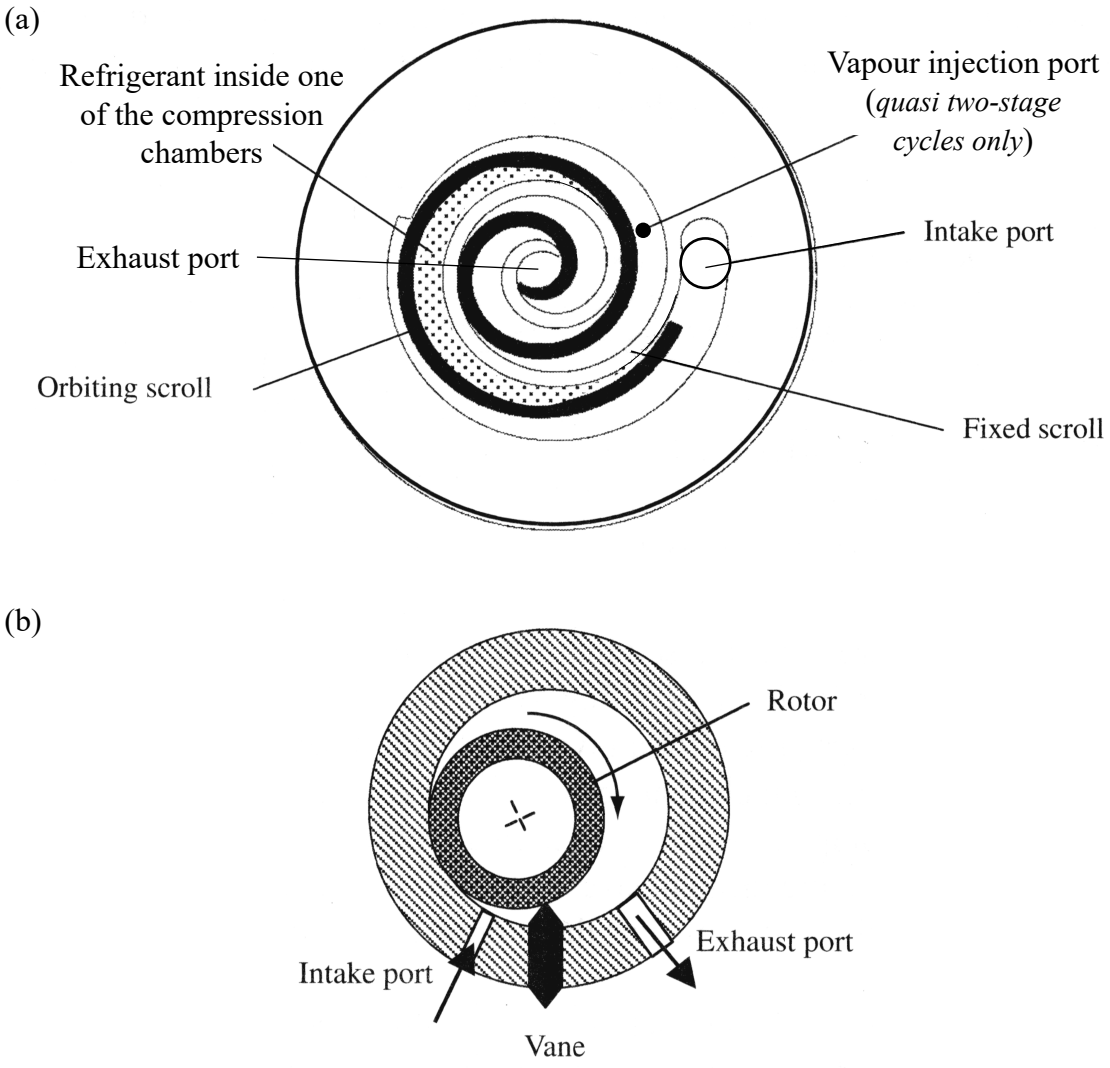

Figure 2.1: Overhead cross-sectional view of (a) a scroll compressor with vapour injection capability and (b) a single rotary (rolling piston) compressor cylinder. Adapted from Mitchell and Braun [8].

between the two sequential compression stages/cylinders [138]. However, this differs from vapour injection in a scroll compressor, in that the vapour is not added directly into a compressor chamber, but instead mixes with partially compressed vapour as it moves between two vertically stacked rotary compression cylinders (like the cylinder

shown in Figure 2.1(b)) [70]. The PUZ-HA36NHA5 model of the Mitsubishi *P-Series with Hyper Heat* (also sold under the Trane and American Standard labels), uses a twin rotary compressor with vapour injection to create a quasi two-stage cycle. The Gree heat pumps in Table 2 (and similar systems under the Kinghome, GE, and Tosot names) also include vapour injection into a two-stage rotary compressor.

2.1.2 Quasi two-stage cycles

A quasi two-stage cycle is used in several cold climate heat pump models including the Mitsubishi *P-Series* with *Hyper Heat* (and similar Trane, and American Standard models), Gree *Unix* and *Flexx* series (and similar units sold under different names), as well as the 3.5 and 4 ton sizes of the LG *RED* series, as seen in Table 2. This cycle type involves an additional process that converts a portion of the liquid refrigerant into vapour after the condenser (without passing it through the evaporator), and then this vapour is re-injected into the system's compressor, part-way through the compression process, as shown in Fig. 2.2 (a) and (b). The result is similar to that of systems referred to as actual "two-stage" cycles, which have two separate compressors, but the use of only one compressor makes the system simpler, less expensive, and more reliable than a two-stage system [6]. There are several benefits of the quasi two-stage cycle for heating, compared to a standard single-stage cycle: increased heating capacity ($\dot{Q}_{\mathrm{H}}$), reduction of compressor discharge temperature (T_3), reduced compressor work ($\dot{W}_{\mathrm{C}}$), and increased specific heating capacity (q_{L}) of the evaporator [39]. All of these benefits directly counteract the negative effects discussed in Section 1.2.5 that occur due to low

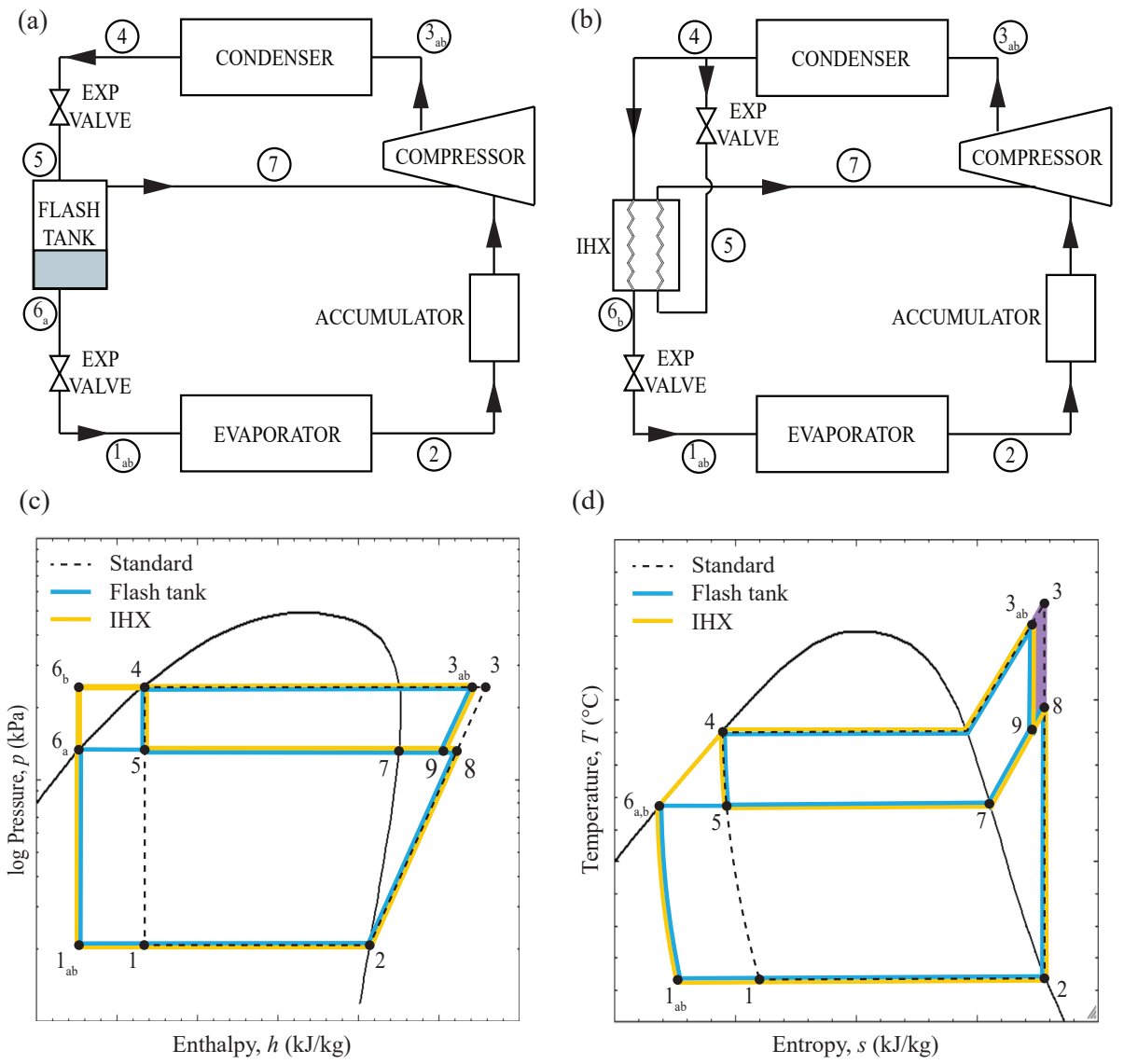

Figure 2.2: (a) Flash tank method selected component layout, (b) IHX method selected component layout, (c) pressure-enthalpy ($p-h$) diagram and (d) temperature-entropy ($T-s$) diagram showing the thermodynamic heating cycle of a quasi two-stage heat pump using both methods (flash tank blue, IHX yellow), with a standard cycle for comparison (dashed line).

evaporator pressure when heating at low outdoor temperatures. There are two main methods by which vapour is extracted from the liquid line for later reinjection: the flash tank method, and the internal heat exchanger method (IHX, also referred to as a subcooler or economizer) [28]. Fig. 2.2 shows the layout of key components for each of these methods, along with the p-h and T-s diagrams of the resulting quasi two-stage cycles. This section explains the thermodynamic effects of the extraction and injection processes in quasi two-stage cycles and the corresponding performance benefits.

Vapour extraction methods

The flash tank vapour extraction method, shown in Fig. 2.2(a), (c), and (d) (blue line), is used in the Gree (and similar) cold climate heat pumps listed in Table 2. In a heat pump using this method, the liquid refrigerant leaving the condenser (point 4) is first expanded to an intermediate pressure, using an additional expansion valve, and the resulting liquid/vapour mixture (point 5) is then separated in a component known as a flash tank. The vapour portion (referred to as "flash", point 7) is diverted through a pipe near the top of the tank which leads to the compressor's vapour injection port, while the liquid portion (point 6_a) drains through a pipe at the bottom of the tank, leading to the second (primary) expansion valve and then the evaporator. Fig. 2.2 shows how the flash separation process (point 5 to points 6_a and 7) results in the liquid entering the evaporator (point 1_{ab}) with a lower specific enthalpy than it would in a standard cycle (point 1), thus increasing the specific heating capacity (q_L) and two-phase heat transfer area, of the evaporator [39]. Since the flash tank method extracts vapour by expanding refrigerant to a liquid/vapour mixture state, the resulting vapour is very close

to saturation [39], and the flow rate of injected vapour is determined by the intermediate pressure in the flash tank. The former is advantageous for maximizing the benefit at reinjection, which is discussed in more detail in Section 2.1.2, but the latter means there is limited control over the flow rate of vapour headed to the compressor [39].

The Mitsubishi *P-Series* and LG *RED* (3.5 and 4 ton) heat pumps listed in Table 2 use the internal heat exchanger (IHX) method for vapour extraction. In this type of system, the liquid line is split into two parts after the condenser, one of which is sent through an additional expansion valve to a lower intermediate pressure and temperature, as shown in Fig. 2 (b) and the yellow line in Figs. 2 (c) and (d). Both parts then pass through an IHX where the hotter refrigerant (still at condenser pressure) is further subcooled (points 4-6_b) as it transfers heat to the cooler refrigerant (at intermediate pressure), causing it to vapourize (points 5-7). In a quasi two-stage cycle, this vapour would then be injected into the compressor's vapour injection port. As in the flash tank method, the liquid line exiting the IHX has lower enthalpy when it passes through the second expansion valve (6-1_{ab}) than in the standard cycle, thereby increasing the specific heating capacity (q_L) and two-phase heat transfer area of the evaporator [39]. The vapour leaving the IHX is typically more superheated than that extracted using a flash tank [39, 139], which is not ideal for reinjection, as explained in Section 2.1.2. However, the injected vapour flow rate, and degree of superheat, may be controlled using the first expansion valve [39, 140]. The IHX method is considered more complex and expensive than the flash tank method, but it also offers greater flexibility around the intermediate pressure [39, 140], and better control of the degree of superheat and flow rate of the resulting injection stream [14]. Ma and Zhao [139] compared a flash

tank system to an IHX system with similar reinjection methods and found that the flash tank system showed better performance and was simpler and easier to construct. This comparative performance outcome was supported by other studies [140, 141]. The main heating performance benefits of these vapour extraction methods are realized upon reinjection of the vapour into the system, which will be described next.

Quasi two-stage vapour injection

After the vapour has been extracted using one of the above methods, the quasi two-stage cycle requires reinjection of the vapour into the compressor partway through the compression process (as seen in Fig. 2.2), where it mixes with the partially compressed vapour inside (point 8) to yield point 9. As outdoor temperature drops, injecting more refrigerant into the compressor at an intermediate pressure can help maintain a higher flow rate in the condenser compared to a standard cycle, by compensating for the reduction in the mass flow rate entering the compressor at its primary suction port (explained in Section 1.2.5) [142]. This allows for higher heating capacity ($\dot{Q}_{\mathrm{H}}$) at cold temperatures without increasing the compressor speed or volume [138]. Furthermore, Fig. 2.2(d) shows that the temperature inside the compressor drops from point 8 to point 9 when the colder injected vapour (point 7) mixes with the partially-compressed vapour (point 8), which is similar to the effect accomplished by "intercooling" [23] or "desuperheating" [143] in two-stage systems. The result is that the discharge temperature (point 3_{ab}) is also reduced, and the portion of the specific work (w_{C}) represented by the purple shaded area in Fig. 2.2(d), is eliminated. This mitigates the high discharge temperature issues that result from cold climate operation (described above in Section 1.2.5) thereby potentially expanding the

heat pump's operating temperature range, and increasing the system COP. The benefits of the quasi two-stage cycle over a standard single-stage cycle for cold climate performance are well-documented in the literature [9,14,39,70,140,144,145]. Wang et al. [140] examined both the flash tank and IHX quasi two-stage system types, and found that both showed an increase in COP and capacity greater than 15 % and 25 % respectively, compared to a single-stage standard cycle at an outdoor temperature of −17.8 °C. Although both extraction methods described in Section 2.1.2 yield benefits, they have different advantages and disadvantages, which make a direct comparison complicated.

A comparison of the performance of quasi two-stage heat pumps with flash tank vapour extraction to those with IHX vapour extraction, must consider the properties and flow rate of the vapour that is injected into the compressor. When flash tank extraction is used, the quantity and quality of the resultant vapour is determined by the intermediate pressure, since all of the vapour in the flash tank is inherently saturated and flows directly to the compressor. This means that injection flow control is not needed, nor possible, and, since saturated vapour is the coldest vapour at a given pressure, it maximizes the intercooling effect that can be achieved upon injection. The downside to the flash tank method is that there is limited control over the injection flow rate, which can lead to compressor flooding at high speeds [141], or the over/under feeding of vapour under widely ranging outdoor temperatures [14]. By contrast, the IHX method has superior control over the injection stream [14,141] since this stream has its own dedicated expansion valve, and with it a wider range of injection operating parameters can be achieved [9,39]. However, systems that use the IHX method tend to inject vapour that is more superheated than those with flash tank extraction, which results in comparatively

higher compressor work and discharge temperatures for IHX systems [9, 39]. For this reason, most studies have found that systems with flash tank extraction perform better than those with IHX extraction [9, 39, 139–141], although theoretically, the two methods should be able to achieve similar performance if the injection parameters are the same (specifically the intermediate pressure and degree of superheat) [39]. Flash tanks are also less expensive than the heat exchanger needed for IHX extraction [14]. In either case, precise and strategic control of intermediate pressure, injection mass flow rate, injection superheat (IHX only), and compressor speed, are required to ensure a net benefit from a quasi two-stage cycle at varying temperatures and loads [39, 146].

2.1.3 Indirect refrigerant injection

Indirect refrigerant injection, used in the Daikin *Sky Air* series heat pumps in Table 2, has been regarded as a simpler and less expensive method to address some of the same performance issues improved by quasi two-stage vapour injection [137, 142]. In this method, refrigerant reinjection takes place before the compressor, as shown in Fig. 2.3, typically either into or before the accumulator (dashed and dotted lines respectively), thus allowing for the use of a simpler, non-injectable compressor [137]. While both of the extraction methods described in Section 2.1.2, may be used to derive vapour for indirect reinjection, the Daikin *Sky Air* series heat pumps use an IHX, and then inject the resulting vapour into the suction line before the accumulator (similar to the dotted line in Fig. 2.3). The 30 kBTU Daikin system shown in Table 2 shows a high heating capacity and high COP at an outdoor temperature of −15 °C compared to the other

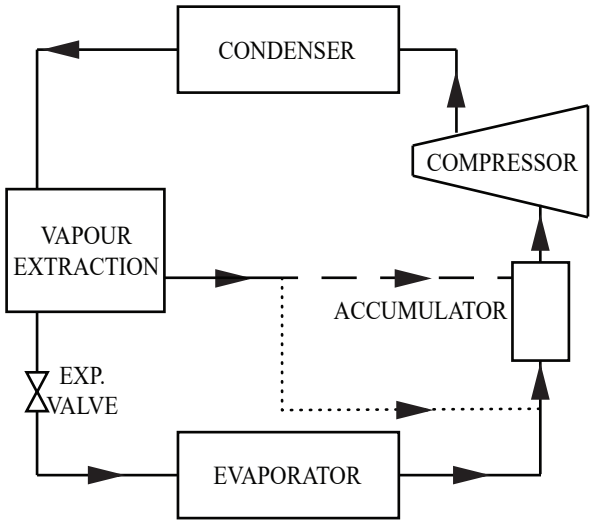

Figure 2.3: Diagram of key components of a single-stage heat pump with indirect vapour injection into (dashed line) or before (dotted line) the accumulator.

market-available cold climate heat pumps. Only a few studies have examined the effect of indirect vapour injection on heat pump performance. Roh and Kim [142] studied a variable-speed design with a scroll compressor and IHX vapour extraction setup similar to that shown in Fig. 2.2 (b), but where injection took place into the accumulator. Lai et al. [147] and Liu et al. [137] both examined experimental designs with vapour extraction using gas-liquid separation (such as a flash tank), where the resulting vapour was sent through a third expansion valve to bring it close to evaporator pressure before injecting it into the suction line. The design by Liu et al. did not include an accumulator [137]. Lai et al. [147] found that, within a suitable range of intermediate pressure and flow rates, improvements could be seen in heating capacity, COP, and power consumption, particularly at outdoor temperatures between 15 °C and 25 °C, and when the degree of superheating at the exit of the evaporator was set to be 0 °C. Similarly, Roh and

Kim [142], and Liu et al. [137] both found that, within certain ranges of injection ratios ($\dot{m}_{\text{inj}}/\dot{m}_{\text{cond}}$), condenser mass flow rate increased, compression ratio decreased, and that the decreased compression ratio resulted in lower discharge temperatures and reduced power consumption. However, when comparing indirect vapour injection to quasi two-stage injection, Roh and Kim [142] found that quasi two-stage generally showed superior performance benefits, particularly if improved heating capacity was the objective. It should be noted that none of the system designs in the literature replicated the one used in the Daikin heat pumps in Table 2 (which use a different IHX extraction configuration referred to as "post-expansion subcooler" by Jian et al. [143]), nor did they specifically examine cold climate heating conditions (the lowest outdoor temperature tested by Roh and Kim [142] , Liu et al. [137], and Lai et al. [147] was −8.3 °C, −5 °C, and 5 °C, respectively). Thus, the apparent success of the Daikin *Sky Air* ccASHPs shows that indirect injection has promise for cold climate heat pumps and indicates that more work can be done to understand and harness the heating performance benefits it offers to this context.

2.1.4 Refrigerant management

One common refrigerant management strategy is to employ accumulators, which are gas-liquid separators located before compressors in heat pump systems (as seen in Fig. 2.2 (a) and (b)) that are primarily used to prevent liquid refrigerant from entering the compressor [14] (causing problems described in Section 1.2.5) and allow for controlled reintroduction of compressor oil. An accumulator is present in at least 19 of the 22 distinct cold climate

heat pump product lines listed in Table 2, which is consistent with the fact that there is an increased risk of liquid entering the compressor in cold climate operation due to frequent mode changes and the potential for incomplete vapourization in the evaporator (described in Section 1.2.5). Additionally, a strategically-sized accumulator can serve as a refrigerant reservoir, which passively removes excess refrigerant from circulation during conditions or modes with lower refrigerant needs [16, 72, 148] to accommodate the wide variation in outdoor temperatures experienced in cold climates (explained in Section 1.2.5).

A component known as a charge compensator is used in the Bryant *Evolution* (280ANV) and Carrier *Infinity* (25VNA0) series heat pumps to manage variation in desired refrigerant charge (discussed in Section 1.2.5) [97, 100]. A charge compensator is a hollow vessel that encases the sealed refrigerant line exiting the outdoor heat exchanger (the

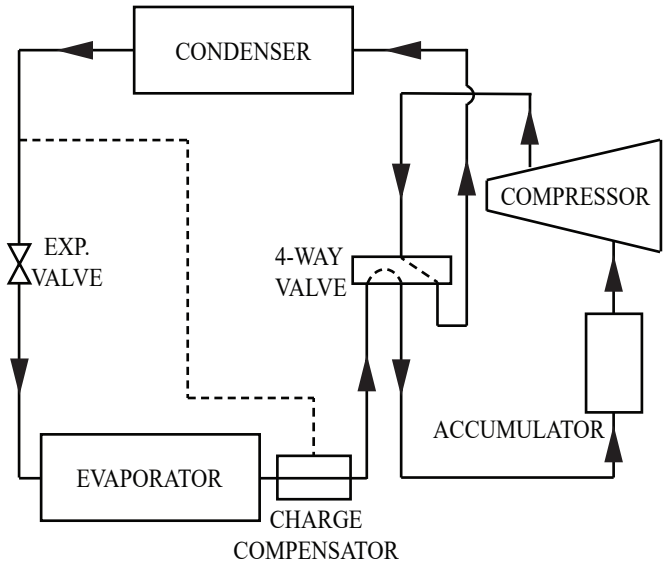

Figure 2.4: Diagram showing the location of the charge compensator in a single-stage standard heat pump cycle with an accumulator, in heating mode.

evaporator in heating mode), which is filled or drained by a pipe connected to the liquid line exiting the indoor heat exchanger (the condenser in heating mode), as shown in Fig. 2.4 [21, 97]. The temperature of the inner sealed line will cause refrigerant in the charge compensator to either condense (pulling refrigerant into the vessel for storage), or vaporize (pushing refrigerant back out into circulation). Other heat pumps have devices for refrigerant management as well, for example many Mitsubishi heat pumps include an additional expansion valve and a component called a "power receiver" which respond to changes in the outdoor temperature [149] and control the optimal refrigerant level [**?**]. The inclusion of components like a charge compensator and power receiver allow these heat pump systems to maintain more optimal operating parameters in cold climates.

A strategy which increases the cold climate capacity and performance of some of the market-available cold climate heat pumps is to change the relative size of the indoor and outdoor units being paired, but this also increases the need for a good refrigerant charge management strategy. Each outdoor unit of the Bryant/Carrier heat pumps in Table 2, can be paired with several different indoor units of various sizes (nominal sizes shown as "var." in the table), yielding a wide range of capacity and performance. In many cases, the pairing of a smaller indoor unit with an outdoor unit capable of a higher capacity results in a system which retains a higher percentage of its rated capacity at a −15 °C outdoor temperature compared to other systems in the same product line with equally-sized indoor/outdoor units. This can be observed in Table 2 in the heat pumps by Gree (and similar), American Standard (*XV18* series), Trane (*Platinum 18* series), and Bosch (*IDS Premium* series). Similarly, the primary difference between the *ESI Ultra* (3 ton only) system from Ecoer in Table 2, and their regular *ESI* series (which

uses the same units, but does not qualify as a cold climate series), is that the *ESI Ultra* pairs the larger 48–60 kBTU outdoor unit with the 36 kBTU indoor unit. Among other variables, heat exchanger size and refrigerant line diameters often differentiate the unit sizes. Thus, changing the size of one of the units may change both the internal volume of the system, and the location of that volume, thereby impacting system pressures and the desired refrigerant charge of the system during different modes. One strategy to address these changes, is the charge compensator found in each outdoor unit of the Bryant 280ANV0 and Carrier 25VNA0 heat pumps in Table 2, which is sized to accommodate the difference in charge between the heating and cooling modes, as well as the difference in required charge between the smallest and largest compatible indoor unit [97, 100]. In heat pumps that do not have a charge compensator or power receiver, management of charge is accomplished through other strategies involving accumulators. This highlights the importance of refrigerant management strategies in cold climate heat pump design.

2.1.5 Defrosting

During cold climate operation, defrosting of the outdoor coil is commonly accomplished using the reverse cycle method, which involves periodically actuating the 4-way valve (shown in Fig. 2.4) to switch the flow of refrigerant from the heating mode to the cooling mode configuration. The frosted outdoor coil then becomes the condenser and receives hot high-pressure refrigerant from the compressor, which melts the frost on the coil [150]. The reverse cycle method is used by all of the market-available heat pumps in Table 2 that specified their defrost strategy, and has been identified as the most common defrost method for air source heat pumps [10, 20, 21, 151]. Eight of the systems examined also

mention the inclusion of a base pan heater coil, which ensures that meltwater drains freely out of the basepan holes, to prevent an accumulation of ice backing up onto the heat exchanger. The exact duration, frequency, transition sequence, and fan behaviour demonstrated by each heat pump's defrost cycle vary depending on the control system and programming used by the heat pump manufacturer. However, typically the outdoor fan is shut off during defrosting [151] since heat transfer to the outdoor air is not desired and would slow the melting process. Many market-available systems also turn off the indoor fan during defrost mode in order to avoid blowing cold air into the home [22]. Those systems which leave the indoor fan running (Fujitsu FO**20RVJCAB, Rheem/Ruud *Prestige*, American Standard *Platinum 18*/Trane *XV18* and American Standard *Platinum 20*/Trane *XV20i*) offer a standard or optional electric heating coil which warms the supply air delivered to the home during defrost mode, and also serves as the auxiliary heating system. A study by Kegel et al. [152], demonstrated that shutting off the interior fan to avoid the need for this auxiliary electric heating during defrosting can result in significant energy savings, despite the fact that it increases the time needed to defrost fully. Zhiyi et al. [21] demonstrated that the inclusion of a charge compensator (as in the Bryant and Carrier heat pumps described in Section 2.1.4) resulted in faster and more effective defrosting, since the refrigerant charge increased when the heat pump is switched to defrost mode, allowing the system to quickly achieve a high discharge pressure (and corresponding high temperature). Defrost cycles are necessary in cold climate heat pumps, but they interrupt heat pump operation and substantially reduce seasonal efficiency; therefore, innovations that prevent or slow frost accumulation or improve defrost speed and efficiency can enhance overall cold climate performance.

2.2 Opportunities

Heat pumps have the inherent potential to deliver superior electrified heating in cold climates, particularly if they can be made to reliably and efficiently meet home heating demands at all winter temperatures, without dependence on a less efficient or higher polluting auxiliary heating system [72]. While some companies are making good progress toward this objective, the majority of market-available cold climate heat pumps still exhibit a significant loss of heating capacity at cold temperatures, and their minimum operating temperatures are above the minimum outdoor temperatures experienced in many cold climates (as seen in Table 2). Meanwhile, there are numerous technologies found in the literature that have yielded promising results for increasing the cold climate performance of air source heat pumps, that are not yet being applied in market-available systems. Additionally, the comparison strategies and industry performance metrics currently used make it difficult to assess the suitability of available and proposed systems for cold climate applications, and to predict comparative operational costs and installed performance. This section will highlight opportunities to improve market-available cold climate VCASHPs for residential heating, by providing an overview of a variety of promising innovations and relevant research gaps that merit further investigation or application. It is organized according to the following sections: alternative refrigerants, cycle types and modifications, refrigerant charge management techniques, compression innovations, expansion loss recovery, frost management, and comparative performance evaluation.

2.2.1 Alternative refrigerants

All of the market-available heat pumps in Table 2 use the current industry standard R410a refrigerant [153], yet ongoing research suggests that other refrigerants could offer equivalent or superior cold climate performance, while posing less of a threat to the environment. The relatively high global warming potential (GWP) of R410a (GWP = 2088 [153]), makes leaks and improper disposal (common in residential units) a concern, motivating research into low GWP alternatives [154–157]. While it has been suggested that reducing the total quantity of refrigerant used could help alleviate this issue [18], switching to an environmentally benign refrigerant provides a more definitive solution. A study by Hakkaki-Fard et al. [158] identified several refrigerant mixtures which, when used as direct replacements for R410a, could improve cold climate performance of a standard air source heat pump, without the need for changes to the mechanical components. Several other studies have demonstrated the influential role that refrigerant choice plays in the performance and optimization of various heat pump designs [9, 143, 159], as well as heat exchanger designs [160]. Lorentzen and Petterson [161] suggested that substances such as CO_2, which are ubiquitous and naturally-occurring, should be prioritized as refrigerants in order to avoid recurring industry overhauls/shifts necessitated by unanticipated negative impacts of refrigerant escape. Thus, there are opportunities to improve cold climate heat pumps by switching to refrigerants which can enhance performance while also reducing the environmental impacts.

Carbon dioxide (CO_2 or R744) has gained a great deal of attention as a refrigerant for heat pumps, since it is naturally-occurring, non-toxic, non-flammable, has a low global

warming potential (GWP = 1), as well as high volumetric heat capacity, excellent heat transfer properties, and relatively high density and saturation pressure at low temperatures [161]. Bansal [46] describes how the thermo-physical properties of CO_2 also lead to superior phase change behaviour and distribution in the evaporator heat exchanger at low temperatures, compared to other refrigerants. CO_2 has a low critical point of 31.1 °C [162], so much of the CO_2 heat pump research focuses on the transcritical cycle, where heat rejection occurs in the gas phase above the critical point, and thus involves a large temperature change (known as temperature glide) without condensation [163]. The transcritical CO_2 cycle takes place at much higher pressures than typical heat pump cycles with other refrigerants, so additional safety precautions are needed [46]. Furthermore, it has a larger pressure ratio between the heat absorption and heat rejection heat exchangers, so expansion losses are greater and thus the potential benefit from integrating expansion loss recovery strategies (discussed later in Section 2.2.5) is high [164,165]. Several review papers have been published regarding developments in transcritical CO_2 heat pumps [46,163,164,166], and some have focused specifically on CO_2 heat pumps for cold climates [167,168], and low temperature refrigeration [46]. CO_2 has shown promising performance as a refrigerant in both subcritical [46] and transcritical [165] low-temperature cascade refrigeration systems, as well as in supercritical cycles for vehicle air conditioners and heat pump water heaters [163].

Another refrigerant group under study for use in cold climate heat pumps is zeotropic refrigerant mixtures, defined as those that demonstrate temperature glide during phase change at constant pressure [169]. Technically R410a is a slightly zeotropic refrigerant, but it shows only a very small temperature glide (< 0.05 °C [169]) at relevant saturation

pressures, which has minimal impact. Hakkaki-Fard et al. conducted a series of studies demonstrating the benefit of zeotropic mixtures with substantial temperature glide (at least 5 °C) for cold climate heating applications [153, 158, 170, 171], which are summarized in a review by Zhang et al. [28]. It has been suggested that a counter flow heat exchanger configuration is preferable when using zeotropic refrigerants [169], but it has also been shown in some scenarios that the heat exchanger configuration had little effect on the performance of the refrigerant mixtures examined [170]. Zuhlsdorf [172] emphasized the importance of the boundary conditions (source and sink temperature glide, and system temperature lift) on determining which zeotropic mixtures will increase performance. Additionally, Roskosch et al. [173] performed a study which showed that the compressor efficiency of the refrigerant mixture had a dominating impact on overall cycle performance that must not be overlooked. Further experimental studies of promising refrigerant mixtures specifically for centrally-ducted cold climate residential heat pumps would be useful to help better understand the performance effects of refrigerant temperature glide in the heat exchanger types and boundary conditions relevant to these systems.

2.2.2 Cycle types and modifications

Modifying the heat pump cycle is a common strategy used to avoid or counteract the challenges that standard VCASHP cycles experience at cold outdoor air temperatures, described in Section 1.2. The market-available ccASHPs examined in this paper utilize two different cycle types, single-stage and quasi two-stage; however there are several

other advantageous cycle types and modifications that will be described in this section including suction internal heat exchangers, improved refrigerant injection cycles, two-stage cycles, cascade cycles, autocascade cycles, multi-stage cycles, and multi-function heat pumps.

Suction internal heat exchangers

A performance improvement strategy described in the literature is to use a suction internal heat exchanger (SIHX) to transfer heat from the liquid line exiting the condenser, to the suction line exiting the evaporator [29]. The effect of this feature is that, as with the IHX described in Section 2.1.2, point 4 in Fig. 1.4 moves to the left, which ensures that only subcooled liquid enters the expansion valve [29], reduces expansion losses (described further in Section 2.2.5), and lowers the enthalpy at point 1, thereby increasing the specific heating capacity inside the evaporator [39]. At the same time, point 2 in Fig. 1.4 also moves to the right as it absorbs heat in the SIHX, which helps to ensure that the refrigerant entering the compressor has fully vapourized and achieved sufficient superheat [29]. This can be beneficial in cold climates when vapourization can be incomplete during cold outdoor conditions (described in Section 1.2.5), but it also can result in excess superheat that would detrimentally increase compressor discharge temperature, and decrease suction density [72]. For this reason, SIHXs are best suited to applications where high discharge temperature is mitigated by another system feature, such as in heat pumps with refrigerant injection (described in Section 2.1.2, 2.1.3 and 2.2.2), or oil injection (described in Section 2.2.4).

Improved refrigerant injection cycles

Improvements to refrigerant injection cycles for quasi two-stage or two-stage cycles have been achieved with more complex vapour extraction methods and two-phase injection. Several papers summarize a large number of alternative vapour extraction configurations, that show better cold climate performance than the IHX and flash tank methods currently found in some market-available heat pumps (described in Section 2.1.2) [28,29,143,174]. Additionally, studies have demonstrated that the injection of refrigerant as a liquid-vapour mixture can yield lower compressor discharge temperature, superior COP, and comparable or superior heating capacity at cold temperatures, relative to the more typical method of injecting vapour alone [175,176]. Application of one or both of these types of modifications could further improve the cold climate performance of quasi two-stage and two-stage heat pumps with refrigerant injection.

Two-stage cycles

Genuine two-stage cycles are not currently found in the market-available heat pumps summarized in Table 2, despite compelling evidence of their suitability for cold climate applications [23]. Two-stage cycles use two separate, sequential compression processes, with a basic example (including refrigerant injection) shown in Fig. 2.5. The use of two compressors in series reduces the pressure ratio that must be achieved by each one, and allows for the incorporation of intercooling/desuperheating processes (such as refrigerant injection) between them, to reduce compressor work and the final discharge temperature. Two-stage cycles can also take advantage of compressors which are separately controlled,

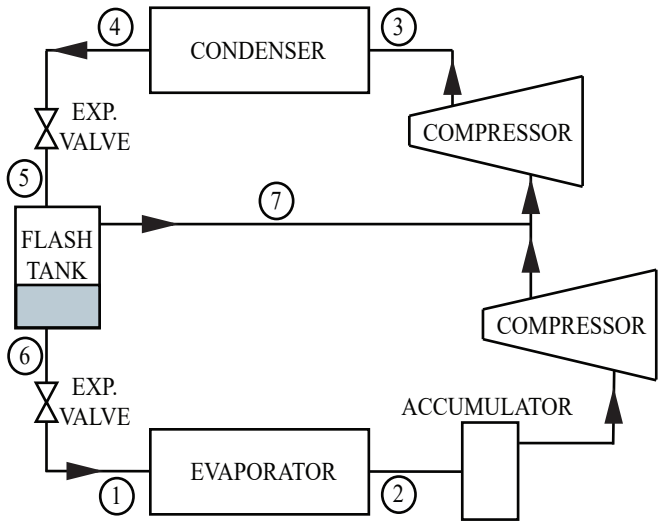

Figure 2.5: Diagram showing the primary component layout of a two-stage heat pump cycle with flash tank vapour injection.

and of two different types or sizes/volumes [58,71,174,177], which can be beneficial for reducing upfront cost, or improving capacity modulation through multi-function operation (discussed in Section 1.3.3). Two-stage heat pumps, particularly those with refrigerant injection, have been the topic of numerous research papers [9, 23, 71, 143, 174, 178], the results of which have reinforced their potential to perform well in cold climates.

Cascade cycles

A review of research on cascade heat pump cycles is provided in Section 1.3.2.

Autocascade cycles

Autocascade heat pumps offer a way to exploit the advantageous properties of different refrigerants at high and low temperatures (similar to a cascade cycle), by separating zeotropic refrigerant mixtures into their constituent pure refrigerants for strategic use in

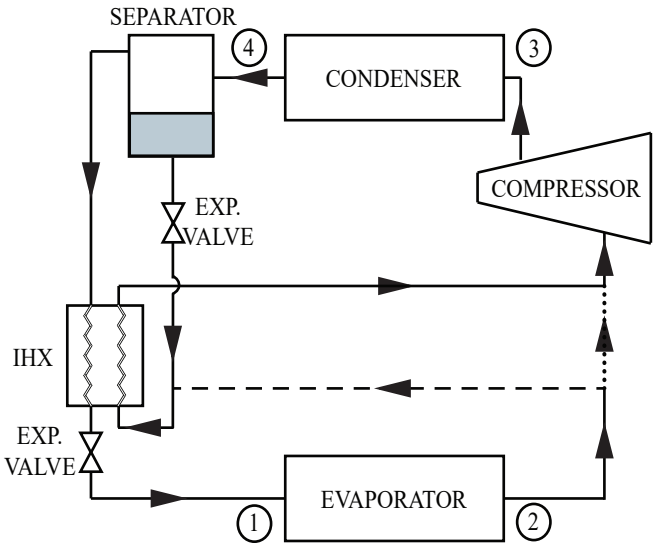

Figure 2.6: Diagram showing two possible configurations for an autocascade heat pump cycle, which differ according to whether the refrigerant exiting the evaporator follows the dashed or dotted line.

different parts of the heat pump cycle. Fig. 2.6 shows two different layouts for a simple autocascade heat pump cycle, represented by the two different paths (dotted or dashed lines) that could be taken by the vapour exiting the evaporator, as described by Zhao et al. [179] and Zuev et al. [66] (dashed version), and Chen et al. (dotted version) [180]. In an autocascade heat pump, the flow exiting the condenser at point 4 is a two-phase mixture, which is then separated into vapour and liquid streams, each primarily composed of a different refrigerant [179]. In the system shown in Fig. 2.6 the vapour stream is condensed in an IHX, expanded, and then sent through the evaporator where it absorbs heat from the outdoor air at a higher saturation pressure than would be possible with the original refrigerant mixture, thereby reducing the pressure difference and subsequent compressor work, and improving the overall system performance [179]. The liquid stream

is expanded, and ultimately merges with the vapour exiting the evaporator, before the compressor. The liquid and vapour streams can merge either before (dashed line) or after (dotted line) the liquid stream is vapourized in the IHX. Three studies were identified that specifically addressed the use of air source autocascade heat pump cycles for heating in cold climates [66, 179, 181], and all concluded that this cycle type is well-suited to cold climate application. In fact, the investigation conducted by Zuev et al. [66] compared the performance of an autocascade and a cascade heat pump for heating at low ambient outdoor temperatures and concluded that, below an outdoor temperature between −20 °C and −25 °C, the heating performance of the autocascade design surpassed that of the cascade system. The majority of the research found examining standard and improved autocascade cycles focused on the related topic of low-temperature refrigeration [180, 182–188]. However, the work completed to date illustrates that there is potential for autocascade cycles to improve the performance of cold climate heat pumps in centrally-ducted residential applications.

Multi-stage cycles

Multi-stage cycles with more than two compression stages are not currently found in the market-available heat pumps summarized in Table 2, despite evidence that heat pump performance increases with each additional compression stage when refrigerant injection is used [28]. However, the practicality and benefits of multi-stage cycles could be limited by the added complexity and expense associated with each additional stage, so Zhang et al. [28] suggest it is more appropriate to realize a multi-stage effect using a single injectable compressor (as in the quasi two-stage cycle) with more than one

supplementary injection port. They cite several studies which explored this type of quasi multi-stage cycle, demonstrating both benefits to cold temperature heating performance and challenges for effective control system design.

Multi-function heat pumps

A review of multi-function heat pumps be found in Section 1.3.3. Multi-function capabilities are not found in the market-available heat pumps in Table 2.

2.2.3 Refrigerant charge management techniques

Heat pump performance can be improved by refrigerant management strategies which adjust the system's refrigerant charge to better suit the wide range of temperature conditions experienced in cold climates (discussed in Section 1.2.5). Currently, the majority of the heat pumps in Table 2 do not include components whose primary function is refrigerant charge management, and instead they rely on the secondary refrigerant storage effect of accumulators, which are reservoirs whose primary purpose is to keep liquid from entering the compressor (as described in Section 2.1.4) [16]. As cold climate heat pump technologies continue to improve, the extended operating temperatures, defrost strategies, cycle types, refrigerants, and components involved enhance the impact of refrigerant charge management, so the development of customized charge management strategies is increasingly important for these systems [14, 21, 150, 189–192]. This section will discuss one passive and one active charge management technique which are not found in the market-available ccASHPs examined: liquid receivers, and variable liquid line length.

Liquid receivers

A liquid receiver is a type of refrigerant reservoir that is not included in the market-available cold climate heat pumps listed in Table 2, despite their prevalence in heat pump systems described in the literature [13,14,71,140], and positive effect on heat pump performance [13]. The closest analogue found in Table 2 is Mitsubishi's "power receiver," which is described in Section 2.1.4. Liquid receivers are located on the high pressure side of heat pump systems [193] and passively alter the refrigerant charge during changing conditions or modes [16]. They are typically placed directly after the condenser to prevent excess liquid refrigerant from backing up into the heat exchanger [13], and to ensure only liquid is sent to the expansion valve [16]. Some considerations discouraging the inclusion of liquid receivers in residential heat pump systems are that they increase the total quantity of refrigerant needed [18] as well as the overall system dimensions/bulk and cost [140]. A study by Menken et al. [193] examined the role of refrigerant reservoir location on heat pump performance by comparing a standard heat pump cycle using a liquid receiver, to one using an accumulator. They concluded that an accumulator is the preferable refrigerant reservoir for cold climate heating conditions, which supports the decision to include accumulators, rather than liquid receivers, in the market-available cold climate heat pumps in Table 2. However, the Mitsubishi (and similar), Carrier (280ANV0**), and Bryant *Evolution Extreme* heat pumps in Table 2 contain more than one refrigerant management component (Section 2.1.4); therefore, including liquid receivers alongside other refrigerant management devices may yet be valuable for cold climate heat pumps.

Variable liquid line length

Another way in which refrigerant charge can be managed to improve performance, is to treat the refrigerant lines as reservoirs, and actively modify the volume of these lines in the heat pump system. Manipulation of the length of the line that carries the liquid phase refrigerant has a large influence on system pressures and can be accomplished through the switching of numerous valves, as demonstrated in a study by Lee et al. [16], and shown in Fig. 2.7. The results showed that their proposed "variable liquid line length" system improved both heating capacity and COP in heat pumps without a liquid receiver, and would be particularly effective at improving seasonal performance in regions with high temperature variations [16], such as cold climates. They also showed that

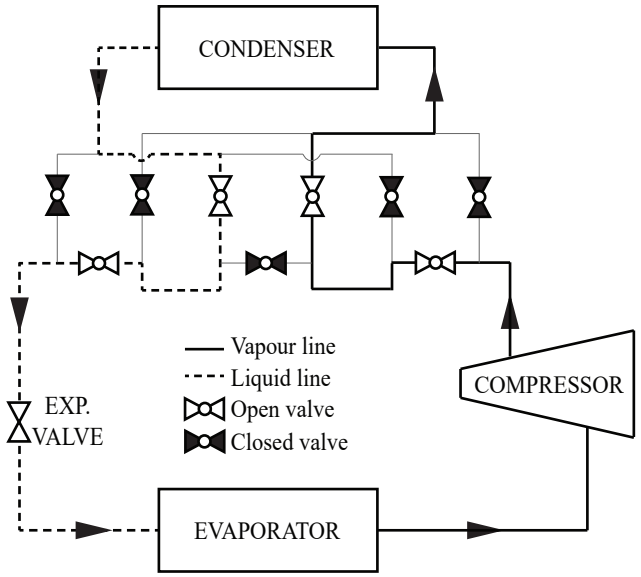

Figure 2.7: Diagram showing the configuration of a heat pump with variable liquid line length based on the system designed by Lee et al. [16]. The ball valves can be opened or closed to adjust the length of the liquid line.

there is potential for active refrigerant control strategies to improve cold climate heat pumps, since these allow for more precise optimization of refrigerant charge than passive refrigerant reservoirs.

2.2.4 Compression innovations

Further improvements to compressor technologies could help heat pumps meet the heating needs in cold climates and eliminate reliance on auxiliary heating, specifically by increasing the max/min capacity ratio (turn down ratio) of cold climate heat pumps [126], and lowering the minimum outdoor temperature at which these systems can deliver their maximum heat output. To increase turn down ratio, compressors must be capable of delivering both very low and very high refrigerant flow rates while maintaining good seal, lubrication, efficiency, and safe operating temperatures. Meanwhile, operating with maximum heat output at increasingly low outdoor temperatures requires mitigating the problems of increased discharge temperature and decreased refrigerant density at low evaporator pressures (discussed in Section 1.2.5). This section presents designs from the literature that could assist in achieving these objectives.

Oil-injected compression

Oil injection or oil flooding has been shown to improve the performance of scroll compressors, reduce discharge temperature during cold temperature heating, and improve heat pump COP [28]. Rather than relying on refrigerant flow to return migrated oil and cool the compressor motor, oil injected compressors have a separate oil circuit to accomplish these tasks, as shown in purple in Fig. 2.8. The oil is injected directly into the compres-

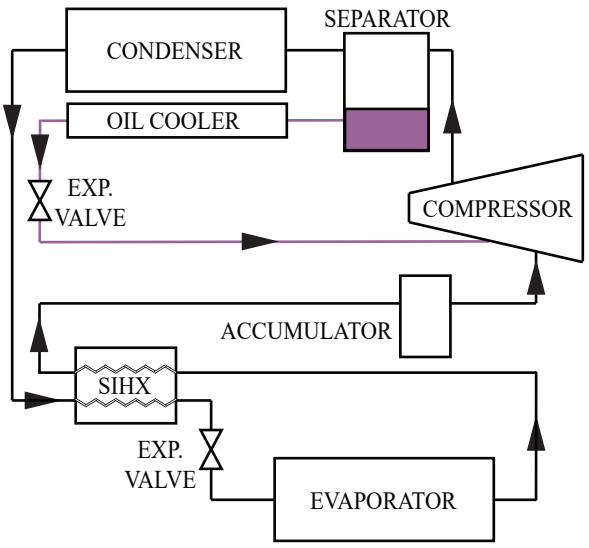

Figure 2.8: Diagram showing the configuration of a heat pump with a compressor oil injection circuit and a suction internal heat exchanger (SIHX), adapted from Ramaraj et al. [194].

sor where it lubricates and absorbs the heat of compression, then it is separated from the discharge stream, cooled (rejecting heat to the indoor air), expanded to evaporator pressure, and returned to the compressor to be injected again [194]. Scroll compressors are ideal for this technique, due to their relatively high tolerance to the wet compression involved [194, 195]. Since the heat of compression is absorbed by the injected oil, oil-injected compression can occur nearly isothermally [194], allowing the inlet refrigerant temperature to be higher without causing excessively high discharge temperature. This is particularly advantageous in systems which incorporate a suction internal heat exchanger (SIHX) (as described in Section 2.2.2), like the one shown in Figure 2.8. Furthermore, the reduced compressor discharge temperature can lower the minimum operating outdoor temperature of the heat pump (explained in Section 1.2.5), thereby reducing reliance on

backup auxiliary heating systems in cold climates [194].

Variable volume compression

Variable volume compression utilizes changes to internal compressor volumes to manipulate the flow or pressure ratio of refrigerant in the compressor, rather than relying solely on modulation of compressor speed. Variable volume compression is not found in the market-available cold climate heat pumps listed in Table 2; however, Gree has employed variable volume compression in some of its other heat pump models that are not centrally-ducted units. Gree developed a three cylinder two-stage rotary compressor that changes modes during low outdoor temperatures to activate a second low-stage cylinder which increases the total suction volume (and decreases the high/low stage volume ratio) thereby counteracting the reduction in flow rate and heating capacity caused by decreased refrigerant density [11] (described in Section 1.2.5). Biao et al. [11] conducted an experimental analysis of Gree's variable volume system and demonstrated that it could operate stably with a COP of 1.52 at an outdoor temperature of −30 °C (sink temperature of 45 °C), when heat pumps using traditional single and two-stage compression could no longer function, and it exceeded the COP of the traditional systems in all of the tested temperature conditions. Wang et al. [196] incorporated variable volume capabilities into an injectable two-stage scroll compressor design that used two separate scroll sets for the low and high pressure stages. The low stage scroll set had a fixed geometry, and therefore a fixed internal pressure ratio as in traditional scroll compressors, while the high stage scroll set could vary its internal pressure ratio using load-off valve blocks and advanced exhaust ports to control the pressure of discharge. Experimental results showed

that the system presented by Wang et al. [196] exceeded the heating COP of four other heat pump cycle configurations discussed in this review (standard single-stage, two-stage with IHX vapour injection, and quasi two-stage with IHX or flash tank vapour injection) at evaporator temperatures ranging from −25 °C to −15 °C, while yielding significantly lower compressor discharge temperatures (a benefit discussed in Section 1.2.5). The design presented by Wang et al. [196] could offer improved performance amid the widely varying conditions experienced in cold climates, while also offering the benefit of scroll compressor's high capacity and relatively high tolerance of liquid slugging. Thus, the variable volume concept shows potential benefits to both scroll and rotary compressors for heat pumps operating in cold climates.

Tandem Compression

Shen et al. [14, 72] examined the potential of tandem compression (two compressors in parallel rather than series), to improve cold climate performance. When compared to standard single "two-stage" compressors, tandem compression offers a larger displacement volume ratio between the high and low stages, yielding a wider capacity range [72]. Shen et al. [72] used a multi-function design that switched from using one to two compressors when operating at low outdoor temperatures, which effectively boosted heating capacity. They examined two configurations: one that was a simple/economical version using tandem single-speed compressors, and a more complex/expensive option using tandem vapour-injected variable-speed compressors. The latter performed marginally better, achieving 88 % rated capacity at an outdoor temperature of −25 °C with a system COP of 2.0, while the single-speed version maintained 76 % capacity and a COP

of 1.9. Both designs exceeded the capabilities of a heat pump with a single vapour injected compressor, and surpassed the US Department of Energy's (DOE) cold climate performance targets of 75 % capacity at −25 °C and a COP of 4.0 at 8.3 °C [72]. Their performance at −25 °C also exceeded the performance reported for most of the market-available heat pumps in Table 2 at a milder outdoor temperature of −15 °C. A follow-up study that involved installing a prototype of the vapour injection tandem system in a home in Alaska, USA, yielded promising outcomes, suggesting tandem compression is well-suited to cold climate heat pumps [14].

2.2.5 Expansion loss recovery

Heat pumps experience losses during the expansion process, which increase as the pressure ratio across the system widens, as in cold temperature heating conditions. Ejectors or expanders are devices that can be used for the primary pressure reduction instead of an expansion valve, in order to recover energy during expansion and use it to reduce the net power input required for the heat pump cycle [197]. Ejectors and expanders are not included in the market-available cold climate heat pumps listed in Table 2, despite their potential benefits to cold climate heat pump performance.

An ejector is an alternative expansion device which mixes a high pressure fluid stream with a low pressure stream to yield an intermediate pressure stream while reducing expansion losses [197], with a simple heat pump application shown in Fig. 2.9. The ejector has been the subject of extensive research as a tool for improving the performance of vapour compression refrigeration and heat pump systems [28, 29, 40, 197–200]. In the standard

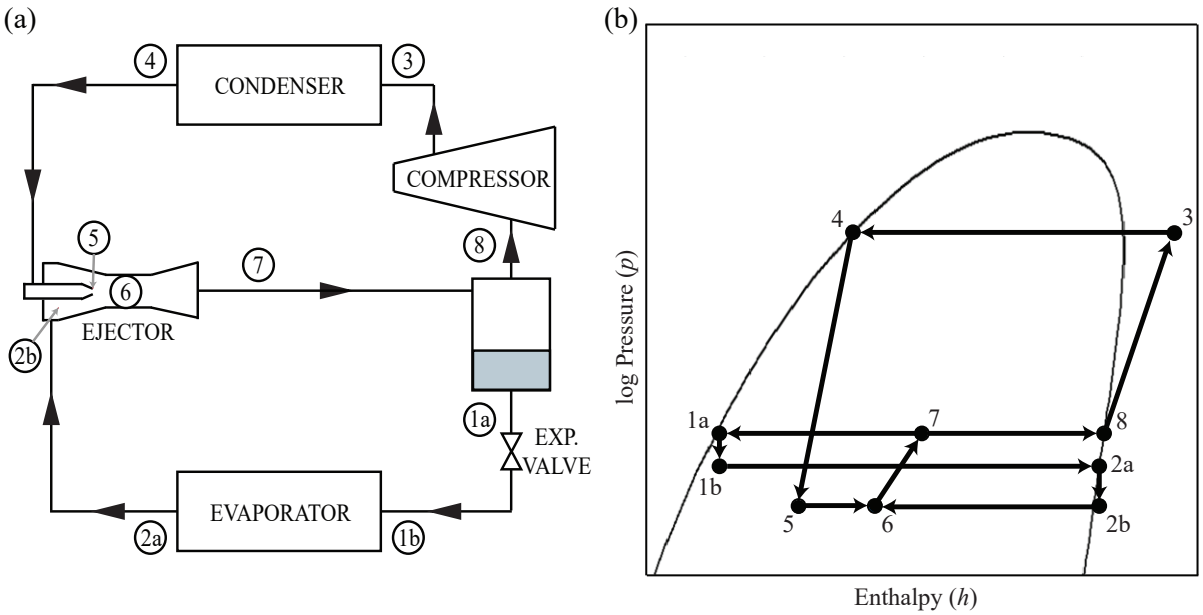

Figure 2.9: Diagram showing the (a) primary component layout and (b) $p-h$ diagram of a single-stage ejector enhanced heat pump (adapted from Zhang et al. [28]).

ejector expansion single-stage heat pump system shown in Fig. 2.9 (proposed by Gay in a 1931 patent [201]), the ejector not only reduces irreversibilities due to expansion, but also increases the suction pressure (at point 8) above that of the evaporator (point 2a), thereby reducing the compressor work [29, 40]. A variety of ejector enhanced vapour compression cycle configurations have been studied including quasi two-stage [202], cascade [198], autocascade [181], transcritical CO_2 [203, 204], and solar-assisted heat pump systems [40]. While much of the earlier research focused on applications for cold temperature refrigeration [28, 205, 206], some studies have specifically investigated the use of ejectors for cold climate heating applications [167, 181, 204, 207, 208]. Since the benefits of the ejector also increase as the pressure difference between the condenser and evaporator increase, they have potential to improve the performance of cold climate heat pumps [28].

The expander is a device which extracts useful work from the expansion process and uses it to reduce (through direct coupling) or offset (through electricity generation) the power consumption of the compressor [10, 29]. Expanders are particularly advantageous when there is a large difference between the condenser and evaporator pressure, such as in transcritical CO_2 heat pumps (described in Section 2.2.1) [209], and much expander research has focused on this cycle type [29, 210, 211]. Elbel and Lawrence [197] outlined several limiting factors for the use of expanders, including that their cost is similar to that of an additional compressor, and suggested that ejectors may be a more promising avenue for expansion recovery. However, Yap et al. [209] proposed an expander-compressor, which would achieve both expansion and compression using a single device, for a more compact design. Some studies have examined the potential use of expanders in subcritical heat pumps [212], but further work could be done to study their effect on cold climate heating performance specifically, and to determine if the inclusion of an expander could be feasible for residential heat pumps, which have strict space and cost constraints.

2.2.6 Frost management

A wide variety of frost delay, removal, and prevention strategies have been explored which could improve upon, or replace, the traditional reverse cycle defrost method employed by market-available ccASHPs. A large number of promising strategies have been summarized in recent reviews by Al Douri et al. [50] and Song et al. [49] including advances in passive and active defrosting methods, methods to slow or prevent frost formation, and optimization strategies for reverse cycle defrosting. Additionally, Zhang et al. [51] com-

pleted an analysis and review of frost-free (dehumidification) technologies for air source heat pump evaporators. Some studies that were not summarized in these reviews are described below. Byrne et al. [213] developed and tested a unique thermosyphon defrost method that allows defrosting to occur simultaneously with heating operation, thereby mitigating the loss of efficiency and heat output typically attributed to the defrost cycle. Additionally, Kim et al. [150] developed a dual hot gas bypass defrosting method with an accumulator heater, which resulted in a 15 % decrease in defrosting time, and a 15 % increase in defrost efficiency compared to a typical reverse defrost cycle. A study by Wei et al. [214] showed that the incorporation of quasi two-stage vapour injection during the defrost cycle lead to a 20.1 % reduction in the time needed to defrost the coil, an 18 % reduction in defrost power consumption, and a 6.2 % increase in defrost efficiency. Long et al. [215] presented a novel defrost system which reduced defrost time by 67 % compared to a reverse cycle method, using only recovered heat from the compressor to defrost the outdoor coil, and allowing normal heating operation to continue during defrosting. Thus, there is potential to improve the defrost performance of market-available cold climate heat pumps through the application of methods already described in the literature.

Heat exchanger design often focuses on efficiency and compactness but it can also have secondary impacts on frost accumulation and removal, which play a substantial role in cold climate heat pump performance. For instance, microchannel heat exchangers are drawing more attention in market-available heat pumps, such as the Samsung, Bryant (280ANV series) and Carrier (25VNA0 series) heat pumps in Table 2, because of the benefits of increased thermal performance, reduced size, and lower refrigerant use [216–218].

However, some past studies have shown that, when used as the evaporator in a heat pump, microchannel heat exchangers can require more frequent defrosting than traditional finned tube heat exchangers [216–218], so care must be taken in their design for cold climate applications. Shao et al. [217] concluded that maldistribution of refrigerant has a dominating negative effect on the rate of frost accumulation in microchannel coils, that could not be remedied by modifying fan speed or fin density. Hong et al. [216] proposed a microchannel heat exchanger design with plain-louvered fins (rather than conventional corrugated-louvered fins), which cut the defrost frequency in half and also improved peak heating capacity. No studies could be found regarding the frosting characteristics or defrost performance of the *Spine Fin* (similar to that described as "serrated fin") coil type used in the American Standard and Trane (18 and 20 series) heat pumps but, given the demonstrated impact that fin density and shape has on frosting/defrosting characteristics [20, 49], further research is recommended. Since defrosting is currently both unavoidable and detrimental to system performance, particularly in cold climates, advancements in outdoor heat exchanger design have great potential to improve cold climate heat pumps.

2.2.7 Comparative performance evaluation

Effective prediction and evaluation of the comparative installed performance of cold climate heat pumps is needed to identify the most promising design innovations to improve market-available systems, as well as to aid policy makers and homeowners in identifying which systems on the market can meet heating needs in cold climates. This section discusses the value of application-specific comparative research studies and improved per-

formance testing and metrics as tools for meaningful, standardized comparisons between different residential cold climate heat pump designs.

Application-specific comparative research

There is a need for more studies that compare the cold climate performance of a wide range of heat pump designs using analogous installed systems with standardized testing conditions, procedures, and metrics for specific applications, such as centrally-ducted home heating. Many studies to date compare the performance of new designs only to a standard single-stage heat pump cycle, rather than to other innovative designs with matching operating conditions [203]. Furthermore, experimental studies of VCASHP technologies often use water as the indoor supply fluid, as would be the case in hydronic space heating, or water heating systems. However, these air-to-water prototypes do not typically use the same heat exchanger type or condenser temperature as centrally-ducted air-to-air systems, thus reducing the relevance of the results, and potentially altering which cycle type will yield the highest performance [179]. By contrast, a comparative study with an application-specific focus would allow for the use of applicable industry testing standards, and would also standardize parameters such as the supply fluid, indoor/outdoor air temperatures, typical heat exchanger type and configuration, unit capacity range, physical size constraints, and refrigerant safety requirements, thereby allowing for more meaningful side-by-side comparison of appropriate technologies. The results of such studies could illuminate which cycles, configurations, and components perform best while meeting the heating needs for centrally-ducted homes in cold climates without reliance on auxiliary heating.

Cold climate performance metrics and testing

Industry standardized performance metrics could allow homeowners and policy-makers to evaluate which heat pumps are the best choice for use in cold regions, but the metrics currently being used do not reflect sufficiently cold climate conditions. In North America, third party certified performance testing is done according to the standards set by the Air Conditioning, Heating, and Refrigeration Institute (AHRI), whose published rating reports include a minimum of the following two metrics for all residential heat pumps: "high heat capacity" (the maximum heating output at the "rated" indoor and outdoor dry bulb temperatures of 21.1 °C and 8.3 °C, respectively), and the heating season performance factor (HSPF) for climate region IV [219]. The "high heat capacity" is included in Table 2, under the title "rated heating capacity" (as it is commonly known). The reporting of the *maximum* heating output at 8.3 °C is both too warm for cold climate contexts, and irrelevant to cold climate heat pumps with variable speed, two-stage, or tandem compression, since they are designed to operate at only partial capacity at such a mild temperature. Similarly, the lowest temperature condition used when calculating HSPF for climate region IV is −8.3 °C, which is still too warm to capture the effects of differences in performance at the extreme cold temperatures regularly experienced in climates colder than region IV, which includes the majority of Canada. Both the US Department of Energy (DOE) and Natural Resources Canada (NRCan) are updating their heat pump testing regulations and energy efficiency standards to better reflect installed performance in cold climates [220]. The "% rated capacity" at −15 °C in Table 2 (compiled by NRCan) is an optional test point derived from the newer American "Appendix

M1" testing standard [220]. However, as a percentage, this metric has limited value as a comparison tool, since it is calculated using each heat pump's individual rated capacity which are not all the same, nor equal to their nominal capacity (described in Section 1.3). The minimum operating temperature (shown in Table 2 from manufacturer data), and COP at that temperature (not reported), are additional pieces of information needed to evaluate the feasibility of relying on a particular heat pump system without auxiliary heating, but they are currently missing from AHRI ratings [221]. Thus, the consideration of colder testing points, colder climate regions, and the reporting of meaningful minimum operating temperature and COP, are recommended for improved evaluation of cold climate heat pump performance.

Current American and Canadian heat pump testing procedures (harmonized test standards *AHRI 210/240* [219] and *CSA C656*) also involve only steady-state operation at fixed conditions, and thus fail to reflect the benefits of variable/multi-speed technology and improved control algorithms (such as defrost controls) on installed, dynamic performance [221–223]. To capture these types of effects, the Canadian Standards Association (CSA) has developed a new dynamic load-based testing procedure, *EXP07:19* [222], which NRCan is currently evaluating [221] and aims to use for cold climate heat pump incentive programs, through voluntary qualified product listings [220]. The new procedure also introduces five separate climate regions found in Canada that cover a wider range of cold climate conditions. Implementation of these types of regulatory changes, and improved testing methods, have the potential to provide more reliable and compelling evidence to inform government policies and rebates, as well as consumers looking to benefit from improved cold climate heat pumps. This will lead to more widespread

use of electric air source heat pumps for residential heating in cold climates as a replacement for current fossil fuel based space heating methods, thus reducing greenhouse gas emissions and combating climate change.

Chapter 3

Comparative thermodynamic analysis

3.1 System descriptions

This study involved thermodynamic modelling of two heat pump systems, shown in Figure 3.1; one, a conventional configuration with auxiliary backup heating, and the other, a new add-on cascade configuration intended to improve cold climate performance. Both of the heat pump systems make use of the same affordable, single-stage, single-speed "primary heat pump" which is composed of an outdoor unit containing the evaporator heat exchanger coil, a thermal expansion valve, a compressor, and a fan, as well as an indoor air handler/fan-coil unit containing the condenser heat exchanger coil and an indoor blower fan. Two refrigerant lines connect the indoor and outdoor units (one carries liquid, the other superheated vapour), and the air handler sends heated supply air into the home's centralized ductwork.

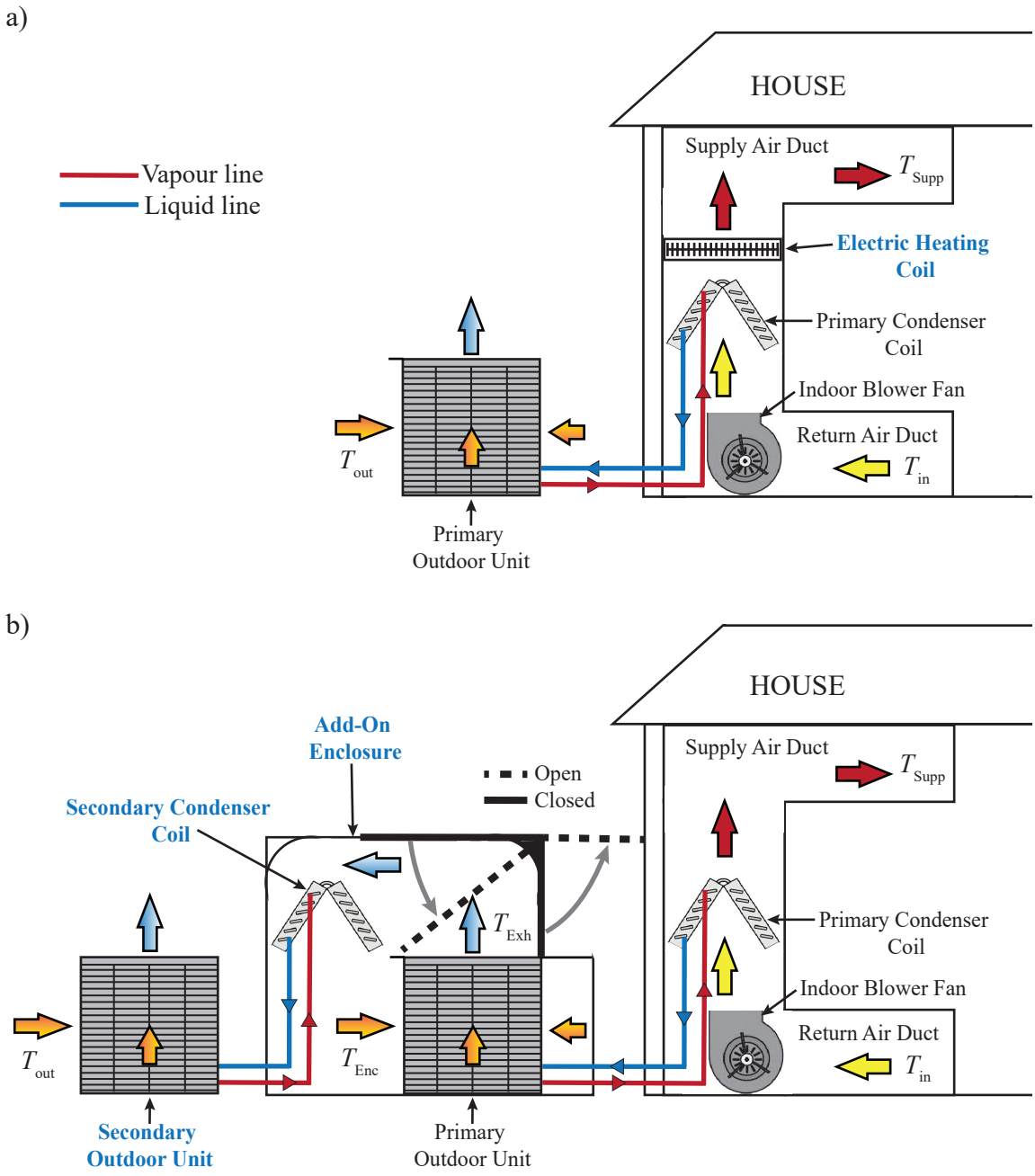

Figure 3.1: Diagrams showing the installed configuration of a) System 1, the baseline heat pump with supplementary electric resistance heating, and (b) System 2, the add-on cascade heat pump configuration.

System 1, used as a baseline for comparison, consists of the primary heat pump with a auxiliary electric resistance heating coil located in the plenum of the air handling unit, as shown in Figure 3.1 (a). This is a typical setup for the use of a standard single-stage/mild climate heat pump in a cold climate. The auxiliary coil adds heat when the primary heat pump's output is insufficient to meet the home's heating load.

System 2 is the proposed cold climate add-on system, which uses the primary heat pump plus a secondary identical heat pump that supplies heat to the primary in a cascade configuration. The primary heat pump delivers heat to the home using the centrally-ducted forced air system, while the secondary heat pump maintains an intermediate temperature microclimate inside of an enclosure installed around the outdoor evaporator unit of the primary heat pump, as seen in Figure 3.1 (b). At cold outdoor air temperatures, the milder microclimate in the enclosure keeps the primary heat pump's evaporator temperature and pressure elevated, for improved heating output and performance. Meanwhile, the secondary heat pump condenser delivers heat to recirculated air that exits the primary evaporator unit at a cooler temperature than inside the home, so its condenser temperatures and pressures are lower than those of the primary, keeping the secondary compression ratio within a safe and effective range. As seen in Figure 3.1 (b), the secondary heat pump has no indoor condenser fan, but rather the outdoor fan of the primary heat pump is used to drive the airflow over both the primary heat pump's evaporator coil and the secondary heat pump's condenser coil, thereby saving the energy input of a second condenser fan. During mild outdoor air temperature conditions, when the primary heat pump alone offers superior performance, the enclosure can be opened (dotted line in Figure 3.1 (b)) to allow the primary heat pump's outdoor unit to draw in

fresh air and send exhaust air to the outdoors, while the secondary heat pump is turned off. Thus, this design is effectively a multi-function cascade heat pump (discussed in Section 1.3.3) but, unlike typical cascade systems that directly link the two heat pump cycles together using a shared heat exchanger (as seen in Figure 1.6), it uses air as an intermediate heat transfer medium so that the two heat pumps can still be operated independently as needed.

The thermodynamic models created of Systems 1 and 2 were used to predict their performance at three outdoor dry bulb temperature conditions (8.3 °C, −8.3 °C and −15 °C). These temperatures were chosen since they are reported by the North American Energy Efficiency Program (NEEP) based on third-party testing for numerous heat pump models, including many of those found in Table 2. This allowed for the standardized comparison to published performance of market-available cold climate heat pump designs, presented in Section 4.4. If an add-on design of this type can provide sufficient heating with competitive efficiency, it would allow Canadians to take advantage of existing and affordable mild-climate electric VCASHP systems to reduce residential GHG emissions from heating.

3.2 Home heating load profile

For consistency, all of the systems compared must meet the entire heating load of a sample home at outdoor air temperatures of 8.3°C, −8.3°C, and −15°C. The building heating load profile in Figure 3.2 was created to represent a two-story Canadian home with a heating load of 45 kBtu/hr (13.19 kW) at an outdoor design (minimum) temperature of

−20 °C and a constant indoor set temperature of 21.1°C. The heating load line hits the x-axis at 18.3 °C (60 °F) since this is the typical temperature above which heating is not needed due to internal and solar gains [224]. The linear equation of this profile was used to determine the required heat output at each of the tested temperature conditions, labelled in Figure 3.2.

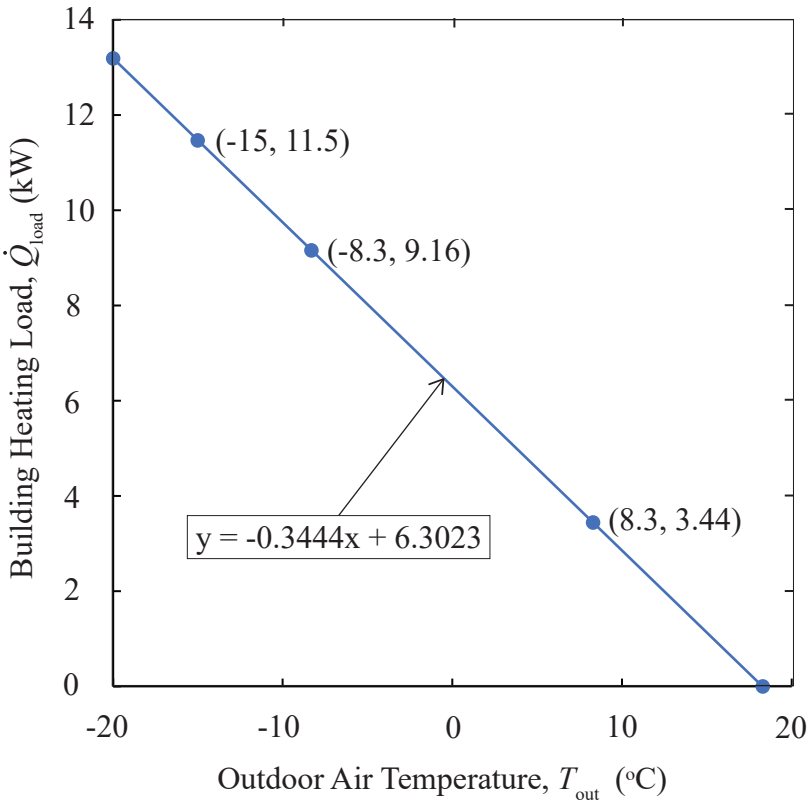

Figure 3.2: Heating load profile of the sample two-story Canadian home heated by the modelled heat pump systems.

3.3 Modelling of System 1: The primary heat pump

The model of the primary heat pump was developed using published specifications and performance data for a market-available 4 ton (48000 Btu/hr) Carrier heat pump which features R410a refrigerant, a thermal expansion valve, and a single-speed compressor. The system is composed of a 25HBC548B**30 outdoor unit and an FX4DNF049 indoor air handler. Engineering Equation Solver (EES) software was used for the modelling, including the built-in fluid property data for R410a and air.

The following assumptions and simplifications were made in the model of the primary heat pump:

- Fans both operate at a single (maximum) speed.
- There are negligible pressure losses in the system.
- There are negligible heat gains/losses in pipe sections.
- The expansion process is isenthalpic ($h_1 = h_4$).
- All air is at standard atmospheric pressure (101.325 kPa).
- Humidity effects are negligible.
- Performance effects of frosting and defrosting are neglected.
- Performance effects due to system cycling at partial load conditions are neglected.
- Degrees of superheating and subcooling are constant at all temperatures.

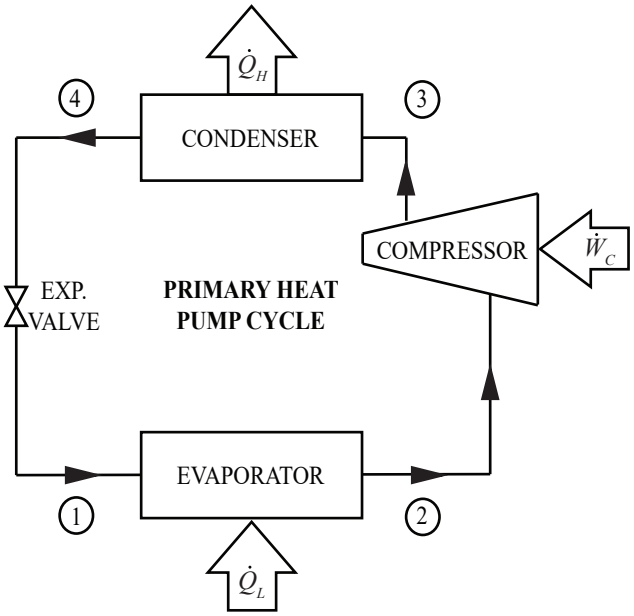

Figure 3.3: Diagram of the components and key state points in the primary heat pump.

Figure 3.3 shows the components of the System 1 heat pump cycle and the location of the four points determined in the model. The state conditions at each of these points were determined using the following energy balance equations for each of the processes in the thermodynamic cycle:

Evaporation (Points 1-2):

$$\dot{m}_{\mathrm{r}} h_1 + \dot{Q}_{\mathrm{L}} = \dot{m}_{\mathrm{r}} h_2 \tag{3.1}$$

Compression (Points 2-3):

$$\mathcal{P}_{\mathrm{C}} + \dot{m}_{\mathrm{r}} h_2 = \dot{m}_{\mathrm{r}} h_3 + \dot{Q}_{\mathrm{C}} \tag{3.2}$$

Condensation (Points 3-4):

$$\dot{m}_{\mathrm{r}} h_3 = \dot{m}_{\mathrm{r}} h_4 + \dot{Q}_{\mathrm{H}} \tag{3.3}$$

Expansion (Points 4-1):

$$\dot{m}_{\mathrm{r}} h_4 = \dot{m}_{\mathrm{r}} h_1 \tag{3.4}$$

Available manufacturer data specified the expected high (p_3, p_4) and low (p_1, p_2) pressures for the heat pump at seven outdoor temperatures ranging from −17.8 °C to 15.6 °C and three indoor temperatures (18.3 °C, 21.1 °C, and 23.9 °C). To incorporate this pressure data into the model, the two data sets at the relevant indoor temperature of 21.1 °C were plotted against outdoor temperature as shown in Figure 3.4. Then, a linear function was fitted to each, and these functions are used to interpolate the pressure values at different outdoor air temperature conditions in the model.

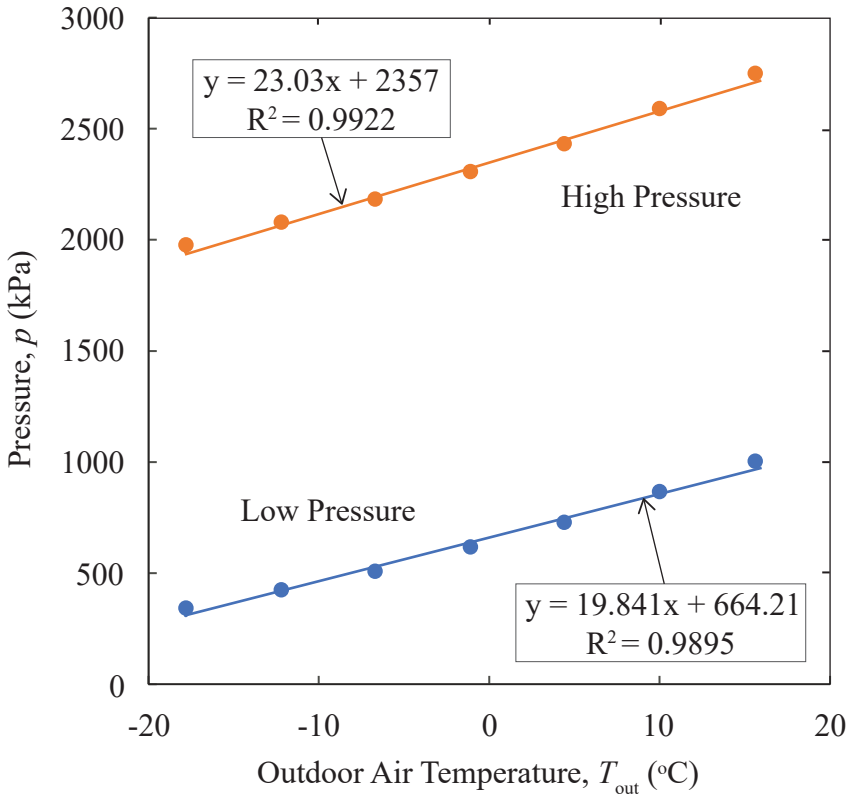

Figure 3.4: Published high and low pressure data points (with computed linear trend-lines) for the primary heat pump at varying outdoor air temperatures, and an indoor set temperature of 21.1 °C [225].

From there, the model determines the state conditions at points 2 and 4 using the interpolated pressure values, along with fixed (inputted) superheat and subcooling values. Subsequently, the state conditions at point 1 are determined using the evaporating pressure, and Equation (3.4).

Performance data from the heat pump manufacturer provided the total system power consumption $\mathcal{P}_{\text{tot}}$ (includes the compressor and both fans) and the heating output ($\dot{Q}_{\text{H}}$)

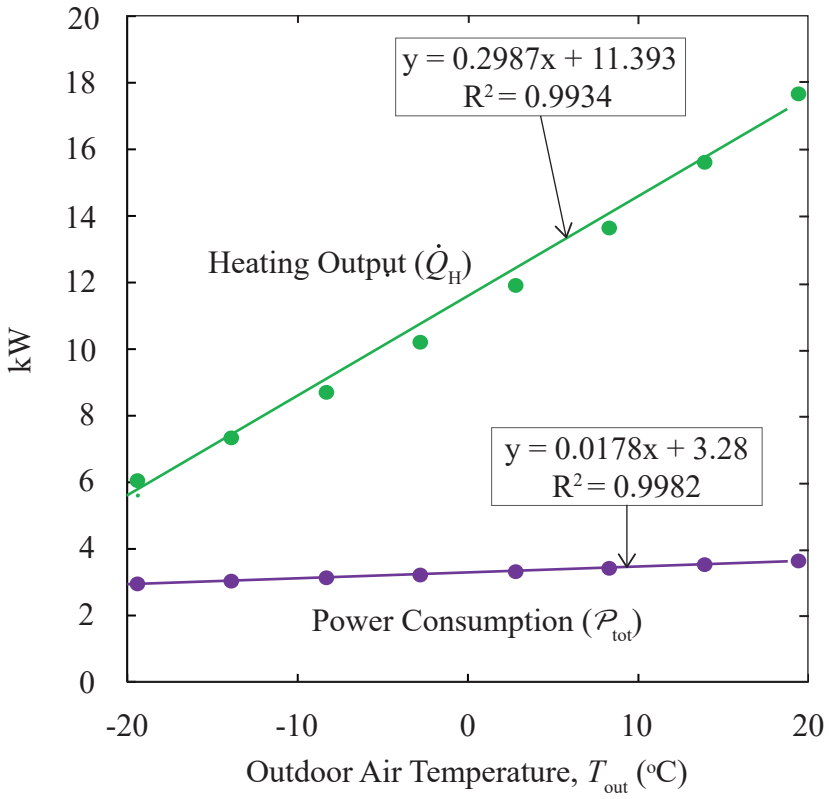

Figure 3.5: Published heating output ($\dot{Q}_{\text{H}}$) and total power consumption ($\mathcal{P}_{\text{tot}}$) data points for the primary heat pump at varying outdoor air temperatures [226], fitted with computed linear trendlines. All data points are for an indoor temperature of 21.1 °C and maximum fan speed.

under various conditions including eight outdoor temperatures ranging from 19.4 °C to −19.4 °C, three indoor temperatures (18.3 °C, 21.1 °C, and 23.9 °C) as well as three indoor fan speeds (1400, 1600, and 1800 CFM). The $\dot{Q}_{\mathrm{H}}$ and $\mathcal{P}_{\mathrm{tot}}$ values at maximum fan speed and an indoor set temperature of 21.1 °C were selected and plotted against outdoor temperature (T_{out}), as shown in Figure 3.5. A linear function was then fitted to each data set to calculate $\mathcal{P}_{\mathrm{tot}}$ and $\dot{Q}_{\mathrm{H}}$ at different outdoor air temperatures in the model.

To isolate the power consumption of the compressor alone ($\mathcal{P}_{\mathrm{C}}$), the power consumption of the indoor (ID) and outdoor (OD) fans was determined and subtracted from the total power consumption values, as shown in Equation (3.6). The power consumption of each fan ($\mathcal{P}_{\mathrm{fan}}$) was calculated based on the horsepower of the fan's motor, found in the product data sheets from the manufacturer (0.25 HP for the outdoor fan, 0.75 HP for the indoor fan [226, 227]), and motor efficiency, using Equation (3.5). The published fan horsepower values were assumed to relate to the maximum airflow rate, and full loading of the motor. Thus, in Equation (3.5) HP is the published motor horsepower, and η_{m} is the full-load motor efficiency. The indoor (ID) fan motor is an electronically commutated motor [227], so it's efficiency was assumed to be 95 %, while the outdoor (OD) fan motor is a single-phase permanent split capacitor motor, with an assumed efficiency of 60 % (both typical full load efficiency values for their respective type and size of motor [228]).

$$\mathcal{P}_{\mathrm{fan}} = \frac{\mathrm{HP} * 746}{\eta_{\mathrm{m}}} \tag{3.5}$$

$$\mathcal{P}_{\mathrm{C}} = \mathcal{P}_{\mathrm{tot}} - \mathcal{P}_{\mathrm{fanID}} - \mathcal{P}_{\mathrm{fanOD}} \tag{3.6}$$

No efficiency factor was applied to the remaining compressor power consumption

($\mathcal{P}_{\mathrm{C}}$), since the motor in a hermetic scroll compressor is cooled by incoming refrigerant, and thus any inefficiencies at the motor are dissipated as heat that is absorbed by the refrigerant. The negative effect of this preheating process on the refrigerant suction density, and thus mass flow rate [229], is already accounted for in the mass flow rate values, since these were based on actual compressor performance data.

Published compressor data provided the ten coefficients needed to calculate the mass flow rate in the compressor based on the dew point temperatures at suction ($T_{2\mathrm{sv}}$) and discharge ($T_{3\mathrm{sv}}$), using Equation (3.7) from the *AHRI Standard 540* [230]. These coefficients are based on a regression analysis performed by the manufacturer using data from compressor testing under rated conditions. The temperatures are inputted into the equation in Farenheit, and the resulting mass flow rate is in pounds per hour, which must then be converted to m^3/hr.

$$\begin{aligned}\dot{m}_{\mathrm{rated}} = C_1 + (C_2 T_{2sv}) + (C_3 T_{3sv}) + (C_4 T_{2sv}^2) + (C_5 T_{2sv} T_{3sv}) + (C_6 T_{3sv}^2) \\ +(C_7 T_{2sv}^3) + (C_8 T_{3sv} T_{2sv}^2) + (C_9 T_{2sv} T_{3sv}^2) + (C_{10} T_{3sv}^3)\end{aligned} \tag{3.7}$$

Since the published compressor coefficients were based on data from testing with a superheat of 20 °F (11.1 °C), the rated mass flow rate values were subsequently corrected to reflect the actual superheat of 5 °C used in the model, according to the superheat correction equation (Equation (3.8)) from *AHRI Standard 540*. Equation (3.8) simplifies to Equation (3.9) when assuming a volumetric efficiency factor (F_{v}) of 1, as suggested by the standard when an F_{v} value is unknown [230].

$$\dot{m}_{\mathrm{r}} = [1 + F_{\mathrm{V}}((\frac{\rho_2}{\rho_{\mathrm{rated}}}) - 1)] * \dot{m}_{\mathrm{rated}} \tag{3.8}$$

$$\dot{m}_{\mathrm{r}} = \frac{\rho_2}{\rho_{\mathrm{rated}}} * \dot{m}_{\mathrm{rated}} \tag{3.9}$$

Having determined the mass flow rate ($\dot{m}_{\mathrm{r}}$), $\dot{Q}_{\mathrm{H}}$, and enthalpy at point 4 (h_4), the state conditions at point 3 can be found starting with h_3 via Equation (3.3). Additionally $\dot{Q}_{\mathrm{L}}$ can be determined using Equation (3.1).

The compressor of an air source heat pump is located in the outdoor unit and therefore is subjected to the airflow generated by the outdoor fan at outdoor air temperatures. For this reason, heat loss from the compressor to the surrounding air ($\dot{Q}_{\mathrm{C}}$) is significant and must be added to the right side of Equation (1.2) yielding Equation (3.2). To determine the compressor heat loss, the actual compression work done on the refrigerant ($\dot{W}_C$) is calculated using Equation (3.10), and then Equation (3.2) is used to solve for $\dot{Q}_{\mathrm{C}}$.

$$\dot{W}_{\mathrm{C}} = \dot{m}_{\mathrm{r}}(h_3 - h_2) \tag{3.10}$$

In System 1, when the home heating load exceeds the heating output ($\dot{Q}_{\mathrm{H}}$) of the primary heat pump, the auxiliary electric resistance heating coil ($\dot{Q}_{\mathrm{aux}}$) in the air handler is used to make up the difference, with an assumed efficiency of 100%. Thus, $\dot{Q}_{\mathrm{aux}}$ is determined by subtracting the primary heat pump's output at the given outdoor temperature condition from the home heating load ($\dot{Q}_{\mathrm{load}}$) at that condition, as in Equation (3.11). The overall system COP for System 1 is then solved for using Equation (3.12).

$$\dot{Q}_{\mathrm{aux}} = \dot{Q}_{\mathrm{load}} - \dot{Q}_{\mathrm{H}} \tag{3.11}$$

$$\mathrm{COP}_{\mathrm{Sys1}} = \frac{\dot{Q}_{\mathrm{H}} + \dot{Q}_{\mathrm{aux}}}{\mathcal{P}_{\mathrm{tot1}} + \dot{Q}_{\mathrm{aux}}} \tag{3.12}$$

3.3.1 Model validation

To validate the model and interpret the results, several additional parameters were calculated and observed. Among these were isentropic efficiency of the compressor (η_{is}), pressure ratio ($\mathrm{R_p}$), percentage of compressor power lost as heat ($\mathrm{R_{lost}}$), supply air tem-

perature (T_{supp}), discharge temperature (T_3), and heat exchanger pinch point temperature differentials (ΔT_{pinchC}, ΔT_{pinchE}).

Isentropic efficiency relates the compression process to one where entropy is constant. It is determined by Equation (3.13), where $h_{3\text{is}}$ is the enthalpy when $s_2 = s_3$.

$$\eta_{\text{is}} = \frac{h_{3\text{i}} - h_2}{h_3 - h_2} \tag{3.13}$$

Underwood et al. used regression analysis to show that the relationship between compressor isentropic efficiency and pressure ratio could be described well using a function

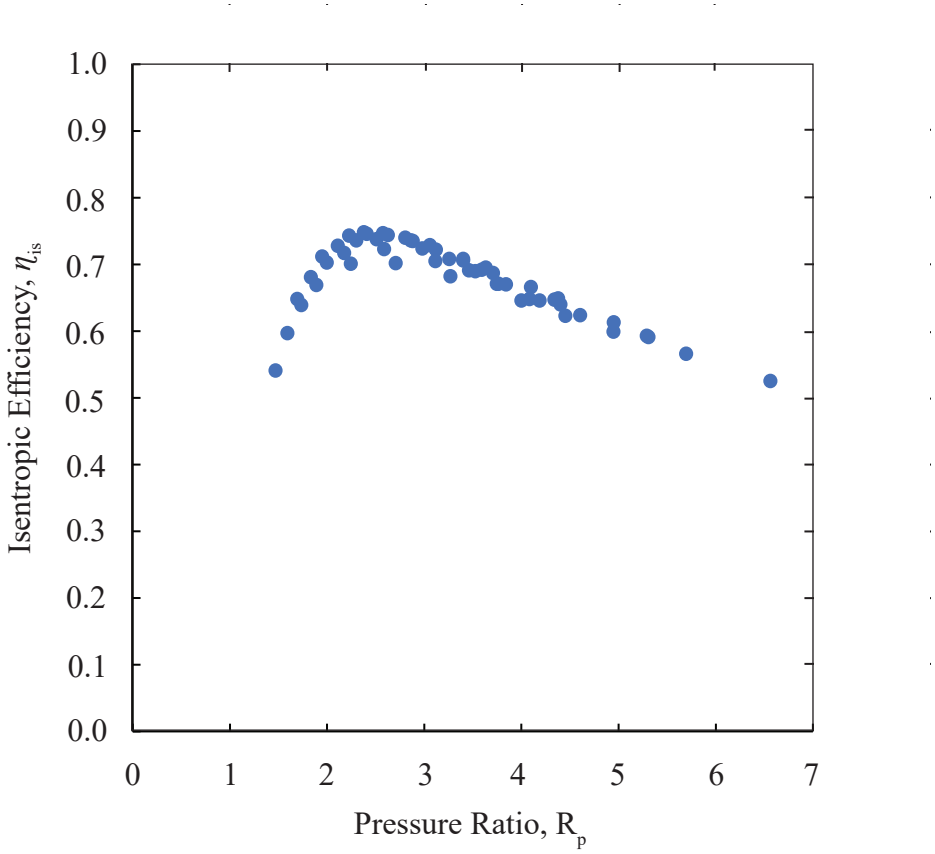

Figure 3.6: Isentropic efficiency (η_{is}) versus pressure ratio (R_p) based on published data for the heat pump compressor [231].

with only four parameters [232]. For the compressor in the primary heat pump, isentropic efficiency values were published for 54 different pressure combinations, so this data was plotted against pressure ratio to reveal their relationship, shown in Figure 3.6. The plot was then used as a benchmark to evaluate if the isentropic efficiencies found for the compression process(es) in the outputs of the model were reasonable, based on pressure ratio. The isentropic efficiency values in the model are expected to be higher than those in Figure 3.6 for comparable pressure ratios, given the additional compressor heat loss that is expected to occur in the actual operating conditions of the modelled heat pump, where the compressor is subjected to forced convective cooling from cold outdoor air drawn over it by the outdoor fan. By contrast, standardized compressor testing is conducted in still air at 35 °C. For this analysis, I assumed that compressor heat loss would not lead to an isentropic efficiency greater than 1, so a realistic isentropic efficiency is defined as one that is greater than the value predicted by Figure 3.6, and less than or equal to 1. Some studies describe compressor heat losses as a percentage of total compressor power consumption (R_{lost}), as shown in Equation (3.14). Based on the literature R_{lost} values are expected to fall between roughly 7% and 30% [12, 233].

$$R_{\text{lost}} = \frac{\dot{Q}_{\text{C}}}{\mathcal{P}_{\text{C}}} * 100\% \tag{3.14}$$

The degrees of superheating and subcooling used in the model were initially chosen to each be 5 °C and then iteratively adjusted as needed, based on the observed effects on certain modelled output parameters. The heat pump in question uses a thermal expansion valve (TXV), so the degrees of superheat at the evaporator exit should be the same at all temperature conditions. A superheat value of 5 °C is common in the literature (e.g. [59]),

so this value was chosen. Additionally it was observed that a superheating value any higher would result in a negative pinch point temperature differential at the evaporator heat exchanger coil exit (Equation (3.15)), which would reverse the direction of heat transfer at that point, and be unacceptable. The pinch point temperature differential is the difference in temperature between the heat transfer fluids (refrigerant and air) at the point in the heat exchanger where their temperatures are the closest. In the case of the evaporator, this occurs when the refrigerant reaches its maximum temperature, at the evaporator outlet.

$$\Delta T_{\text{Epinch}} = T_{\text{out}} - T_2 \tag{3.15}$$

The subcooling value has less of a significant impact on pinch point temperature (since the condenser pinch point does not occur at point 4 in the A-coil heat exchanger used) but rather it has a notable impact on the compression process in the model, since it dictates the enthalpy at point 3 in Equation (3.2). Since the $\dot{Q}_{\text{H}}$ and condenser pressure, and mass flow rate for each condition are already fixed, a greater degree of subcooling, results in higher heat loss ($\dot{Q}_{\text{C}}$) and isentropic efficiency values of the compression process. The heat pump installation manual refers to subcooling values ranging from 8 °F–18 °F (4.4 °C–10 °C). In the end, the degree of subcooling value was chosen to be 6.5 °C, since it was the lowest value that does not result in an isentropic efficiency value greater than 1 within the operating range of the heat pump, but the R_{lost} values still fall within the expected range for all but the most extreme high and low outdoor temperature values (−21 °C and below, 14 °C and above), where they dropped below 7 %.

The supply air temperature delivered was determined based on the total heat transferred to the air, using Equation (3.16), the mass flow rate of the air ($\dot{m}_{\text{air}}$) of the indoor

air handler (based on manufacturer flow rate), and the set temperature (T_{in}) as the return air temperature (T_{ret}). It is important to ensure that the supply air remains within a comfortable temperature range for building inhabitants (typically 32.2 °C and above [234]).

$$\dot{Q}_{\text{H}} = \dot{m}_{\text{air}} c_{\text{p}} (T_{\text{supp}} - T_{\text{ret}}) \tag{3.16}$$

3.4 Modelling of System 2: Proposed add-on design

The primary heat pump model from System 1 (excluding electric resistance auxiliary heat) was replicated as the primary heat pump for System 2, with the intermediate enclosure temperature (T_{enc}) used in place of the outdoor air temperature. An additional version of this primary heat pump model was then adapted for the secondary heat pump to create the cascade system. This secondary heat pump model uses key data inputs from the primary heat pump model ($\dot{Q}_{\text{L}}$, ΔT_{cond}, and T_{exh}), and the same equations (unless otherwise stated below) with state points 1, 2, 3, and 4 replaced with their low-stage cycle counterparts 5, 6, 7, and 8, respectively. Additionally, several other outputs were renamed with an additional subscript of 2, to indicate they pertain to the secondary heat pump cycle (e.g. $\dot{Q}_{\text{H2}}$, $\dot{W}_{\text{C2}}$, $\dot{m}_{\text{r2}}$). System 2 was also modelled using EES software. Figure 3.7 shows the components and key points in the System 2 heat pump cycles.

The same assumptions and simplifications listed in the description of the primary heat pump model were also applied to the cycles in the add-on cascade model. However, the following *additional* assumption was also made:

- The enclosure is perfectly insulated.

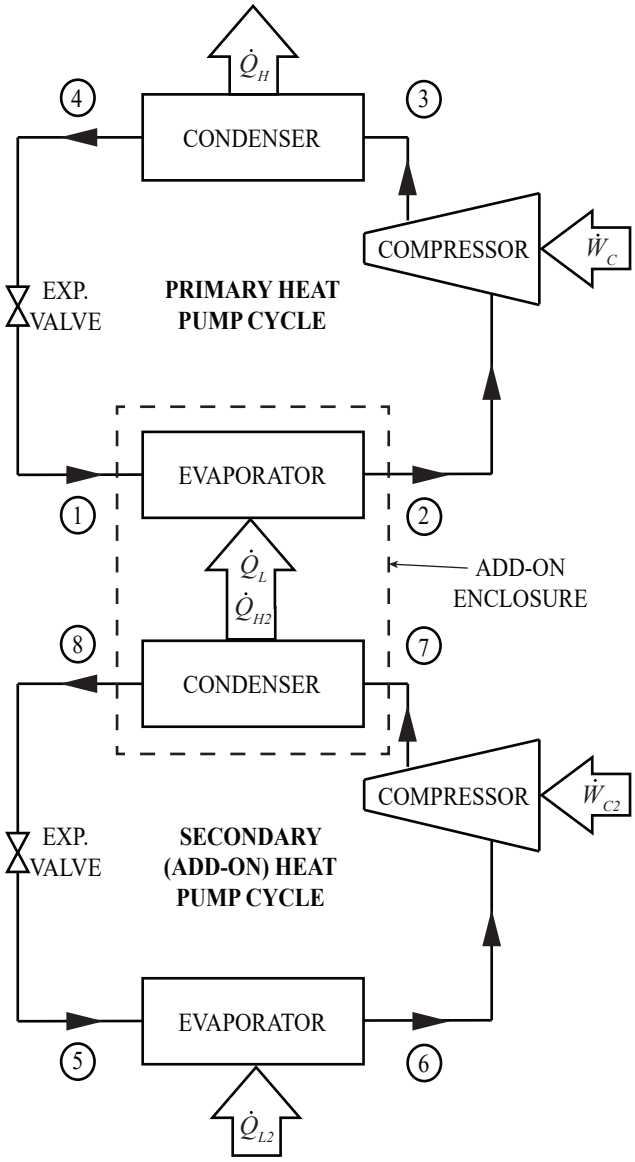

Figure 3.7: Diagram of the cycle components and key state points in System 2.

To maintain a constant temperature inside the enclosure at a given outdoor temperature condition, the secondary heat pump must supply heat to the enclosure air at the same rate as it is being removed by the primary heat pump's evaporator. Thus, the $\dot{Q}_{\mathrm{L}}$ value from the primary heat pump is used as the $\dot{Q}_{\mathrm{H2}}$ input for the secondary heat pump at each temperature condition.

The pressure of the secondary evaporator (p_5 and p_6) was determined based on the outdoor air temperature using the same linear relationship as for the primary heat pump, since this pressure was assumed to behave independently of the condenser temperature. However, the condenser pressure of the secondary heat pump was not determined from the linear relation derived from the manufacturer data, since the data was based on a constant indoor air temperature of 21.1 °C, and the secondary condenser rejects heat to the enclosure at a lower (and varying) temperature for which data was unavailable. Thus, the condenser pressure of the second heat pump was instead determined by setting ΔT_{cond2} equal to ΔT_{cond1}, found using Equations (3.17) and (3.18) where the condenser temperature is the average of the saturated vapour (T_{sv}) temperature and the saturated liquid (T_{sl}) temperature at the condenser pressure, since R410a is slightly zeotropic (explained in Section 2.2.1) [230]. In the corresponding equations for the secondary condenser, points 3 and 4 are replaced with 7 and 8, and T_{in} is replaced with the temperature of the exhaust air (T_{exh}) exiting the top of the primary heat pump evaporator unit. This exhaust air temperature is determined by finding the enthalpy value of the air (h_{exh}) using the energy balance in Equation (3.19), where h_{enc} is the enthalpy of the air at the enclosure temperature.

$$T_{\text{cond1}} = \frac{T_{\text{sl}} + T_{\text{sv}}}{2} \tag{3.17}$$

$$\Delta T_{\text{cond1}} = T_{\text{cond1}} - T_{\text{in}} \tag{3.18}$$

$$\dot{m}_{\text{air}} h_{\text{enc}} = \dot{m}_{\text{air}} h_{\text{exh}} + \dot{Q}_{\text{L}} \tag{3.19}$$

A key determinant of the performance and viability of System 2 is the temperature inside of the enclosure (T_{enc}) , which falls somewhere between the outdoor air temperature (T_{out}) and 18.3 °C, (the temperature at which heating is no longer required). The

enclosure temperature determines the heating output ($\dot{Q}_{\mathrm{H}}$) of the primary heat pump, which cannot be less than the full heating load of the home at the given outdoor temperature condition if auxiliary heating is to be avoided. Additionally, the range of possible enclosure temperatures is constrained to those which keep the compressor discharge temperatures (T_3 and T_7) below the cutoff temperature of the compressor (135 °C), and the evaporator pressure above the recommended minimum (234 kPa) [235]. Within the acceptable range, the enclosure temperature chosen should then be the one which yields the highest overall $\mathrm{COP}_{\mathrm{Sys2}}$ (ideally exceeding that of the compared system(s)). To select the most appropriate enclosure temperature for each outdoor temperature condition, a parametric analysis was performed to observe the outcomes of different enclosure temperatures, ranging from 0.5 °C above the outdoor temperature to 18 °C, at intervals of 0.5 °C.

The overall COP of the add-on cascade system ($\mathrm{COP}_{\mathrm{Sys2}}$) was calculated using Equations (3.22), (3.20), and (3.23). In Equation (3.21), compressor power consumption is approximated by assuming a heat loss factor of 10 % of the compressor power input, since total power consumption data was not available for the heat pump at such a low condenser pressure. Additionally the fan power consumption ($\mathcal{P}_{\mathrm{fan2}}$) for the secondary heat pump is only that of the secondary evaporator fan, since the condenser airflow is driven by the evaporator fan of the primary heat pump.

$$\dot{W}_{\mathrm{C2}} = \dot{m}_{\mathrm{r2}}(h_7 - h_6) \tag{3.20}$$

$$\mathcal{P}_{\mathrm{C2}} = \frac{\dot{W}_{\mathrm{C2}}}{0.9} \tag{3.21}$$

$$\mathcal{P}_{\mathrm{tot2}} = \mathcal{P}_{\mathrm{C2}} + \mathcal{P}_{\mathrm{fan2}} \tag{3.22}$$

$$\mathrm{COP}_{\mathrm{Sys2}} = \frac{\dot{Q}_{\mathrm{H}}}{\mathcal{P}_{\mathrm{tot1}} + \mathcal{P}_{\mathrm{tot2}}} \tag{3.23}$$

Chapter 4

Results and discussion

4.1 Primary heat pump model outcomes

The primary heat pump model was run for outdoor temperatures ranging from 18 °C to −30 °C temperatures at increments of 0.5 °C, and the generated parameters demonstrated the expected trends for a standard single-stage heat pump as outdoor temperature decreases (described in Chapter 1):

- Supply air temperature decreased with outdoor temperature.
- Mass flow rate decreased with outdoor temperature.
- T_3 (compressor discharge temperature) rose excessively starting below −12 °C.

The resulting isentropic efficiency (η_{is}) values followed a curve similar to that generated from published compressor data (Figure 3.6), as well as those found in the literature [232], in that it initially rose to a peak (in this case at a pressure ratio, R_p, of around 3.4), then decreased with increasing pressure ratio.

The minimum operating temperature of a heat pump is typically limited by the operating range of the compressor. Protective features in the compressor model used in this heat pump shut the system off when the discharge temperature reaches 135 °C [235], which modelling results showed occurs just above an outdoor temperature of −23 °C. Similarly, the suction pressure (p_2) drops below the minimum recommended pressure for the compressor (234 kPa, [235]) below an air temperature of −21.5 °C. Thus, the primary heat pump is assumed to shut off at −21.5 °C.

Figure 4.1 shows the primary heat pump's capacity at various outdoor temperatures,

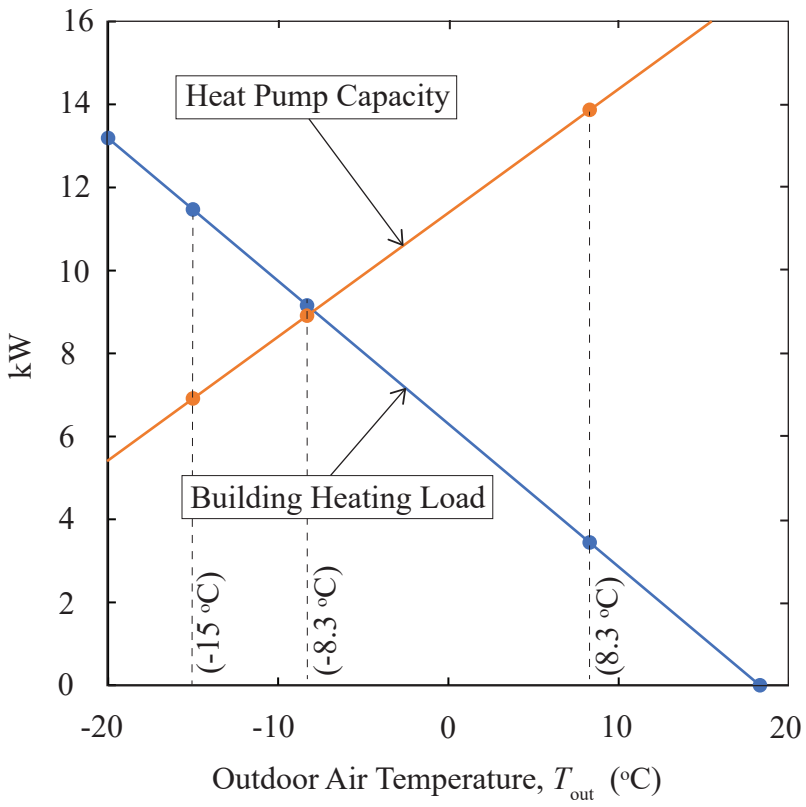

Figure 4.1: Graph showing the building heating load profile, heat pump capacity, and thermal balance point.

superimposed on the building heating load profile. Where the two lines intersect (known as the thermal balance point) indicates the temperature below which the heat pump alone can no longer supply the entire heating load and requires supplementation. For this system and sample home, the thermal balance point is reached at −7.9 °C. Additionally, with a single fan speed (as modelled), the supply air temperature drops below the comfortable 32.2 °C (90 °F) range at temperatures below 0.5 °C. Therefore, as expected, the primary heat pump alone would be unsuitable for heating the sample home in a cold climate.

4.2 System 1 results

Figure 4.2 shows the cycle of the primary heat pump operating at each of the three main test temperatures on a $T-s$ diagram, and Table 3 summarizes the results of the System 1 performance analysis. The primary heat pump requires no auxiliary heating at an outdoor temperature of 8.3 °C, a small amount at −8.3 °C, and substantial supplementation at −15 °C. $\mathrm{COP}_{\mathrm{Sys1}}$ decreases with the outdoor temperature and the supply air temperature predicted by the model is lower than the recommended minimum comfortable temperature of 32.2 °C [234] in the two negative outdoor temperature cases. The latter is true because, the heat pump only delivers supply air above 32.2 °C, when the heat pump capacity is 11.5 kW or higher. The outdoor air temperature that demands this capacity (although the heat pump cannot deliver it) is approximately −15°C, so in that particular temperature case the electric heating coil which delivers the remainder of the required heating will bring the supply air up to temperature. It should be noted

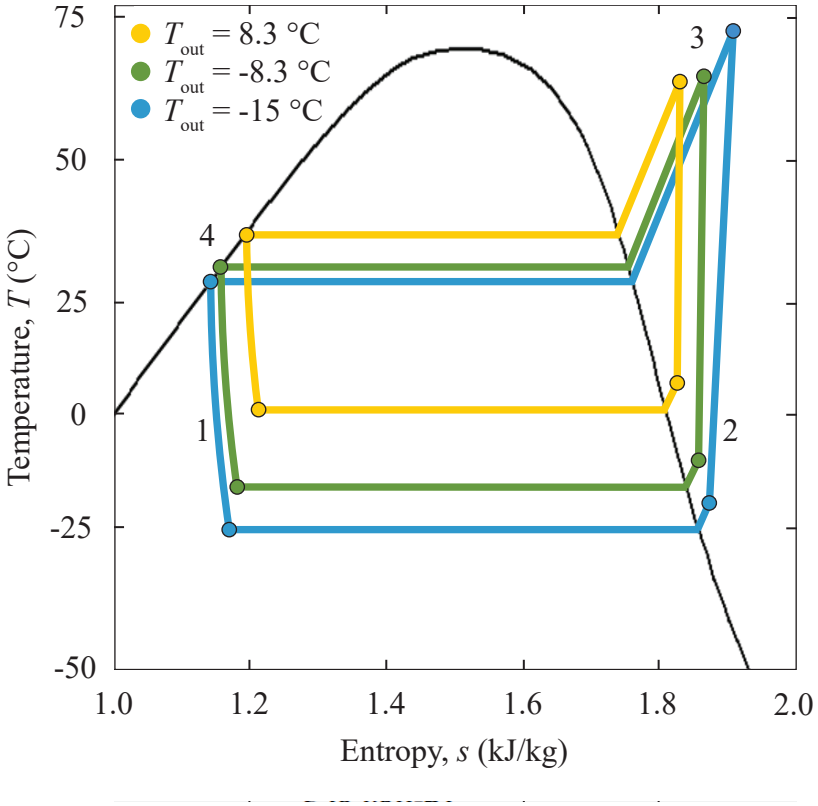

Figure 4.2: $T - s$ diagram showing the modelled heating cycle of the primary heat pump at each of the three tested outdoor air temperatures.

Table 3: Modelled performance of System 1 at the three tested outdoor air temperatures.

$T_{\mathbf{out}}$	8.3 °C	−8.3 °C	−15 °C
Home Heating Load (kW)	3.44	9.16	11.5
$\dot{Q}_{\mathbf{H}}$ **(kW)**	13.9	8.91	6.91
$\mathcal{P}_{\mathbf{tot}}$ **(kW)**	3.43	3.13	3.01
$\dot{Q}_{\mathbf{aux}}$ **(kW)**	0	0.247	4.56
$\mathbf{COP_{Sys1}}$	4.05	2.71	1.52

that this is only the case because the auxiliary coil is located inside the plenum of the air handler after the condenser heat exchanger. Supplementary heating inside the rooms (such as baseboard heating) would not have the same effect. Additionally, between 0.5 °C and −15 °C, auxiliary heating will not solve the supply air temperature issue, unless the heating output is intentionally increased to 11.5 kW. This is one reason why the actual heat pump has three indoor fan speeds which would keep supply air up to temperature in outdoor conditions down to −7.9 °C, as explained in Section 4.3.1.

4.3 System 2 results

For the analysis of the add-on cascade heat pump model, an enclosure temperature needed to be identified for each outdoor temperature case which would yield operating parameters that meet several requirements: sufficient heating output ($\dot{Q}_{\mathrm{H}}$, primary heat pump) to meet the home heating load at that outdoor temperature, comfortable supply air temperature (32.2 °C or higher), safe discharge temperature in both compressors (< 135 °C), and reasonable isentropic efficiency for both compression processes (defined in the previous section). At every outdoor temperature condition, the $\mathrm{COP}_{\mathrm{Sys2}}$ value increased with decreasing enclosure temperature, so the *minimum* enclosure temperature that met the other parameter requirements was selected in each case. This strategy also avoided unnecessary excess heating output that could lead to short-cycling (see Section 1.2.5).

At an outdoor air temperature of 8.3 °C, the add-on cascade model shows that there is no enclosure temperature that results in acceptable values for all of the observed operating parameters. However, 8.3 °C is a mild outdoor temperature for heating (suitable for a

single-speed heat pump) so the primary heat pump alone already performs very well at this temperature, as seen in Table 3. Therefore, the 8.3 °C outdoor temperature condition represents a scenario where the outdoor enclosure would be opened to allow the primary heat pump to operate alone, with the secondary heat pump turned off.

When T_{out} is −8.3 °C, all of the enclosure temperatures tested will result in sufficient heating output to the home, but the optimal enclosure temperature is 2 °C because this is the lowest temperature that also yields a reasonable compressor isentropic efficiency (η_{is}) value for the secondary compressor, and a supply air temperature of at least 32.2 °C. At this enclosure temperature, COP_{Sys2} is lower than COP_{Sys1} (2.43 versus 2.71). However, the cascade configuration has already extended the useful operating range of the primary heat pump by maintaining a comfortable supply air temperature at a colder outdoor temperature than could be achieved by the primary heat pump alone. The cycles performed by the heat pumps in System 2 when T_{out} is −8.3 °C are included in the $T - s$ diagram in Figure 4.3, with an enclosure temperature of 2 °C.

When the outdoor air temperature is −15 °C, both the heating output of the primary heat pump and the supply air temperature limit the enclosure temperature to a minimum of 0.5 °C. When T_{enc} is set to 0.5 °C, the resulting COP_{Sys2} is 1.64 compared to the System 1 COP of 1.52, so the add-on cascade system appears to be the more efficient option. However, the isentropic efficiency of the secondary compressor at that enclosure temperature is unrealistically low (0.34), as demonstrated by the unreasonable location of point 7_{a} in the blue secondary heat pump cycle in Figure 4.3. This outcome is a reflection of the low mass flow rate through the secondary compressor when the outdoor temperature is −15 °C, which is caused by lowered suction density (ρ_6) due to low

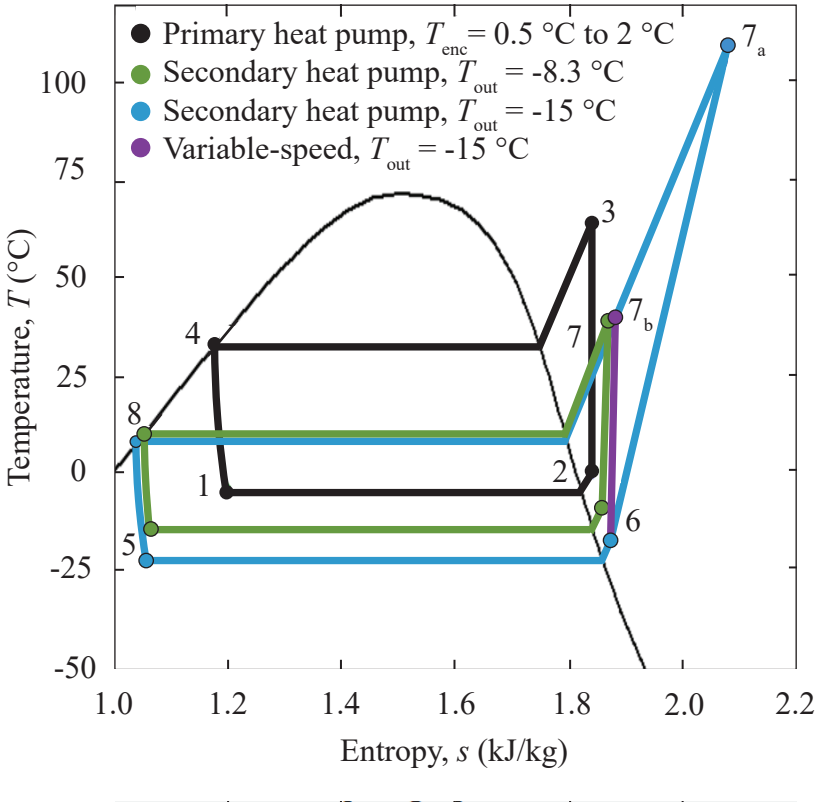

Figure 4.3: A $T-s$ diagram showing the modelled heating cycles of System 2 at outdoor temperatures of -8.3 °C and -15 °C. The purple line represents the alternate compression process at -15 °C when the mass flow rate is increased (as with a variable-speed compressor) but the enclosure temperature remains the same (0.5 °C).

evaporator pressure. In the System 2 model, Equation (3.3) dictates the location of state point 7, since all of the other variables in that equation are already determined. Too small of a mass flow rate requires a higher magnitude of $(h_7 - h_6)$ to achieve the required $\dot{Q}_{H2}$ value (which is also larger at low outdoor temperatures), so h_7 must increase (point 7 moves to the right on the $p-h$ diagram), decreasing the isentropic efficiency of the compression process, and increasing the compressor discharge temperature (T_7). Thus,

with a fixed compressor speed tying suction density to mass flow rate, the add-on cascade design cannot operate with all parameters within acceptable limits when T_{out} is −15 °C or lower.

However, if the mass flow rate of the secondary compressor could be increased from 0.0309 kg/s to 0.0395 kg/s (a 28 % increase) by using a variable-speed compressor, then the isentropic efficiency of the secondary compressor would be 0.98, which is more reasonable for the pressure ratio (R_{p2}). This change significantly decreases the compression work ($\dot{W}_{C2}$ = 1.41 kW rather than 3.17 kW) and allows for up to 2.70 kW of secondary compressor heat loss (R_{lost2} of 66 %) while still matching the COP of System 1. Assuming a more realistic heat loss of 10 %, the resulting COP_{Sys2} is 2.28, which is substantially higher than the System 1 COP of 1.52. Figure 4.3 shows the heat pump cycles of System 2 when T_{out} is −8.3 °C and −15 °C. The cycle of the primary heat pump (black lines) is nearly the same for both temperature conditions since the enclosure differs by only 1.5 °C, whereas the secondary heat pump cycle (green for −8.3 °C and blue for −15 °C) differs with the outdoor air temperature. The purple line represents the System 2 cycle with the previously-described 28 % increase in mass flow rate, resulting in point 7_{b} for a more reasonable discharge temperature (T_7) and isentropic efficiency (η_{C2}).

Based on the results at −8.3 °C and −15 °C, I concluded that the potential temperature range where System 2 is superior, as well as the cutoff temperature for that system, must occur between those two outdoor temperatures. Therefore, I re-ran the model at several additional temperature conditions (−8 °C through −15 °C in increments of 1 °C) to locate these transition points. The results showed that the COP of System 2 surpassed that of System 1 starting at −10 °C, and that System 2 can no longer maintain

reasonable operating parameters when the outdoor temperature reaches −13 °C.

In light of the benefits that resulted from modifying the mass flow rate when T_{out} is −15 °C, which allowed System 2 to continue to operate at that temperature within acceptable parameters, I replicated this mass flow modification for all of the temperature cases, always assuming an η_2 value of 0.98, and a secondary compressor heat loss (R_{lost2}) of 10 %. I also expanded the tested outdoor temperatures to include −20 °C, −21.5 °C (the cutoff point of System 1), −23 °C, and −25 °C, in order to locate the minimum operating temperature of System 2 with a variable-speed compressor. However, when the variable-speed compressor is introduced, two viable enclosure temperature options arise: one that has maximal COP_{Sys2}, and the other which has minimal excess heating capacity ($\dot{Q}_{\text{exc}}$) to reduce efficiency losses from short-cycling (discussed in Section 1.2.5). In the end, both of these selection methods were used at each temperature, resulting in the grey and yellow lines (respectively) in Figure 4.4.

Figure 4.4 compares the overall COP of System 1 and the three versions of System 2 that were ultimately modelled. The performance lines overlap when T_{out} is −7.9 °C or higher since in those conditions the primary heat pump operates independently in all of the designs. The operating range of System 1 extends down to the minimum operating temperature of the primary heat pump (−23 °C), using heat from a supplementary electric coil starting below −7.9 °C when the primary heat pump can no longer meet the home heating load, but it still delivers an uncomfortably cool supply air temperature between outdoor temperatures of −7.9 °C and −15 °C. In System 2, which has no supplementary electric heating coil, −7.9 °C is the point at which the enclosure is closed to recirculate the air inside and the secondary heat pump is activated. The addition of

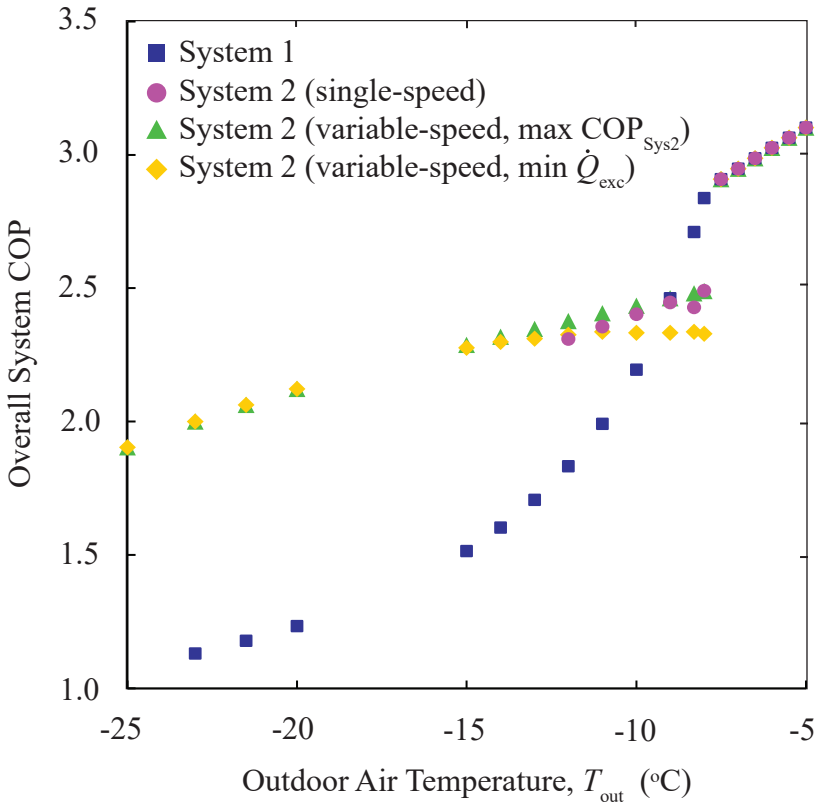

Figure 4.4: Graph of overall system COP versus outdoor air temperature comparing all of the modelled systems.

the enclosure and secondary single-speed heat pump (orange System 2 line) extends the effective operating range of the primary heat pump by enabling it to supply sufficiently warm air, and meet the entire home heating load, down to −12 °C, while offering superior overall COP (compared to System 1) starting below −9 °C. However, System 2 could continue to operate down to an even colder temperature of −20 °C, or even −25 °C, if it used a variable-speed compressor capable of operating at the evaporator pressures required, and of increasing the mass flow rate by a factor of 2.1–5.1, respectively. Both variable-speed versions of System 2 result in superior overall COP compared to System

1 at all outdoor temperatures below −9 °C, while meeting all of the other operating parameter requirements.

4.3.1 Effects of modified airflow rate

According to Equation 3.16, when $\dot{Q}_{\mathrm{H}}$ and T_{ret} are constant, lowering the indoor fan speed (and therefore $\dot{m}_{\mathrm{air}}$) results in a higher supply air temperature (T_{supp}). The heat pump models developed assume a constant maximum indoor fan speed, but in reality, the heat pump has a three-speed indoor fan. The ratio between the minimum indoor airflow rate and the maximum is 1400/1800 CFM or 0.78, so switching to the the minimum fan speed will cause the temperature change of the air to be increased by a factor of 1.3. Thus, when examining the results, outdoor temperatures which yield supply air temperatures as low as 29.6 °C could be brought up into the comfortable range, simply by switching to the lowest fan speed. This aligns well with the outcomes of the primary heat pump model since, below 0.5 °C, the supply temperature is insufficient, but still within the range that can be compensated for by a reduction of the indoor fan speed, down to the thermal balance point (−7.9 °C) when the secondary heat pump kicks in to augment the supply temperature and heating output. The variable-speed System 2 design which minimizes system oversizing relies on this fan modulation to maintain sufficient supply air temperature at the lowered enclosure temperatures that yield the results shown by the yellow line in Figure 4.4.

The fact that the airflow over the secondary condenser is driven by the primary evaporator should further increase the System 2 performance. This is because the air flow

rate of the outdoor evaporator fan is 4046 CFM (1.91 m^3/s) rather than the maximum of 1800 CFM (0.850 m^3/s) of the indoor fan that would otherwise be used. In both cases, the air would be directed through a box of equal cross sectional area containing the condenser coil, so using the evaporator fan results in a velocity that is approximately 2.25 times higher. An increased air velocity will increase the convective heat transfer coefficient for the secondary heat pump condenser, thereby improving heat transfer and potentially allowing for a lower ΔT_{cond2}. A lower ΔT_{cond2} would mean the condensing pressure could be lowered, reducing the work of the secondary compressor, and improving the overall COP of the system.

4.4 Comparative performance evaluation

For comparison, the data from Table 2 was used to determine overall system COP for each market-available cold climate heat pump when made to deliver the full heating load of the sample home at −15 °C. First the capacity of each heat pump at −15 °C was determined using the rated capacity and the percent rated capacity at −15 °C. Then, the published COP value at −15 °C was used to determine the power consumption using Equation (1.1). Finally, a $\dot{Q}_{\text{aux}}$ value was introduced to make up any missing capacity to meet the home heating load, and a new COP_{Sys} was calculated using Equation (3.12). Table 4 shows a comparison of the market-available systems which yielded the five highest overall COP_{Sys} values, to the systems modelled in this study. The original System 2 design (with both compressors being single-speed) is not included since it ceases to function below −12 °C. However, both of the variable-speed System 2 designs offer

Table 4: Performance of each modelled system compared to selected market-available cold climate heat pumps when operating at an outdoor temperature of −15 °C.

System Name	**Rated Heating Cap. (kBTU/hr)**	$\dot{Q}_{\mathbf{load}}$ **(kW)**	$\dot{Q}_{\mathbf{H}}$ **(kW)**	$\mathcal{P}_{\mathbf{tot}}$ **(kW)**	$\dot{Q}_{\mathbf{aux}}$ **(kW)**	**System COP**
System 1	48	11.5	6.91	3.01	4.56	1.52
System 2 - VS, max COP	48	11.5	12.6	2.15	0	2.29
System 2 - VS, min $\dot{Q}_{\text{exc}}$	48	11.5	11.5	1.78	0	2.28
LG (LUU480HHV)	50	11.5	14.7	6.94	0	2.11
Bryant (280ANV036)	35.4	11.5	9.75	3.56	1.75	2.17
Bryant (280ANV048)	45.5	11.5	11.1	4.94	0.43	2.14
Carrier (25VNA036)	35.4	11.5	9.75	3.56	1.75	2.17
Carrier (25VNA048)	45.5	11.5	11.1	4.94	0.43	2.14

a superior overall COP compared to System 1 and all of the market-available systems. The most competitive systems on the market were the Bryant (280ANV036) and Carrier (25VNA036), which are both single-stage variable-speed heat pumps with no other distinct cold climate features, but both contain a charge compensator (discussed further in Section 2.1.4). Further analysis would be required to determine which of the compared systems offers the best overall seasonal efficiency when performance at all relevant temperatures, partial load cycling losses, and defrosting are factored in. However, even this simple comparison at one temperature condition with an equal load demonstrates how standardized comparative analyses are helpful in identifying the most effective cold climate heat pump technologies for a specific application.

4.5 Reliability of the model

By making reasonable assumptions, the heat pump models developed in this study were able to meet the design objectives, while predicting realistic operating parameters which fall within the capabilities of the actual systems and components involved. Nonetheless,

heat pump performance is influenced by a large number of variables which can be challenging to model accurately. Thus, the thermodynamic models and assumptions used in this study should be validated against empirical operational data (where it was lacking), or a prototype, in order to be fully confident in design criteria for the add-on unit. In particular, the variable-speed analysis could be re-done using manufacturer data for a suitable variable-speed heat pump, and its actual compressor. Currently, the compressor mass flow rate equation of the single-speed compressor (Equation 3.7) is being applied in the variable-speed designs as well.

Additionally, the models were developed based on the parameters of a specific heat pump, and specific home heating profile, so the preferred enclosure temperatures likely only apply to this particular system. An add-on heat pump and its control system would need to be customized for each product line with significantly different performance, and the heating load profile to which it is being applied. Nonetheless this study has provided a meaningful comparison demonstrating the potential of this design to offer excellent cold climate performance, and the feasibility of creating such a system with existing heat pumps.

4.6 Design limitations and advantages

The proposed design has some limitations, which may be mitigated or offset by advantages and opportunities that it offers.

- *Cycling losses*: Since the primary heat pump is single-speed, Figure 3.12 shows that the output will be excessive at temperatures above -7.9 °C. This will inevitably

result in efficiency losses during partial load conditions and cooling mode (not examined in this study) due to the system cycling on and off. However, there are some expected efficiency gains that are also not quantified in this study, which would help to offset these losses. First, the heat lost from the primary compressor would be recovered in the enclosure, thereby reducing the actual heating output required from the secondary heat pump. Additionally, the absence of a second condenser fan will save energy, and the higher airflow rate from using the primary evaporator fan inside the enclosure will increase the heat transfer coefficient at the secondary condenser, which may improve its performance. It would be worthwhile to model a version of the proposed design which uses the variable-speed unit as the *primary* heat pump (with a single-speed secondary) so that it is the more flexible variable-speed heat pump that operates alone during times of low demand, thereby reducing short-cycling.

- *Space*: The design will require more outdoor space than a typical heat pump system, which may be a deterrent to some homeowners with space constraints. However, other single-speed heat pumps exist that are of the "side discharge" variety, which have a much slimmer profile than the Carrier unit that was modelled. Using side discharge heat pumps could make the proposed design much more compact.

- *Cost*: The proposed add-on cascade system will use more materials than the all-in one ccASHP designs on the market, but this does not necessarily translate to a higher upfront cost for the homeowner due to differences in the component types and complexity involved, as well as the possibility of utilizing an existing furnace

air-handler or heat pump system to minimize the new components that must be purchased. Performing a complete and accurate cost analysis of the proposed design was not possible during this study, since manufacturer component prices are not available to the general public, and HVAC installers only provide quotes that include complete system installation. A prototype should be built to determine the actual upfront cost of the system for comparison to other cold climate heat pumps, as well as to conduct installed seasonal performance testing to determine comparative payback periods. The superior cold weather performance of the cascade add-on design demonstrated by this study could result in an accelerated payback period for the proposed system, due to reduced energy consumption. Additionally, the enclosure protects the evaporator unit of the primary heat pump from winter weather, which could result in extended lifespan of the primary unit. The enclosure design could also allow for the inclusion of a sensor inside to immediately alert the homeowner of a refrigerant leak, resulting in faster repair of the issue. This could help minimize refrigerant loss (and associated global warming effects), as well as prevent performance losses or compressor damages due to low refrigerant charge.

Chapter 5

Conclusions

5.1 Conclusions

This thesis encompassed two main parts: 1) an analysis of cold climate heat pump technologies used in market-available residential systems and opportunities for further advancement described in the literature, and 2) thermodynamic modelling and comparative analysis of a new add-on cascade heat pump design using two existing and affordable heat pumps. The market analysis showed that cold climate heat pumps available today use inverter driven variable-speed compressors and some brands also incorporate more complex cycle types and additional, specialized components requiring more sophisticated controls. These features lead to increased upfront costs, but yield a significant extension of operating temperature range, and increased capacity at low outdoor temperatures compared to a traditional single-speed heat pump. Nonetheless, most market-available ccASHPs still experience significant reductions in heating capacity by -15 °C, and most shut off at a minimum temperature that is within the range of temperatures commonly

experienced in many cold climates, when reliable home heating is most critical. Thus, further improvements to cold climate heat pumps are still needed, and will help to make ccASHPs an attractive and reliable choice for Canadian homeowners.

The thermodynamic modelling analysis of the baseline (System 1) and proposed system (System 2) showed that, when composed of two identical single-speed heat pumps, System 2 can only operate down to a temperature of around −12 °C, but offers superior supply air temperature below −7.9 °C, and a superior COP below −9 °C. Additionally, the use of a variable-speed compressor in the secondary heat pump could expand the operating range of System 2 to that of System 1 (−21.5 °C) or lower, while offering a substantially higher overall COP at all temperatures below −9 °C. Furthermore, by making use of the multi-speed capabilities of the indoor fan, the variable-speed version of System 2 can operate at lower enclosure temperatures that match the heating output of the primary heat pump to the demand of the home, virtually eliminating cycling due to oversizing once the add-on system is activated (below the thermal balance point of −7.9 °C).

The overall system COP of the proposed add-on cascade system (System 2) with a variable-speed secondary compressor exceeds that of System 1 (a single-speed heat pump with auxiliary electric heating) as well as the five market-available cold climate heat pumps which exhibit the highest overall COP at −15 °C for the required heating load (supplemented as needed with electric resistance heating). While only six heat pump models on the market could meet the full heating load of the sample home at −15 °C without auxiliary heating, the proposed add-on cascade system with a variable-speed compressor in the secondary heat pump, could meet the full heating demand of the home

at even colder temperatures, with the minimum outdoor temperature determined by the speed modulation and pressure ranges of the secondary compressor.

5.2 Recommendations

Given the promising results of this study, I would recommend that the following additional work be completed:

1. Identify variable-speed heat pumps that could serve as the secondary heat pump, and incorporate performance data from this heat pump and its variable-speed compressor into the model to validate the results and determine the full potential operating temperature range.

2. Explore the effect of using a variable-speed heat pump as the primary, with a single-speed heat pump as the secondary, as in the multi-function cascade design proposed by Yang et al. [58]. Such a design might allow for greater flexibility in heating output that would help to minimize cycling losses during partial load conditions (and cooling conditions), but have a similar upfront cost and performance benefits.

3. Build a prototype and conduct further comparative studies which consider cycling of the primary heat pump during partial load conditions, control requirements, defrosting performance, cooling operation, as well as comparative operational and upfront costs.

4. Explore the use of alternative refrigerants in one or both systems, including low GWP drop-in replacements suggested by Hakkaki-Fard et al. [158], to determine if

performance and operating range of System 2 could be further improved without the need to modify the components of the heat pumps.

5.3 Contributions

The market overview and analysis conducted in this thesis provides the first comprehensive review of market-available residential cold climate heat pump technologies and their capabilities, as well as offers a summary of additional developments found in the literature which present opportunities to further improve cold climate heat pump performance. This thesis has also introduced a previously unexplored cascade heat pump design which uses a shared air-space as a heat transfer medium between two sequential heat pump systems. Such a design has potential for other applications, such as large-scale refrigeration, which might make productive use of this cool-temperature enclosed space during the heating season. The analysis presented here is also the first to explore and demonstrate the potential for using relatively simple, inexpensive, and well-established market-available heat pumps to create a multi-function cascade system for cold climate use. By leveraging existing production lines, supply chains, technician training, and distribution streams, such a design has the potential to expedite the uptake of electric heat pumps for home heating in cold climates around the world, leading to a rapid and significant reduction of GHG emissions from the residential building sector.

Bibliography

[1] UN. Sustainable development goal 13 - Take urgent action to combat climate change and its impacts. Accessed: Oct. 6, 2022. https://www.un.org/sustainabledevelopment/climate-change/.

[2] H.-O. Pörtner, D. C. Roberts, H. Adams, C. Adler, P. Aldunce, E. Ali, R. A. Begum, R. Betts, R. B. Kerr, R. Biesbroek, et al. Climate change 2022: Impacts, adaptation and vulnerability. *IPCC Sixth Assessment Report*, 2022.

[3] Natural Resources Canada. Residential space heating system stock share. Accessed Jul. 7, 2022. https://oee.nrcan.gc.ca/.

[4] Natural Resources Canada. Residential GHG emissions by energy source and end use. Accessed Jul. 7, 2022. https://oee.nrcan.gc.ca/.

[5] A. Szekeres and J. Jeswiet. Heat pumps in Ontario. *International Journal of Energy and Environmental Engineering*, 10(2):157–179, 2019.

[6] W. Wei, L. Ni, L. Xu, Y. Yang, and Y. Yao. Application characteristics of variable refrigerant flow heat pump system with vapor injection in severe cold region. *Energy & Buildings*, 211:109798, 2020.

[7] Statistics Canada. Primary heating systems and type of energy. Table 39-10-0286-01. Accessed Jun. 28, 2022. https://doi.org/10.25318/3810028601-eng.

[8] J. W. Mitchell and J. E. Braun. *Principles of heating, ventilation, and air conditioning in buildings*. John Wiley & Sons, 2013.

[9] A. Redón, E. Navarro-Peris, M. Pitarch, J. Gonzálvez-Macia, and J. M. Corberán. Analysis and optimization of subcritical two-stage vapor injection heat pump systems. *Applied Energy*, 124:231–240, 2014.

[10] S. Jiang. Air-source heat pump systems. In R. Wang and X. Zhai, editors, *Handbook of Energy Systems in Green Buildings*, pages 349–391. Springer, 2018.

[11] X. Biao, H. Tongyi, H. Lin, Y. Yan, S. Yuying, and W. Wei. Experimental study of an improved air-source heat pump system with a novel three-cylinder two-stage variable volume ratio rotary compressor. *International Journal of Refrigeration*, 100:343–353, 2019.

[12] B. Huang, Q. Jian, L. Luo, and J. Zhao. Experimental study of enhancing heating performance of the air-source heat pump by using a novel heat recovery device designed for reusing the energy of the compressor shell. *Energy Conversion and Management*, 138:38–44, 2017.

[13] L. Rajapaksha and K. O. Suen. Influence of liquid receiver on the performance of reversible heat pumps using refrigerant mixtures. *International Journal of Refrigeration*, 27(1):53–62, 2004.

[14] B. Shen, O. Abdelaziz, V. Baxter, and E. Vineyard. Cold climate heat pump using tandem vapor-injection compressors. In *springer Proceedings in Energy – Cold Climate HVAC 2018*, pages 429–439. Springer, 2019.

[15] J. M. Corberán, I. O. Martínez, and J. Gonzálvez. Charge optimisation study of a reversible water-to-water propane heat pump. *International Journal of Refrigeration*, 31(4):716–726, 2008.

[16] D. Lee, M. Lee, W. Cho, and Y. Kim. Performance improvement of heat pumps by optimizing refrigerant charge using novel variable liquid-line length system. *Applied Thermal Engineering*, 196:117287, 2021.

[17] S. B. Hong, J. W. Yoo, and M. S. Kim. A theoretical refrigerant charge prediction equation for air source heat pump system based on sensor information. *International Journal of Refrigeration*, 104:335–343, 2019.

[18] J. Sieres, I. Ortega, F. Cerdeira, and E. Álvarez. Influence of the refrigerant charge in an R407C liquid-to-water heat pump for space heating and domestic hot water production. *International Journal of Refrigeration*, 110:28–37, 2020.

[19] T. Kropas, G. Streckienė, and J. Bielskus. Experimental investigation of frost formation influence on an air source heat pump evaporator. *Energies*, 14(18):5737, 2021.

[20] S. Li, D. Bacellar, C. Martin, C. Lee, S. Beaini, and J. Leverette. Experimental evaluation of frost development on tube-fin heat exchangers: Fin types, fin

densities, (super) hydrophobic and icephobic coatings. *ASHRAE Transactions*, 127(1):487–495, 2021.

[21] W. Zhiyi, W. Xinmin, and D. Zhiming. Defrost improvement by heat pump refrigerant charge compensating. *Applied Energy*, 85(11):1050–1059, 2008.

[22] M. Qu, L. Xia, S. Deng, and Y. Jiang. Improved indoor thermal comfort during defrost with a novel reverse-cycle defrosting method for air source heat pumps. *Building and Environment*, 45(11):2354–2361, 2010.

[23] S. S. Bertsch and E. A. Groll. Two-stage air-source heat pump for residential heating and cooling applications in northern U.S. climates. *International Journal of Refrigeration*, 31(7):1282–1292, 2008.

[24] H. Cheung and J. E. Braun. Performance comparisons for variable-speed ductless and single-speed ducted residential heat pumps. *International Journal of Refrigeration*, 47:15–25, 2014.

[25] K. P. Kone and N. Fumo. Dehumidification performance of a variable speed heat pump and a single speed heat pump with and without dehumidification capabilities in a warm and humid climate. *Energy Reports*, 6:1696–1701, 2020.

[26] J. D. Munk, R. K. Jackson, A. O. Odukomaiya, and A. C. Gehl. Field study of performance, comfort, and sizing of two variable-speed heat pumps installed in a single 2-story residence. *ASHRAE Transactions*, 120(2), 2014.

[27] IEA Heat Pump Conference 2005. *Review of air-source heat pumps for low temperature climates*, 8, 2005.

[28] L. Zhang, Y. Jiang, J. Dong, and Y. Yao. Advances in vapor compression air source heat pump system in cold regions: A review. *Renewable and Sustainable Energy Reviews*, 81:353–365, 2018.

[29] C. Park, H. Lee, Y. Hwang, and R. Radermacher. Recent advances in vapor compression cycle technologies. *International Journal of Refrigeration*, 60:118–134, 2015.

[30] A. S. Gaur, D. Z. Fitiwi, and J. Curtis. Heat pumps and our low-carbon future: A comprehensive review. *Energy Research & Social Science*, 71:101764, 2021.

[31] K. J. Chua, S. K. Chou, and W. M. Yang. Advances in heat pump systems: A review. *Applied Energy*, 87(12):3611–3624, 2010.

[32] L. Ni, J. Dong, Y. Yao, C. Shen, D. Qv, and X. Zhang. A review of heat pump systems for heating and cooling of buildings in China in the last decade. *Renewable Energy*, 84:30–45, 2015.

[33] I. Staffell, D. Brett, N. Brandon, and A. Hawkes. A review of domestic heat pumps. *Energy & Environmental Science*, 5(11):9291–9306, 2012.

[34] N. Serey, D. Ahmad, and H. Jouhara. Air-to-air heat pump: review of recent advances and future potential. In *E3S Web of Conferences*, volume 116, page 00074. EDP Sciences, 2019.

[35] R. Valancius, R. M. Singh, A. Jurelionis, and J. Vaiciunas. A review of heat pump systems and applications in cold climates: Evidence from Lithuania. *Energies*, 12(22):4331, 2019.

[36] P. Carroll, M. Chesser, and P. Lyons. Air source heat pumps field studies: a systematic literature review. *Renewable and Sustainable Energy Reviews*, 134:110275, 2020.

[37] N. Enteria, O. Cuartero-Enteria, and T. Sawachi. Review of the advances and applications of variable refrigerant flow heating, ventilating, and air-conditioning systems for improving indoor thermal comfort and air quality. *International Journal of Energy and Environmental Engineering*, 11(4):459–483, 2020.

[38] C. W. Roh, J. W. Yoo, and M. S. Kim. Vapor refrigerant injection techniques for heat pump systems: the latest literature review and discussion. *International Journal of Air-Conditioning and Refrigeration*, 22(01):1430002, 2014.

[39] X. Xu, Y. Hwang, and R. Radermacher. Refrigerant injection for heat pumping/air conditioning systems: literature review and challenges discussions. *International Journal of Refrigeration*, 34(2):402–415, 2011.

[40] J. Sarkar. Ejector enhanced vapor compression refrigeration and heat pump systems – a review. *Renewable and Sustainable Energy Reviews*, 16(9):6647–6659, 2012.

[41] P. Gullo, A. Hafner, K. Banasiak, S. Minetto, and E. E. Kriezi. Multi-ejector concept: A comprehensive review on its latest technological developments. *Energies*, 12(3):406, 2019.

[42] Z. Aidoun, K. Ameur, M. Falsafioon, and M. Badache. Current advances in ejector modeling, experimentation and applications for refrigeration and heat pumps. Part 1: Single-phase ejectors. *Inventions*, 4(1):15, 2019.

[43] Z. Aidoun, K. Ameur, M. Falsafioon, and M. Badache. Current advances in ejector modeling, experimentation and applications for refrigeration and heat pumps. Part 2: two-phase ejectors. *Inventions*, 4(1):16, 2019.

[44] S. Boahen and J. Choi. Research trend of cascade heat pumps. *Science China Technological Sciences*, 60(11):1597–1615, 2017.

[45] M. Pan, H. Zhao, D. Liang, Y. Zhu, Y. Liang, and G. Bao. A review of the cascade refrigeration system. *Energies*, 13(9):2254, 2020.

[46] P. Bansal. A review–Status of CO_2 as a low temperature refrigerant: Fundamentals and R&D opportunities. *Applied Thermal Engineering*, 41:18–29, 2012.

[47] M. Mohanraj, C. Muraleedharan, and S. Jayaraj. A review on recent developments in new refrigerant mixtures for vapour compression-based refrigeration, air-conditioning and heat pump units. *International Journal of Energy Research*, 35(8):647–669, 2011.

[48] M. S. Patil, J.-H. Seo, and M.-Y. Lee. Heat transfer characteristics of the heat exchangers for refrigeration, air conditioning and heat pump systems under frosting, defrosting and dry/wet conditions–a review. *Applied Thermal Engineering*, 113:1071–1087, 2017.

[49] M. Song, S. Deng, C. Dang, N. Mao, and Z. Wang. Review on improvement for air source heat pump units during frosting and defrosting. *Applied Energy*, 211:1150–1170, 2018.

[50] J. Al Douri, K. S. Hmood, V. Apostol, H. Pop, S. J. Alqaisy, and E. B. Ibrean. Review regarding defrosting methods for refrigeration and heat pump systems. In *E3S Web of Conferences*, volume 286, page 01012. EDP Sciences, 2021.

[51] Y. Zhang, G. Zhang, A. Zhang, Y. Jin, R. Ru, and M. Tian. Frosting phenomenon and frost-free technology of outdoor air heat exchanger for an air-source heat pump system in China: An analysis and review. *Energies*, 11(10):2642, 2018.

[52] Z. Zhang, D. Wang, C. Zhang, and J. Chen. Electric vehicle range extension strategies based on improved AC system in cold climate–A review. *International Journal of Refrigeration*, 88:141–150, 2018.

[53] A. M. Bahman, E. A. Groll, W. T. Horton, and J. E. Braun. Technologies to improve the performance of A/C systems in hot climate regions. In *Proc. International Refrigeration and Air Conditioning Conference*, 2014.

[54] Z.-R. Peng, G.-B. Wang, and X.-R. Zhang. Thermodynamic analysis of novel heat pump cycles for drying process with large temperature lift. *International Journal of Energy Research*, 43(8):3201–3222, 2019.

[55] O. Bamigbetan, T. M. Eikevik, P. Nekså, and M. Bantle. Review of vapour compression heat pumps for high temperature heating using natural working fluids. *International Journal of Refrigeration*, 80:197–211, 2017.

[56] A. Mota-Babiloni, M. M. Joybari, J. Navarro-Esbrí, C. Mateu-Royo, Á. Barragán-Cervera, M. Amat-Albuixech, and F. Molés. Ultralow-temperature refrigeration

systems: Configurations and refrigerants to reduce the environmental impact. *International Journal of Refrigeration*, 111:147–158, 2020.

[57] M. Jesper, F. Schlosser, F. Pag, T. G. Walmsley, B. Schmitt, and K. Vajen. Large-scale heat pumps: Uptake and performance modelling of market-available devices. *Renewable and Sustainable Energy Reviews*, 137:110646, 2021.

[58] Y. Yang, R. Li, Y. Zhu, Z. Sun, and Z. Zhang. Experimental and simulation study of air source heat pump for residential applications in northern China. *Energy & Buildings*, 224:110278, 2020.

[59] J. Shen, T. Guo, Y. Tian, and Z. Xing. Design and experimental study of an air source heat pump for drying with dual modes of single stage and cascade cycle. *Applied thermal engineering*, 129:280–289, 2018.

[60] E. Bellos and C. Tzivanidis. A theoretical comparative study of CO_2 cascade refrigeration systems. *Applied Sciences*, 9(4):790, 2019.

[61] I. S. Hwang and Y. L. Lee. Cascade heat pump dryer performance improvement using a solar collector. *Journal of Engineering and Applied Sciences*, 10(2):782–787, 2015.

[62] M. Qu, T. Li, S. Deng, Y. Fan, and Z. Li. Improving defrosting performance of cascade air source heat pump using thermal energy storage based reverse cycle defrosting method. *Applied Thermal Engineering*, 121:728–736, 2017.

[63] M. Qu, Y. Tang, T. Zhang, Z. Li, and J. Chen. Experimental investigation on the multi-mode heat discharge process of a PCM heat exchanger during TES based

reverse cycle defrosting using in cascade air source heat pumps. *Applied Thermal Engineering*, 151:154–162, 2019.

[64] Y. Song, D. Li, D. Yang, L. Jin, F. Cao, and X. Wang. Performance comparison between the combined R134a/CO_2 heat pump and cascade R134a/CO_2 heat pump for space heating. *International Journal of Refrigeration*, 74:592–605, 2017.

[65] W. Wang, Q. Zhou, G. Tian, B. Hu, Y. Li, and F. Cao. The intermediate temperature optimization for cascade refrigeration system and air source heat pump via extreme seeking control. *International Journal of Refrigeration*, 117:150–162, 2020.

[66] O. A. Zuev, S. A. Garanov, E. V. Ivanova, and A. S. Karpukhin. Investigation of the efficiency of autocascade and cascade heat pumps in cold climate. *Chemical and Petroleum Engineering*, 56(5–6):448–455, 2020.

[67] R. Soltani, I. Dincer, and M. A. Rosen. Comparative performance evaluation of cascaded air-source hydronic heat pumps. *Energy Conversion and Management*, 89:577–587, 2015.

[68] D. H. Kim, H. S. Park, and M. S. Kim. Characteristics of R134a/R410a cascade heat pump and optimization. In *Proc. International Refrigeration and Air Conditioning Conference*. Purdue University, 2012.

[69] D. H. Kim, H. S. Park, and M. S. Kim. The effect of the refrigerant charge amount on single and cascade cycle heat pump systems. *International journal of refrigeration*, 40:254–268, 2014.

[70] G. Yan, Q. Jia, and T. Bai. Experimental investigation on vapor injection heat pump with a newly designed twin rotary variable speed compressor for cold regions. *International Journal of Refrigeration*, 62:232–241, 2016.

[71] C. Tian, N. Liang, W. Shi, and X. Li. Development and experimental investigation on two-stage compression variable frequency air source heat pump. In *Proc. International Refrigeration and Air Conditioning Conference*. Purdue University, 2006.

[72] B. Shen, O. Abdelaziz, C. K. Rice, V. D. Baxter, and P. Hung. Cold climate heat pumps using tandem compressors. Technical report, Oak Ridge National Laboratory, Oak Ridge, TN, 2016.

[73] R. K. Johnson. Measured performance of a low temperature air source heat pump. Technical report, National Renewable Energy Laboratory, Golden, CO, 2013.

[74] R. S. Kamel, A. S. Fung, and P. R. H. Dash. Solar systems and their integration with heat pumps: A review. *Energy and Buildings*, 87:395–412, 2015.

[75] D. L. Loveday. Solar-assisted heat pump systems: Assessment of an example using profiled steel cladding. *Building services engineering research & technology*, 13(1):37–42, 1992.

[76] Mistubishi. *Heat pump service manual. Document#: OCH750B.* Tokyo, Japan, 2021. https://www.mitsubishitechinfo.ca/.

[77] Mistubishi. *Heat pump service manual. Document#: OCH607A.* Tokyo, Japan, 2021. Accessed October 31, 2022. https://www.mitsubishitechinfo.ca/.

[78] Mistubishi. *Heat pump service manual. Document#: OCH567.* Tokyo, Japan, 2014. Accessed October 31, 2022. https://www.mitsubishitechinfo.ca/.

[79] Mistubishi. Heat pump submittal data: PVA-A30AA7 & PUZ-HA30NHA5. Form # SB_PVA-A30AA7_PUZ-HA30NHA5_201806, 2017.

[80] Mistubishi. Heat pump submittal data: PVA-A36AA7 & PUZ-HA36NHA5. Form #: SB_PVA-A36AA7_PUZ-HA36NHA5_201806, 2017.

[81] Mistubishi. Heat pump submittal data: PVA-A42AA7 & PUZ-HA42NKA. Form #: SB_PVA-A42AA7_PUZ-HA42NKA_201806, 2017.

[82] Mistubishi. Heat pump submittal data: PVAA30AA7 & PUZHA30NKA. Form #: SB_PVA-A36AA7_PUZ-HA36NKA_202103, 2021.

[83] Mistubishi. Heat pump submittal data: PVAA36AA7 & PUZHA36NKA. Form No. SB_PVA-A36AA7_PUZ-HA36NKA_202103, 2021.

[84] Mistubishi. Heat pump submittal data: PVAA42AA7 & PUZHA42NKA1. Form #: PVA-A42AA7 & PUZ-HA42NKA1 - 202103, 2021.

[85] Tosot. T-Unix universal DC inverter ducted central heat pump. Accessed: Oct. 6, 2022. https://www.tosot-na.com/tosot-t-unix/t-unix/.

[86] Tosot. *DC inverter heat pump condensing unit service manual.* Accessed: Oct. 30, 2022. https://www.tosot-na.com/tosot-doc/service-manuals/Unix/Service-Manual_Unix.pdf.

[87] LG. *Single zone LG RED vertical air handler unit engineering manual. Document #: EM_SZ_LGRED_VAHU_07_21.* Alpharetta, GA, USA, 2021. Accessed Oct. 31, 2022. https://lghvac.com/resources/.

[88] Northeast Energy Efficiency Partnerships, Inc. NEEP's cold climate air source heat pump list. Accessed July 19, 2022. https://ashp.neep.org/.

[89] LG. *Air conditioner service manual. Document #: MFL68082948*, 2019. Accessed Oct. 31, 2022. https://www.lgdfs.ca/en/productliterature.

[90] Daikin. *SkyAir* series single zone heating and cooling systems brochure. Document #: CB-SKYHPAC_06-22, 2022.

[91] Daikin. *Sky Air* heat pump submittal data sheet. Document #: FTQ42TAVJUD-RZQ42TAVJUA v1, 2020.

[92] Samsung. Single zone (CAC) split systems HVAC guide specifications, 2021. Accessed Oct. 31, 2022. https://www.samsunghvac.com/downloads-single-zone-duct-systems/MPAH-Single-Zone.

[93] Samsung Electronics. *Max Heat* technical data book. AC***KNZDCH/AA (indoor unit), AC***JXSCCH/AA (outdoor unit), version 1.3, 2020.

[94] Samsung Electronics. Heat pump technical data book, model AC***KNZDCH/AA (indoor unit), AC***JXADCH/AA (outdoor unit), version 1.4, 2018.

[95] Bryant. *186CNV / 284ANV Evolution Extreme series heat pump service manual. Catalog #: SM186CNV-284ANV-01*, 2020.

[96] Bryant. 284ANV *Evolution Extreme* series heat pump product data. Catalog #: PDS284ANV-01, 2020.

[97] Bryant. *280ANV Evolution Extreme heat pump unit training manual. Catalog #: 06-B20-665*, 2012.

[98] Bryant. 280A *Evolution Extreme* series heat pump product data. Catalog #: PDS280A–04, 2019.

[99] Carrier. 25VNA *Infinity* variable speed heat pump product data. Catalog #: 25VNA–01PD, 2011.

[100] Carrier. *25VNA Infinity heat pump unit training manual. Catalog #: 06-C20-665*, 2011.

[101] Bryant. *Preferred* series heat pump submittal data sheet, outdoor model 38MAQB30R–3. Catalog #: 38MAR-30-3-06SB, 2019.

[102] Bryant. *Preferred series 38MA*R heat pump service manual. Catalog #: SG-38MAR-02*. Indianapolis, IN, USA, 2017.

[103] Fujitsu. FO*20R series variable speed heat pump specifications. Form #: PFJ-811 Rev. 1.

[104] Fujitsu. Variable speed R-410A heat pump outdoor units installation instructions. Document #: 92-105074-16-01.

[105] Fujitsu. *Heat pump service manual. Document #: SR_AR024EF_01*, 2020.

[106] Rheem. *Prestige* (RP20) series variable speed heat pumps. Form #: P11-811 Rev. 10, 2021.

[107] Ruud. *Ultra* (UP20) series variable speed heat pumps. Form #: P22-811 Rev. 10, 2021.

[108] Ecoer. Up to 5 ton inverter split system heat pump EODA18H-4860 outdoor unit - submittal data, 2019.

[109] Ecoer. *ESI (Ultra) unitary service manual*. Fairfax, VA, USA, 2019.

[110] Ecoer. *ESI (Ultra)* series outdoor unit heat pump specifications, 2019.

[111] Bosch. *IDS 2.0 split system heat pump service manual. Document #: BTC 761702111 A*, 2021.

[112] Bosch. *BOVB 18* split system heat pump - product specifications. Document #: BTC 761701314 A, 2020.

[113] Bosch. IDS BOVB36-18 & BOVB60-18 split system heat pump spare parts list. Document #: BTC 761711109 A, 2020.

[114] Zephyr. Inverter central brochure. https://tticlimatisation.com/docs/Zephyr_central_inverter.pdf.

[115] Zephyr. *Manuel d'utilization et d'installation, thermopompe. Version #: 2169405, A*. Longueuil, QC, Canada.

[116] Haxxair. 2020 Catalogue de produits secteur résidentiel secteur commercial, 2020.

[117] *American Standard. Variable speed AccuLink heat pumps and air conditioners - service facts. Document #: 4A-V8-SF-1G-EN*, 2017.

[118] Variable speed *Acculink* heat pumps - product data. Document #: 12-1353-1B-EN, 2017.

[119] *American Standard. Variable speed AccuLink heat pumps and air conditioners - service facts. Document #: 4A-V0-SF-1G-EN*, 2017.

[120] American Standard. Variable speed *Acculink* heat pumps - product data. Document #: 12-1354-1D-EN, 2019.

[121] Government of Canada. Eligible product lists for air source heat pumps and cold climate heat pumps under the Canada Greener Homes Grant. Record ID: 4717f11d-b018-4fd3-ae66-e38e8fdef5d7.

[122] A. Gużda and N. Szmolke. Compressors in heat pumps. *Machine Dynamics Research*, 39(2):71–83, 2016.

[123] T. Matsuzaka and S. Nagatomo. Rolling piston type rotary compressor performance analysis. page 386. International Refrigeration and Air Conditioning Conference, Purdue University, 1982.

[124] G. Shoukas, E. Bonnema, G. Paranjothi, R. Faramarzi, and L. Klun. Performance assessment of high efficiency variable speed air-source heat pump in cold climate applications. Technical report, National Renewable Energy Lababoratory, Golden, CO, 2022.

[125] Air Conditioning Contractors of America Association Inc., Alexandria, VA. *Manual S - Residential Equipment Selection*, 2 edition, 2014.

[126] A. B. Guada, T. Kingston, and P. Glanville. Right-sizing electric heat pump and auxiliary heating for residential heating systems based on actual performance associated with climate zone. *ASHRAE Transactions*, 126:316–324, 2020.

[127] J. Sager, T. Mackintosh, G. St-Onge, E. McDonald, and M. Kegel. Detailed performance assessment of variable capacity inverter-driven cold climate air source heat pumps. In *Springer Proceedings in Energy – Cold Climate HVAC 2018*, pages 441–451. Springer, 2019.

[128] T. Q. Qureshi and S. A. Tassou. Variable-speed capacity control in refrigeration systems. *Applied Thermal Engineering*, 16(2):103–113, 1996.

[129] X. Pang and M. Liu. Prevention of compressor short cycling in direct-expansion (DX) rooftop units–Part 1: Theoretical analysis and simulation. *ASHRAE Transactions*, 117(2):666–676, 2011.

[130] Y. Zhu, G. He, W. Sun, M. Shimoji, and X. Chen. Investigation on the characteristics of oil supply system for a hermetic variable speed rotary compressor. *International Journal of Refrigeration*, 118:150–160, 2020.

[131] Lg. R1 compressor introduction (video), 2019. Accessed: Oct. 6, 2022. https://www.youtube.com/watch?v=mC0Pw76d9-4.

[132] S. Prud'homme, S. Breton, J. Tamasauskas, A. Lachance, and M. Kegel. Studying the impact factors influencing variable-capacity heat pump energy performance

through simulation. In *E3S Web of Conferences – Cold Climate HVAC & Energy 2021*, volume 246, page 06005. EDP Sciences, 2021.

[133] S. Krishnamoorthy, M. Modera, and C. Harrington. Efficiency optimization of a variable-capacity/variable-blower-speed residential heat-pump system with ductwork. *Energy and Buildings*, 150:294–306, 2017.

[134] R. Adhikari, N. Aste, M. Manfren, and D. Marini. Energy savings through variable speed compressor heat pump systems. *Energy Procedia*, 14:1337–1342, 2012.

[135] C. Cuevas and J. Lebrun. Testing and modelling of a variable speed scroll compressor. *Applied Thermal Engineering*, 29(2-3):469–478, 2009.

[136] J. P. Ore, N. P. Salts, and E. A. Groll. Evaluation of fixed and variable speed compressor energy consumption in a residential environment before and after building renovations. *ASHRAE Transactions*, 126(1), 2020.

[137] H. Liu, K. Nagano, T. Katsura, and Y. Han. Experimental investigation on a vapor injection heat pump system with a single-stage compressor. *Energies*, 13(12):3133, 2020.

[138] J. Heo, M. W. Jeong, and Y. Kim. Effects of flash tank vapor injection on the heating performance of an inverter-driven heat pump for cold regions. *International Journal of Refrigeration*, 33(4):848–855, 2010.

[139] G.-Y. Ma and H.-X. Zhao. Experimental study of a heat pump system with flash-tank coupled with scroll compressor. *Energy and Buildings*, 40(5):697–701, 2008.

[140] X. Wang, Y. Hwang, and R. Radermacher. Two-stage heat pump system with vapor-injected scroll compressor using R410A as a refrigerant. *International Journal of Refrigeration*, 32(6):1442–1451, 2009.

[141] J. Heo, M. W. Jeong, C. Baek, and Y. Kim. Comparison of the heating performance of air-source heat pumps using various types of refrigerant injection. *International Journal of Refrigeration*, 34(2):444–453, 2011.

[142] C. W. Roh and M. S. Kim. Comparison of the heating performance of an inverter-driven heat pump system using R410A vapor-injection into accumulator and compressor. *International Journal of Refrigeration*, 35(2):434–444, 2012.

[143] S. Jiang, S. Wang, Y. Yu, Z. Ma, and J. Wang. Further analysis of the influence of interstage configurations on two-stage vapor compression heat pump systems. *Applied Thermal Engineering*, 184:116050, 2021.

[144] D. Zhang, J. Li, J. Nan, and L. Wang. Thermal performance prediction and analysis on the economized vapor injection air-source heat pump in cold climate region of China. *Sustainable Energy Technologies and Assessments*, 18:127–133, 2016.

[145] B. J. Dechesne, F. M. Tello-Oquendo, S. Gendebien, and V. Lemort. Residential air-source heat pump with refrigerant injection and variable speed compressor: Experimental investigation and compressor modeling. *International Journal of Refrigeration*, 108:79–90, 2019.

[146] C. W. Roh and M. S. Kim. Effects of intermediate pressure on the heating performance of a heat pump system using R410A vapor-injection technique. *International Journal of Refrigeration*, 34(8):1911–1921, 2011.

[147] J.-C. Lai, W.-J. Luo, J.-Y. Wu, D. Faridah, C.-M. Lin, F. R. Fasya, M. Nuriyadi, and W.-B. Ng. Performance analysis of single-stage air source heat pump utilizing indirect vapor injection design. *Advances in Mechanical Engineering*, 10(4):1–12, 2018.

[148] S. M. Finlayson and T. R. Dickson. Accumulator sizing and evaluation technique based on theoretical optimum system performance. *SAE Transactions*, 114:2557–2562, 2005.

[149] Mistubishi. Nv-Series and P-Series catalog. SKU: TR_RS_1060_02-20, 2020.

[150] J. Kim, H.-J. Choi, and K. C. Kim. A combined dual hot-gas bypass defrosting method with accumulator heater for an air-to-air heat pump in cold region. *Applied Energy*, 147:344–352, 2015.

[151] D. Huang, X. Yuan, and X. Zhang. Effects of fan-starting methods on the reverse-cycle defrost performance of an air-to-water heat pump. *International Journal of Refrigeration*, 27(8):869–875, 2004.

[152] M. Kegel, J. Sager, M. Thomas, D. Giguere, and R. Sunye. Performance testing of cold climate air source heat pumps. In *Proc. 12th IEA Heat Pump Conference*, 2017.

[153] A. Hakkaki-Fard, Z. Aidoun, and M. Ouzzane. Improving cold climate air-source heat pump performance with refrigerant mixtures. *Applied Thermal Engineering*, 78:695–703, 2015.

[154] B. Shen and M. R. Ally. Energy and exergy analysis of low-global warming potential refrigerants as replacement for R410A in two-speed heat pumps for cold climates. *Energies*, 13(21):5666, 2020.

[155] B. Shen and M. R. Ally. Comparative performance of low global warming potential (GWP) refrigerants as replacement for R-410A in a regular 2-speed heat pump for sustainable cooling. *Sustainability*, 13(15):8199, 2021.

[156] K. Uddin, S. Arakaki, and B. B. Saha. Thermodynamic analysis of low-GWP blends to replace R410A for residential building air conditioning applications. *Environmental Science and Pollution Research*, 28(3):2934–2947, 2021.

[157] Q. Tian, D. Cai, L. Ren, W. Tang, Y. Xie, G. He, and F. Liu. An experimental investigation of refrigerant mixture R32/R290 as drop-in replacement for HFC410A in household air conditioners. *International Journal of Refrigeration*, 57:216–228, 2015.

[158] A. Hakkaki-Fard, Z. Aidoun, and M. Ouzzane. Applying refrigerant mixtures with thermal glide in cold climate air-source heat pumps. *Applied Thermal Engineering*, 62(2):714–722, 2014.

[159] A. Chabot and F. Mathieu-Potvin. Numerical analysis of heat pumps: Selection of the best fluids for maximizing the coefficient of performance. *International Journal of Refrigeration*, 112:281–302, 2020.

[160] P. A. Domanski, D. Yashar, and M. Kim. Performance of a finned-tube evaporator optimized for different refrigerants and its effect on system efficiency. *International Journal of Refrigeration*, 28(6):820–827, 2005.

[161] G. Lorentzen and J. Pettersen. A new, efficient and environmentally benign system for car air-conditioning. *International Journal of Refrigeration*, 16(1):4–12, 1993.

[162] P. Nekså. CO_2 heat pump systems. *International Journal of Refrigeration*, 25(4):421–427, 2002.

[163] Y. Ma, Z. Liu, and H. Tian. A review of transcritical carbon dioxide heat pump and refrigeration cycles. *Energy*, 55:156–172, 2013.

[164] R. U. Rony, H. Yang, S. Krishnan, and J. Song. Recent advances in transcritical CO_2 (R744) heat pump system: a review. *Energies*, 12(3):457, 2019.

[165] M. Yari and S. M. S. Mahmoudi. Thermodynamic analysis and optimization of novel ejector-expansion TRCC (transcritical CO_2) cascade refrigeration cycles (novel transcritical CO_2 cycle). *Energy*, 36(12):6839–6850, 2011.

[166] B. T. Austin and K. Sumathy. Transcritical carbon dioxide heat pump systems: A review. *Renewable and sustainable energy reviews*, 15(8):4013–4029, 2011.

[167] K. Ameur and Z. Aidoun. Two-phase ejector enhanced carbon dioxide transcritical heat pump for cold climate. *Energy Conversion and Management*, 243:114421, 2021.

[168] D. Wang, B. Yu, J. Hu, L. Chen, J. Shi, and J. Chen. Heating performance characteristics of CO_2 heat pump system for electrical vehicle in a cold climate. *International Journal of Refrigeration*, 85:27–41, 2018.

[169] L. Rajapaksha. Influence of special attributes of zeotropic refrigerant mixtures on design and operation of vapour compression refrigeration and heat pump systems. *Energy Conversion and Management*, 48(2):539–545, 2007.

[170] A. Hakkaki-Fard, Z. Aidoun, and M. Ouzzane. Air-source heat pumps with refrigerant mixtures for cold climates. page 1397. IEA Heat Pump Conference, ResearchGate, 05 2014.

[171] A. Hakkaki-Fard, Z. Aidoun, and P. Eslami-Nejad. Evaluation of refrigerant mixtures in three different cold-climate residential air-source heat pumps. *ASHRAE Transactions*, 122(2), 2016.

[172] B. Zühlsdorf, J. K. Jensen, S. Cignitti, C. Madsen, and B. Elmegaard. Analysis of temperature glide matching of heat pumps with zeotropic working fluid mixtures for different temperature glides. *Energy*, 153:650–660, 2018.

[173] D. Roskosch, V. Venzik, J. Schilling, A. Bardow, and B. Atakan. Beyond temperature glide: The compressor is key to realizing benefits of zeotropic mixtures in heat pumps. *Energy Technology*, 9(4):2000955, 2021.

[174] S. Jiang, S. Wang, X. Jin, and T. Zhang. A general model for two-stage vapor compression heat pump systems. *International Journal of Refrigeration*, 51:88–102, 2015.

[175] D. Kim, Y. Jeon, D. S. Jang, and Y. Kim. Performance comparison among two-phase, liquid, and vapor injection heat pumps with a scroll compressor using R410A. *Applied Thermal Engineering*, 137:193–202, 2018.

[176] Q. Tu, W. Bai, Z. Xu, L. Zhang, X. Guo, Y. Xu, J. Zhang, and C. Deng. Effects of subcooling degree and injection super-heating degree on performance of an air source heat pump with subcooler. *International Journal of Energy Research*, 43(14):7970–7987, 2019.

[177] S. Jiang, S. Wang, X. Jin, and Y. Yu. Optimum compressor cylinder volume ratio for two-stage compression air source heat pump systems. *International journal of refrigeration*, 67:77–89, 2016.

[178] B. Shen, C. K. Rice, O. Abdelaziz, and S. Shrestha. Development of cold climate heat pump using two-stage compression. Technical report, Oak Ridge National Lab (ORNL), Oak Ridge, TN, 2015.

[179] L. Zhao, N. Zheng, and S. Deng. A thermodynamic analysis of an auto-cascade heat pump cycle for heating application in cold regions. *Energy and Buildings*, 82:621–631, 2014.

[180] J. Chen, J. Yu, and G. Yan. Performance analysis of a modified autocascade refrigeration cycle with an additional evaporating subcooler. *Applied Thermal Engineering*, 103:1205–1212, 2016.

[181] C. Fan, G. Yan, and J. Yu. Theoretical study on a modified heat pump cycle with zeotropic mixture R32/R290 for district heating in cold region. *Applied Thermal Engineering*, 156:702–707, 2019.

[182] B. Yu, J. Yang, D. Wang, J. Shi, and J. Chen. Modeling and theoretical analysis of a CO_2-propane autocascade heat pump for electrical vehicle heating. *International Journal of Refrigeration*, 95:146–155, 2018.

[183] K. Du, S. Zhang, W. Xu, and X. Niu. A study on the cycle characteristics of an auto-cascade refrigeration system. *Experimental Thermal and Fluid Science*, 33(2):240–245, 2009.

[184] Y. Liu and J. Yu. Performance analysis of an advanced ejector-expansion autocascade refrigeration cycle. *Energy*, 165:859–867, 2018.

[185] J. Liu, Y. Liu, G. Yan, and J. Yu. Theoretical study on a modified single-stage autocascade refrigeration cycle with auxiliary phase separator. *International Journal of Refrigeration*, 122:181–191, 2021.

[186] S. G. Kim and M. S. Kim. Experiment and simulation on the performance of an autocascade refrigeration system using carbon dioxide as a refrigerant. *International Journal of Refrigeration*, 25(8):1093–1101, 2002.

[187] M. Sobieraj. Experimental investigation of the effect of a recuperative heat exchanger and throttles opening on a CO_2/isobutane autocascade refrigeration system. *Energies*, 13(20):5285, 2020.

[188] J. Chen and J. Yu. Performance of a new refrigeration cycle using refrigerant mixture R32/R134a for residential air-conditioner applications. *Energy and Buildings*, 40(11):2022–2027, 2008.

[189] J.-M. Corberán, I. Martínez-Galván, S. Martínez-Ballester, J. Gonzálvez-Maciá, and R. Royo-Pastor. Influence of the source and sink temperatures on the optimal refrigerant charge of a water-to-water heat pump. *International Journal of Refrigeration*, 34(4):881–892, 2011.

[190] H. Cho, C. Ryu, Y. Kim, and H. Y. Kim. Effects of refrigerant charge amount on the performance of a transcritical CO_2 heat pump. *International Journal of Refrigeration*, 28(8):1266–1273, 2005.

[191] D. Wang, Z. Zhang, B. Yu, X. Wang, J. Shi, and J. Chen. Experimental research on charge determination and accumulator behavior in trans-critical CO_2 mobile air-conditioning system. *Energy*, 183:106–115, 2019.

[192] M. M. Hazarika, M. Ramgopal, S. Bhattacharyya, and R. L. Doménech. Role of receiver on the performance of a transcritical co2 based air-conditioning unit with single-stage and two-stage expansion. *Science and Technology for the Built Environment*, 27(5):1–28, 2021.

[193] J. C. Menken, T. Weustenfeld, and J. Köhler. Experimental comparison of the refrigerant reservoir position in a primary loop refrigerant cycle with optimal operation. page 1397. International Refrigeration and Air Conditioning Conference, Purdue University, 2014.

[194] S. Ramaraj, J. E. Braun, E. A. Groll, and W. T. Horton. Performance analysis of liquid flooded compression with regeneration for cold climate heat pumps. *International Journal of Refrigeration*, 68:50–58, 2016.

[195] K. Seong, D. Lee, and J. Lee. The effects of wet compression by the electronic expansion valve opening on the performance of a heat pump system. *Applied Sciences*, 7(3):248, 2017.

[196] J. Wang, D. Qv, L. Ni, and Y. Yao. Experimental study on an injection-assisted air source heat pump with a novel two-stage variable-speed scroll compressor. *Applied Thermal Engineering*, 176:115415, 2020.

[197] S. Elbel and N. Lawrence. Review of recent developments in advanced ejector technology. *International Journal of Refrigeration*, 62:1–18, 2016.

[198] Z. Zhang, X. Feng, D. Tian, J. Yang, and L. Chang. Progress in ejector-expansion vapor compression refrigeration and heat pump systems. *Energy Conversion and Management*, 207:112529, 2020.

[199] K. Sumeru, H. Nasution, and F. N. Ani. A review on two-phase ejector as an expansion device in vapor compression refrigeration cycle. *Renewable and Sustainable Energy Reviews*, 16(7):4927–4937, 2012.

[200] B. M. Tashtoush, M. A. Al-Nimr, and M. A. Khasawneh. A comprehensive review of ejector design, performance, and applications. *Applied Energy*, 240:138–172, 2019.

[201] N. H. Gay. Refrigerating system, Dec 1931.

[202] H. Qi, F. Liu, and J. Yu. Performance analysis of a novel hybrid vapor injection cycle with subcooler and flash tank for air-source heat pumps. *International Journal of Refrigeration*, 74:540–549, 2017.

[203] E. Brodal and O. Eiksund. Optimization study of heat pumps using refrigerant blends–Ejector versus expansion valve systems. *International Journal of Refrigeration*, 111:136–146, 2020.

[204] Y. Zhu, Y. Huang, C. Li, F. Zhang, and P.-X. Jiang. Experimental investigation on the performance of transcritical CO_2 ejector–expansion heat pump water heater system. *Energy Conversion and Management*, 167:147–155, 2018.

[205] X. Chen, S. Omer, M. Worall, and S. Riffat. Recent developments in ejector refrigeration technologies. *Renewable and Sustainable Energy Reviews*, 19:629–651, 2013.

[206] J. Chen, S. Jarall, H. Havtun, and B. Palm. A review on versatile ejector applications in refrigeration systems. *Renewable and Sustainable Energy Reviews*, 49:67–90, 2015.

[207] J. Liu and Z. Lin. A novel dual-temperature ejector-compression heat pump cycle - exergetic and economic analyses. *International Journal of Refrigeration*, 126:155–167, 2021.

[208] X. Chen, Y. Zhou, and J. Yu. A theoretical study of an innovative ejector enhanced vapor compression heat pump cycle for water heating application. *Energy and Buildings*, 43(12):3331–3336, 2011.

[209] K. S. Yap, K. T. Ooi, and A. Chakraborty. Analysis of the novel cross vane expander-compressor: Mathematical modelling and experimental study. *Energy*, 145:626–637, 2018.

[210] B. Zhang, L. Chen, L. Liu, X. Zhang, M. Wang, C. Ji, and K.-I. Song. Parameter sensitivity study for typical expander-based transcritical CO_2 refrigeration cycles. *Energies*, 11(5):1279, 2018.

[211] M. Wang, Y. Zhao, F. Cao, G. Bu, and Z. Wang. Simulation study on a novel vane-type expander with internal two-stage expansion process for R-410A refrigeration system. *International Journal of Refrigeration*, 35(4):757–771, 2012.

[212] N. Zheng and L. Zhao. The feasibility of using vapor expander to recover the expansion work in two-stage heat pumps with a large temperature lift. *International Journal of Refrigeration*, 56:15–27, 2015.

[213] P. Byrne, L. Serres, R. Ghoubali, and J. Miriel. Experimental study and simulation of a thermosiphon defrosting technique for air-source heat pumps. *ASHRAE Transactions*, 119(1), 2013.

[214] W. Wei, L. Ni, Q. Dong, W. Wang, J. Ye, L. Xu, Y. Yang, and Y. Yao. Experimental investigation on improving defrosting performance of air source heat pump through vapor injection. *Energy & Buildings*, 256:111696, 2022.

[215] Z. Long, D. Jiankai, J. Yiqiang, and Y. Yang. A novel defrosting method using heat energy dissipated by the compressor of an air source heat pump. *Applied Energy*, 133:101–111, 2014.

[216] S. H. Hong, D. S. Jang, S. Yun, J. H. Baek, and Y. Kim. Performance improvement of heat pumps using novel microchannel heat exchangers with plain-louver fins during periodic frosting and defrosting cycles in electric vehicles. *Energy Conversion and Management*, 223:113306, 2020.

[217] L.-L. Shao, L. Yang, and C.-L. Zhang. Comparison of heat pump performance using fin-and-tube and microchannel heat exchangers under frost conditions. *Applied Energy*, 87(4):1187–1197, 2010.

[218] J.-H. Kim and E. A. Groll. Performance comparisons of a unitary split system using microchannel and fin-tube outdoor coils. *ASHRAE Transactions*, 109:219–229, 2003.

[219] *2017 Standard for performance rating of unitary air-conditioning & air-source heat pump equipment*. Arlington, VA, USA, 2019.

[220] L. Chung. Assessing residential air conditioners/heat pumps energy performance in Canada, 2021.

[221] A. Lachance, J. Tamasauskas, S. Breton, and S. Prud'homme. Simulation based assessment on representativeness of a new performance rating procedure for cold climate air source heat pumps. In *E3S Web of Conferences - Cold Climate HVAC & Energy 2021*, volume 246, page 06004. EDP Sciences, 2021.

[222] *Load-based and climate-specific testing and rating procedures for heat pumps and air conditioners*, 2019.

[223] P. Dhillon, W. T. Horton, and J. E. Braun. Comparison of steady-state and dynamic load-based performance evaluation methodologies for a residential air conditioner. 2021.

[224] Natural Resources Canada. *Air-source heat pump sizing and selection guide*, 1 edition, 2020.

[225] Carrier. Heating check chart. Catalog No: 25HCC5–1HCC, 2019.

[226] Carrier. 25HBC5 *Comfort 15* heat pump with *Puron* refrigerant, 1-1/2 to 5 nominal tons - product data. Catalog #: 25HBC5 -7PD, 2019.

[227] Carrier. FX4D *Comfort* series fan coil sizes 019 thru 061 - product data. Catalog #: FX4D-01PD, 2010.

[228] National Institutes of Health - Office of Management. ECM motors: An energy saving opportunity, 2016. https://orf.od.nih.gov/TechnicalResources/.

[229] X. Wang, Y. Hwang, and R. Radermacher. Investigation of potential benefits of compressor cooling. *Applied Thermal Engineering*, 28(14-15):1791–1797, 2008.

[230] *2015 Standard for performance rating of positive displacement refrigerant compressors and compressor units*. Arlington, VA, USA, 2015.

[231] Emerson Climate Technologies, Inc. ZP42K6E-PFV autogenerated compressor performance, 2017.

[232] C. Underwood, M. Royapoor, and B. Sturm. Parametric modelling of domestic air-source heat pumps. *Energy and Buildings*, 139:578–589, 2017.

[233] 12th IEA Heat Pump Conference. *An instrumented method for the evaluation of compressor heat losses in heat pumps on-field*, 2017.

[234] M. Brown, M. Burke-Scoll, and J. Stebnicki. Air source heat pump efficiency gains from low ambient temperature operation using supplemental electric heating, 2011.

[235] Emerson Climate Technologies, Inc. Application engineering bulletin - 1 to 5 ton ZP*K6 R-410A Copeland scroll compressors. Document #: AE4-1400 R2, 2015.